

PUBLISHED VERSION

Aad, G.;...; Jackson, Paul Douglas; ... et al.; ATLAS Collaboration
[Combined search for the Standard Model Higgs boson in pp collisions at root s=7 TeV with the ATLAS detector](#)

Physical Review. D. Particles, Fields, Gravitation and Cosmology, 2012; 86(3):032003-1-032003-31

© 2012 CERN, for the ATLAS Collaboration. Creative Commons 3.0 Unported (CC BY 3.0)

<http://prd.aps.org/abstract/PRD/v86/i3/e032003>

PERMISSIONS

<http://publish.aps.org/authors/transfer-of-copyright-agreement>

“The author(s), and in the case of a Work Made For Hire, as defined in the U.S. Copyright Act, 17 U.S.C.

§101, the employer named [below], shall have the following rights (the “Author Rights”):

[...]

3. The right to use all or part of the Article, including the APS-prepared version without revision or modification, on the author(s)' web home page or employer's website and to make copies of all or part of the Article, including the APS-prepared version without revision or modification, for the author(s)' and/or the employer's use for educational or research purposes.”

1st May 2013

<http://hdl.handle.net/2440/76954>

Combined search for the Standard Model Higgs boson in pp collisions at $\sqrt{s} = 7$ TeV with the ATLAS detector

G. Aad *et al.**

(ATLAS Collaboration)

(Received 2 July 2012; published 2 August 2012)

A combined search for the Standard Model Higgs boson with the ATLAS detector at the LHC is presented. The data sets used correspond to integrated luminosities from 4.6 fb^{-1} to 4.9 fb^{-1} of proton-proton collisions collected at $\sqrt{s} = 7$ TeV in 2011. The Higgs boson mass ranges of 111.4 GeV to 116.6 GeV, 119.4 GeV to 122.1 GeV, and 129.2 GeV to 541 GeV are excluded at the 95% confidence level, while the range 120 GeV to 560 GeV is expected to be excluded in the absence of a signal. An excess of events is observed at Higgs boson mass hypotheses around 126 GeV with a local significance of 2.9 standard deviations (σ). The global probability for the background to produce an excess at least as significant anywhere in the entire explored Higgs boson mass range of 110–600 GeV is estimated to be $\sim 15\%$, corresponding to a significance of approximately 1σ .

DOI: [10.1103/PhysRevD.86.032003](https://doi.org/10.1103/PhysRevD.86.032003)

PACS numbers: 14.80.Bn, 12.15.Ji, 13.85.Rm

I. INTRODUCTION

Probing the mechanism for electroweak symmetry breaking (EWSB) is one of the prime objectives of the Large Hadron Collider (LHC). In the Standard Model (SM) [1–3], the electroweak interaction is described by a local gauge field theory with an $SU(2)_L \otimes U(1)_Y$ symmetry, and EWSB is achieved via the Higgs mechanism with a single $SU(2)_L$ doublet of complex scalar fields [4–9]. After EWSB the electroweak sector has massive W^\pm and Z bosons, a massless photon, and a massive CP -even, scalar boson, referred to as the Higgs boson. Fermion masses are generated from Yukawa interactions with couplings proportional to the masses of fermions. The mass of the Higgs boson, m_H , is a free parameter in the SM. However, for a given m_H hypothesis the cross sections of the various Higgs boson production processes and the branching fractions of the decay modes can be predicted, allowing a combined search with data from several search channels.

Combined searches at the CERN LEP e^+e^- collider excluded the production of a SM Higgs boson with mass below 114.4 GeV at 95% confidence level (CL) [10]. The combined searches at the Fermilab Tevatron $p\bar{p}$ collider excluded the production of a SM Higgs boson with a mass between 147 GeV and 179 GeV, and between 100 GeV and 106 GeV at 95% CL [11]. Precision electroweak measurements are sensitive to m_H via radiative corrections and indirectly constrain the SM Higgs boson mass to be less than 158 GeV [12] at 95% CL.

*Full author list given at the end of the article.

Published by the American Physical Society under the terms of the [Creative Commons Attribution 3.0 License](https://creativecommons.org/licenses/by/3.0/). Further distribution of this work must maintain attribution to the author(s) and the published article's title, journal citation, and DOI.

In 2011, the LHC delivered an integrated luminosity of 5.6 fb^{-1} of proton-proton (pp) collisions at a center-of-mass energy of 7 TeV to the ATLAS detector [13]. Of the 4.9 fb^{-1} collected, the integrated luminosity used in the individual Higgs search channels is between 4.6 fb^{-1} and 4.6 fb^{-1} , depending on the data quality requirements specific to each channel.

This paper presents a combined search for the SM Higgs boson in the decay modes $H \rightarrow \gamma\gamma$, $H \rightarrow ZZ^{(*)}$, $H \rightarrow WW^{(*)}$, $H \rightarrow \tau^+\tau^-$, and $H \rightarrow b\bar{b}$, with subsequent decays of the W , Z , and τ leading to different final states. Some searches are designed to exploit the features of the production modes $pp \rightarrow H$ (gluon fusion), $pp \rightarrow qqH$ (vector boson fusion), and $pp \rightarrow VH$ with $V = W^\pm$ or Z (associated production with a gauge boson). In order to enhance the search sensitivity, the various decay modes are further subdivided into subchannels with different signal and background contributions and different sensitivities to systematic uncertainties. While the selection requirements for individual search channels are disjoint, each selection is, in general, populated by more than one combination of Higgs boson production and decay. For instance, Higgs boson production initiated by vector boson fusion (VBF) can contribute significantly to a search channel optimized for gluon fusion production.

The ATLAS Collaboration has previously published a similar but less extensive combined search for the Higgs boson [14] in data taken at the LHC in 2011. The CMS Collaboration has also performed a combined analysis of Higgs searches with data collected in 2011 and has obtained similar results [15]. In comparison to the analysis of Ref. [14], the $H \rightarrow \tau^+\tau^-$ and $H \rightarrow b\bar{b}$ channels have been added, the $H \rightarrow WW^{(*)} \rightarrow \ell^+\nu\ell^-\bar{\nu}$ analysis has been updated and extended to cover the mass range of 110–600 GeV, and the $H \rightarrow WW \rightarrow \ell\nu q\bar{q}'$, $H \rightarrow ZZ \rightarrow \ell^+\ell^-\nu\bar{\nu}$, and $H \rightarrow ZZ \rightarrow \ell^+\ell^-q\bar{q}$ analyses have been

TABLE I. Summary of the individual channels entering the combination. The transition points between separately optimized m_H regions are indicated when applicable. The symbols \otimes and \oplus represent direct products or sums over sets of selection requirements. The details of the subchannels are given in Sec. III.

Higgs decay	Subsequent decay	Subchannels	m_H range (GeV)	$\int L dt$ (fb $^{-1}$)	Reference
$H \rightarrow \gamma\gamma$	\dots	9 subchannels $\{p_T, \otimes \eta_\gamma \otimes \text{conversion}\}$	110–150	4.9	[16]
$H \rightarrow ZZ^{(*)}$	$\ell\ell'\ell'$	$\{4e, 2e2\mu, 2\mu2e, 4\mu\}$	110–600	4.8	[17]
	$\ell\ell\nu\bar{\nu}$	$\{ee, \mu\mu\} \otimes \{\text{low, high pileup periods}\}$	200–280–600	4.7	[18]
	$\ell\ell q\bar{q}$	$\{b\text{-tagged, untagged}\}$	200–300–600	4.7	[19]
$H \rightarrow WW^{(*)}$	$\ell\nu\ell\nu$	$\{ee, e\mu, \mu\mu\} \otimes \{0\text{-jet, 1-jet, 2-jet}\} \otimes \{\text{low, high pileup periods}\}$	110–200–300–600	4.7	[20]
	$\ell\nu q\bar{q}'$	$\{e, \mu\} \otimes \{0\text{-jet, 1-jet, 2-jet}\}$	300–600	4.7	[21]
$H \rightarrow \tau^+\tau^-$	$\tau_{\text{lep}}\tau_{\text{lep}}$	$\{e\mu\} \otimes \{0\text{-jet}\} \oplus \{\ell\ell\} \otimes \{1\text{-jet, 2-jet, VH}\}$	110–150	4.7	
	$\tau_{\text{lep}}\tau_{\text{had}}$	$\{e, \mu\} \otimes \{0\text{-jet}\} \otimes \{E_T^{\text{miss}} < 20 \text{ GeV}, E_T^{\text{miss}} \geq 20 \text{ GeV}\} \oplus \{e, \mu\} \otimes \{1\text{-jet}\} \oplus \{\ell\} \otimes \{2\text{-jet}\}$	110–150	4.7	[22]
$VH \rightarrow b\bar{b}$	$\tau_{\text{had}}\tau_{\text{had}}$	$\{1\text{-jet}\}$	110–150	4.7	
	$Z \rightarrow \nu\bar{\nu}$	$E_T^{\text{miss}} \in \{120\text{--}160, 160\text{--}200, \geq 200 \text{ GeV}\} \text{ GeV}$	110–130	4.6	
	$W \rightarrow \ell\nu$	$p_T^W \in \{<50, 50\text{--}100, 100\text{--}200, \geq 200 \text{ GeV}\}$	110–130	4.7	[23]
	$Z \rightarrow \ell\ell$	$p_T^Z \in \{<50, 50\text{--}100, 100\text{--}200, \geq 200 \text{ GeV}\}$	110–130	4.7	

updated to use the full 2011 data set. Both the $H \rightarrow WW^{(*)} \rightarrow \ell^+\nu\ell^-\bar{\nu}$ and $H \rightarrow WW \rightarrow \ell\nu q\bar{q}'$ analyses include a specific treatment of the 2-jet final state, which is targeted at the VBF production process.

The different channels entering the combination are summarized in Table I. After describing the general approach to statistical modeling in Sec. II, the individual channels and the specific systematic uncertainties are described in Secs. III and IV, respectively. The statistical procedure is described in Sec. V and the resulting exclusion limits and compatibility with the background-only hypothesis are presented in Secs. VI and VII, respectively.

II. STATISTICAL MODELING

In this combined analysis, a given search channel, indexed by c , is defined by its associated event selection criteria, which may select events from various physical processes. In addition to the number of selected events, n , each channel may make use of an invariant or transverse mass distribution of the Higgs boson candidates. The discriminating variable is denoted x and its probability density function (pdf) is written as $f(x|\alpha)$, where α represents both theoretical parameters such as m_H and nuisance parameters associated with various systematic effects. These distributions are normalized to unit probability. The predicted number of events satisfying the selection requirements is parametrized as $\nu(\alpha)$. For a channel with n selected events, the data consist of the values of the discriminating variables for each event $\mathcal{D} = \{x_1, \dots, x_n\}$. The probability model for these types of data is referred to as an unbinned extended likelihood or marked Poisson model f , given by

$$f(\mathcal{D}|\alpha) = \text{Pois}(n|\nu(\alpha)) \prod_{e=1}^n f(x_e|\alpha). \quad (1)$$

For each channel several signal and background scattering processes contribute to the total rate ν and the overall pdf $f(x|\alpha)$. Here, the term *process* is used for any set of scattering processes that can be added incoherently. The total rate is the sum of the individual rates

$$\nu(\alpha) = \sum_{k \in \text{processes}} \nu_k(\alpha) \quad (2)$$

and the total pdf is the weighted sum

$$f(x|\alpha) = \frac{1}{\nu(\alpha)} \sum_{k \in \text{processes}} \nu_k(\alpha) f_k(x|\alpha). \quad (3)$$

Using e as the index over the n_c events in the c th channel, x_{ce} is the value of the observable x for the e th event in channels 1 to c^{max} . The total data are a collection of data from individual channels: $\mathcal{D}_{\text{com}} = \{\mathcal{D}_1, \dots, \mathcal{D}_{c^{\text{max}}}\}$. The combined model can then be written as follows:

$$f_{\text{com}}(\mathcal{D}_{\text{com}}|\alpha) = \prod_{c=1}^{c^{\text{max}}} \left[\text{Pois}(n_c|\nu_c(\alpha)) \prod_{e=1}^{n_c} f_c(x_{ce}|\alpha) \right]. \quad (4)$$

A. Parametrization of the model

The parameter of interest is the overall signal strength factor μ , which acts as a scale factor to the total rate of signal events. This global factor is used for all pairings of production cross sections and branching ratios. The signal strength is defined such that $\mu = 0$ corresponds to the background-only model and $\mu = 1$ corresponds to the SM Higgs boson signal. It is convenient to separate the full list of parameters α into the parameter of interest μ , the Higgs boson mass m_H , and the nuisance parameters θ , i.e. $\alpha = (\mu, m_H, \theta)$.

Each channel in the combined model uses either the reconstructed transverse mass or the invariant mass of the Higgs candidate as a discriminating variable. Two approaches are adopted to model the signal pdfs at intermediate values of m_H where full simulation has not been performed. The first, used in the $H \rightarrow \gamma\gamma$ channel, is based on a continuous parametrization of the signal as a function of m_H using an analytical expression for the pdf validated with simulated Monte Carlo (MC) samples. The second, used in channels where pdfs are modeled with histograms, is based on an interpolation procedure using the algorithm of Ref. [24].

B. Auxiliary measurements

The nuisance parameters represent uncertain aspects of the model, such as the background normalization, reconstruction efficiencies, energy scale and resolution, luminosity, and theoretical predictions. These nuisance parameters are often estimated from auxiliary measurements, such as control regions, sidebands, or dedicated calibration measurements. A detailed account of these measurements is beyond the scope of this paper and is given in the references for the individual channels [16–23].

Each parameter α_p with a dedicated auxiliary measurement $f_{\text{aux}}(\mathcal{D}_{\text{aux}}|\alpha_p, \boldsymbol{\alpha}_{\text{other}})$ provides a maximum likelihood estimate for α_p , a_p , and a standard error σ_p . Thus, the detailed probability model for an auxiliary measurement is approximated as

$$f_{\text{aux}}(\mathcal{D}_{\text{aux}}|\alpha_p, \boldsymbol{\alpha}_{\text{other}}) \rightarrow f_p(a_p|\alpha_p, \sigma_p). \quad (5)$$

The $f_p(a_p|\alpha_p, \sigma_p)$ are referred to as constraint terms.

The fully frequentist procedure applied for the present analysis includes randomizing the a_p when constructing the ensemble of possible experiment outcomes. In the hybrid frequentist-Bayesian procedures used at LEP and the Tevatron, the a_p are held constant and the nuisance parameters α_p are randomized according to the prior probability density

$$\pi(\alpha_p|a_p) \propto f(a_p|\alpha_p, \sigma_p)\eta(\alpha_p), \quad (6)$$

where $\eta(\alpha_p)$ is an original prior, usually taken to be constant.

The set of nuisance parameters constrained by auxiliary measurements is denoted \mathbb{S} and the set of estimates of those parameters, also referred to as global observables, which augments \mathcal{D}_{com} , is denoted $\mathcal{G} = \{a_p\}$ with $p \in \mathbb{S}$. Including the constraint terms explicitly, the model can be rewritten as

$$f_{\text{tot}}(\mathcal{D}_{\text{com}}, \mathcal{G}|\boldsymbol{\alpha}) = \prod_{c=1}^{c_{\text{max}}} \left[\text{Pois}(n_c|\nu_c(\boldsymbol{\alpha})) \prod_{e=1}^{n_c} f_c(x_{ce}|\boldsymbol{\alpha}) \right] \cdot \prod_{p \in \mathbb{S}} f_p(a_p|\alpha_p, \sigma_p). \quad (7)$$

The use of a Gaussian constraint term $f_p(a_p|\alpha_p, \sigma_p) = \text{Gauss}(a_p|\alpha_p, \sigma_p)$ is problematic if the parameter is intrinsically non-negative, as is the case for event yields and energy scale uncertainties. This is particularly important when the relative uncertainty is large. An alternative constraint term defined only for positive parameter values is the log-normal distribution, which is given by

$$f_p(a_p|\alpha_p) = \frac{1}{\sqrt{2\pi \ln \kappa}} \frac{1}{a_p} \exp\left[-\frac{(\ln(a_p/\alpha_p))^2}{2(\ln \kappa)^2}\right]. \quad (8)$$

The conventional choice $\kappa = 1 + \sigma_{\text{rel}}$ is made, where σ_{rel} is the relative uncertainty σ_p/a_p from the observed auxiliary measurement [25].

Using the log-normal distribution for a_p is equivalent to having a Gaussian constraint for the transformed parameter $a'_p = \ln a_p$ and $\alpha'_p = \ln \alpha_p$.

For channels that use histograms based on simulated MC samples, the parametric pdf $f(x|\boldsymbol{\alpha})$ is formed by interpolating between histogram variations evaluated at $\alpha_p = a_p \pm \sigma_p$. Since the variations need not be symmetric, the function is treated in a piecewise way using a sixth-order polynomial to interpolate in the range $\alpha_p \in [a_p - \sigma_p, a_p + \sigma_p]$ with coefficients chosen to match the first and second derivatives [26]. Henceforth, the prime will be suppressed and α_p will refer to the transformed nuisance parameter.

Not all systematic uncertainties have an associated auxiliary measurement. For example, uncertainties associated with the choice of renormalization and factorization scales and missing higher-order corrections in a theoretical calculation are not statistical in nature. In these cases, the frequentist form of the constraint term is derived assuming, by convention, a log-normal prior probability density on these parameters and inverting Eq. (6).

III. INDIVIDUAL SEARCH CHANNELS

All the channels combined to search for the SM Higgs boson use the complete 2011 data set passing the relevant quality requirements. The Higgs boson decays considered are $H \rightarrow \gamma\gamma$, $H \rightarrow WW^{(*)}$, $H \rightarrow ZZ^{(*)}$, $H \rightarrow \tau^+\tau^-$, and $H \rightarrow b\bar{b}$. In modes with a W or Z boson, an electron or muon is required for triggering. In the $H \rightarrow \tau^+\tau^-$ channel, almost all combinations of subsequent τ decays are considered. The results in the $\gamma\gamma$ and $\ell^+\ell^-\ell^+\ell^-$ modes are the same as in the previously published combination [14], but all other channels have been updated. A summary of the individual channels contributing to this combination is given in Table I.

The invariant and transverse mass distributions for the individual channels are shown in Figs. 1 and 2, with several subchannels merged.

- (1) $H \rightarrow \gamma\gamma$: This analysis is unchanged with respect to the previous combined search [14,16] and is carried out for m_H hypotheses between 110 GeV and

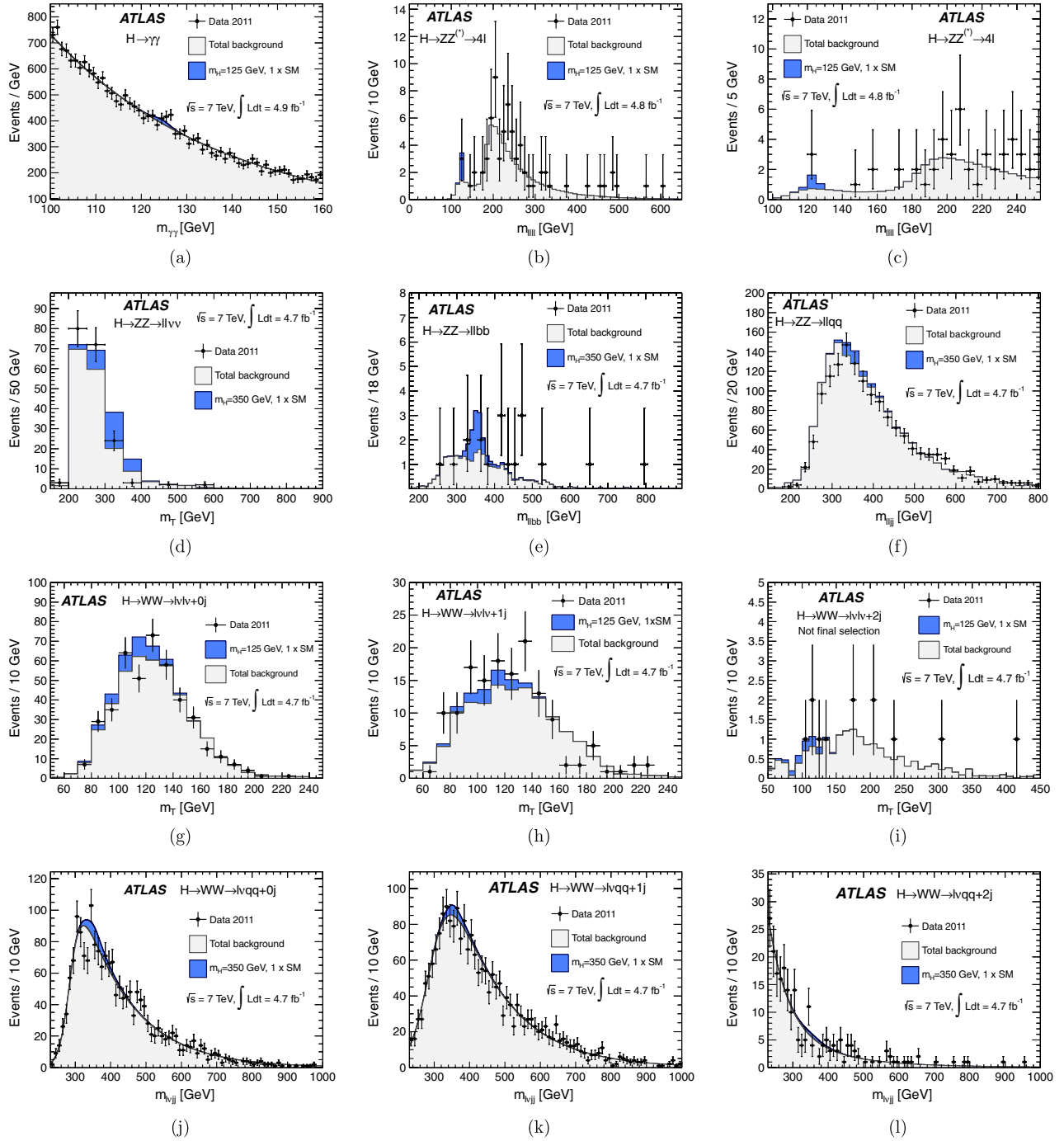


FIG. 1 (color online). Invariant or transverse mass distributions for the selected candidate events, the total background and the signal expected in the following channels: (a) $H \rightarrow \gamma\gamma$, (b) $H \rightarrow ZZ^{(*)} \rightarrow \ell^+\ell^-\ell^+\ell^-$ in the entire mass range, (c) $H \rightarrow ZZ^{(*)} \rightarrow \ell^+\ell^-\ell^+\ell^-$ in the low mass range, (d) $H \rightarrow ZZ \rightarrow \ell^+\ell^-\nu\bar{\nu}$, (e) b -tagged selection and (f) *untagged* selection for $H \rightarrow ZZ \rightarrow \ell^+\ell^-q\bar{q}$, (g) $H \rightarrow WW^{(*)} \rightarrow \ell^+\nu\ell^-\bar{\nu} + 0$ -jet, (h) $H \rightarrow WW^{(*)} \rightarrow \ell^+\nu\ell^-\bar{\nu} + 1$ -jet, (i) $H \rightarrow WW^{(*)} \rightarrow \ell^+\nu\ell^-\bar{\nu} + 2$ -jet, (j) $H \rightarrow WW \rightarrow \ell\nu q\bar{q}' + 0$ -jet, (k) $H \rightarrow WW \rightarrow \ell\nu q\bar{q}' + 1$ -jet, and (l) $H \rightarrow WW \rightarrow \ell\nu q\bar{q}' + 2$ -jet. The $H \rightarrow WW^{(*)} \rightarrow \ell^+\nu\ell^-\bar{\nu} + 2$ -jet distribution is shown before the final selection requirements are applied.

150 GeV. Events are separated into nine independent categories of varying sensitivity. The categorization is based on the pseudorapidity of each photon, whether it was reconstructed as a converted

or unconverted photon, and the momentum component of the diphoton system transverse to the diphoton thrust axis ($p_{T\perp}$). The mass resolution is approximately 1.7% for $m_H \sim 120$ GeV.

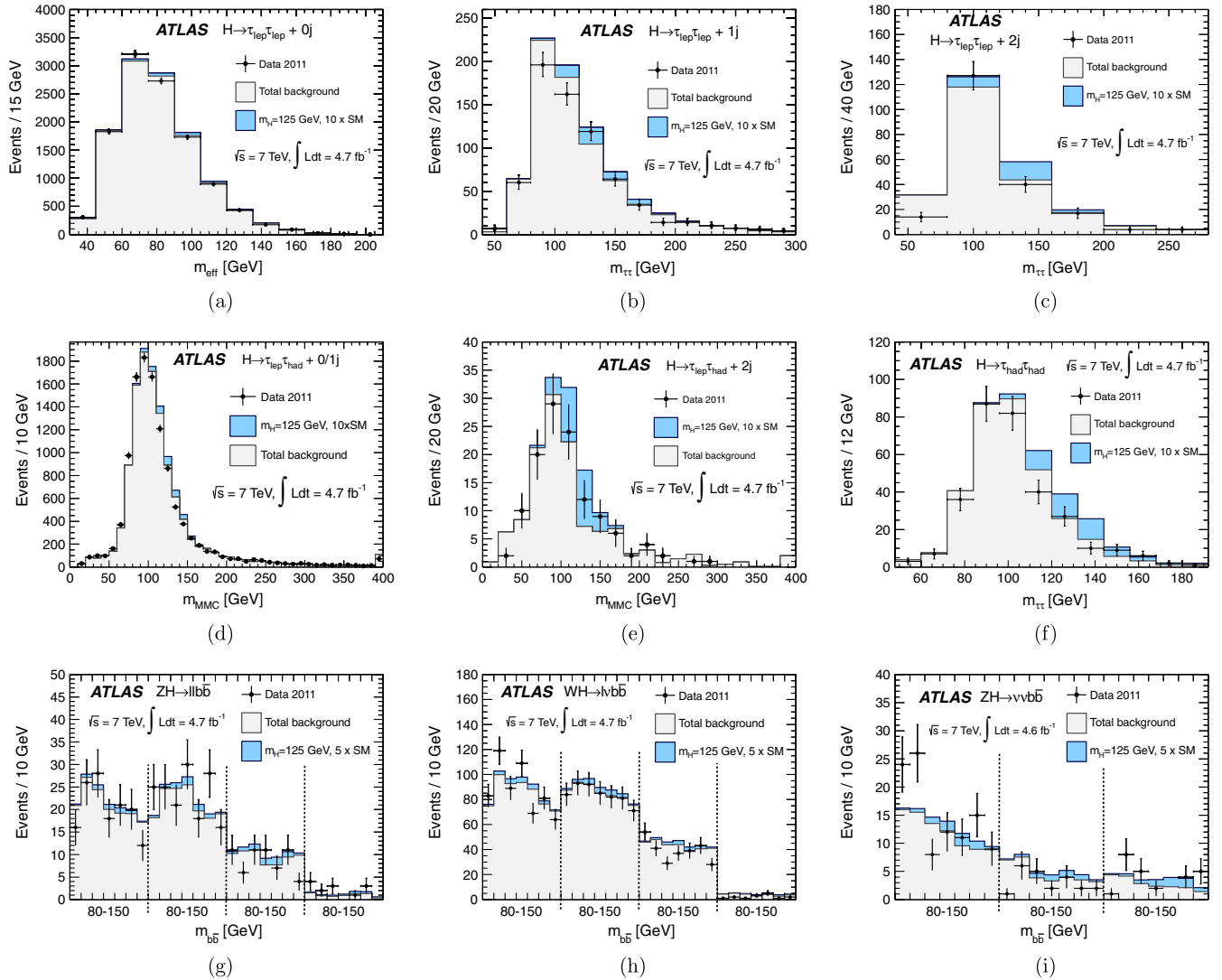


FIG. 2 (color online). Invariant or transverse mass distributions for the selected candidate events, the total background and the signal expected in the following channels: (a) $H \rightarrow \tau_{\text{lep}}\tau_{\text{lep}} + 0\text{-jet}$, (b) $H \rightarrow \tau_{\text{lep}}\tau_{\text{lep}} + 1\text{-jet}$, (c) $H \rightarrow \tau_{\text{lep}}\tau_{\text{lep}} + 2\text{-jet}$, (d) $H \rightarrow \tau_{\text{lep}}\tau_{\text{had}} + 0/1\text{-jet}$, (e) $H \rightarrow \tau_{\text{lep}}\tau_{\text{had}} + 2\text{-jet}$, and (f) $H \rightarrow \tau_{\text{had}}\tau_{\text{had}}$. The $b\bar{b}$ invariant mass for (g) the $ZH \rightarrow \ell^+\ell^-b\bar{b}$, (h) the $WH \rightarrow \ell\nu b\bar{b}$, and (i) the $ZH \rightarrow \nu\bar{\nu}b\bar{b}$ channels. The vertical dashed lines illustrate the separation between the mass spectra of the subcategories in p_T^Z , p_T^W , and E_T^{miss} , respectively. The signal distributions are lightly shaded where they have been scaled by a factor of 5 or 10 for illustration purposes.

- (2) $H \rightarrow ZZ^{(*)}$: In the $ZZ^{(*)}$ decay mode at least one Z is required to decay to charged leptons, while the other decays to either leptons, neutrinos, or jets.
- (i) $H \rightarrow ZZ^{(*)} \rightarrow \ell^+\ell^-\ell^+\ell^-$: This analysis, described in Ref. [17], is performed for m_H hypotheses in the 110 GeV to 600 GeV mass range and is unchanged with respect to the previous combined search [14]. The main irreducible $ZZ^{(*)}$ background is estimated using a combination of Monte Carlo simulation and the observed data. The reducible $Z + \text{jets}$ background, which mostly impacts the low four-lepton invariant mass region, is estimated from control regions in the data. The top-quark ($t\bar{t}$) background normalization is validated using a dedicated control

sample. Four categories of events are defined by the lepton flavor combinations and the four-lepton invariant mass is used as a discriminating variable. The mass resolution is approximately 1.5% in the four-muon channel and 2% in the four-electron channel for $m_H \sim 120$ GeV.

- (ii) $H \rightarrow ZZ \rightarrow \ell^+\ell^-\nu\bar{\nu}$: This analysis [18] is split into two regimes according to the level of pileup, i.e. the average number of pp collisions per bunch crossing. The first 2.3 fb^{-1} of data had an average of about six pileup collisions per event and the subsequent 2.4 fb^{-1} had an average of about 12. The search is performed for m_H hypotheses ranging from 200 GeV to 600 GeV. The analysis is further

categorized by the flavor of the leptons from the Z decay. The selection is optimized separately for Higgs boson masses above and below 280 GeV. The $\ell^+\ell^-$ invariant mass is required to be within 15 GeV of the Z boson mass. The inverted requirement is applied to same-flavor leptons in the $H \rightarrow WW^{(*)} \rightarrow \ell^+\nu\ell^-\bar{\nu}$ channel to avoid overlap in the selection. The transverse mass (m_T), computed from the dilepton transverse momentum and the missing transverse momentum, is used as a discriminating variable.

- (iii) $H \rightarrow ZZ \rightarrow \ell^+\ell^-q\bar{q}$: This search is performed for m_H hypotheses ranging from 200 GeV to 600 GeV and is separated into search regions above and below $m_H = 300$ GeV, for which the event selections are independently optimized. The dominant background arises from $Z + \text{jets}$ production, which is estimated using sidebands of the dijet invariant mass distribution in data. To profit from the relatively large rate of b -jets from Z boson decays present in the signal compared to the rate of b -jets found in the $Z + \text{jets}$ background, the analysis is divided into two categories. The first category contains events in which the two jets are b -tagged and the second uses events with less than two b -tags. The analysis [19] takes advantage of a highly efficient b -tagging algorithm [27] and the sideband to constrain the background yield. Using the Z boson mass constraint improves the mass resolution of the $\ell^+\ell^-q\bar{q}$ system by more than a factor of 2. The invariant mass of the $\ell^+\ell^-q\bar{q}$ system is used as a discriminating variable.
- (3) $H \rightarrow WW^{(*)}$: Two sets of channels are devoted to the decay of the Higgs boson into a pair of W bosons, namely, the $\ell^+\nu\ell^-\bar{\nu}$ and $\ell\nu q\bar{q}'$ channels.
- (i) $H \rightarrow WW^{(*)} \rightarrow \ell^+\nu\ell^-\bar{\nu}$: The updated analysis [20] is performed for m_H values from 110 GeV up to 600 GeV. Events with two leptons are classified by the number of associated jets (0, 1 or 2), where the 2-jet category has selection criteria designed to enhance sensitivity to the VBF production process. The events are further divided by the flavors of the charged leptons, ee , $e\mu$, and $\mu\mu$, where the mixed mode ($e\mu$) has a much smaller background from the Drell-Yan process. As in the case of $H \rightarrow ZZ \rightarrow \ell^+\ell^-\nu\bar{\nu}$, the samples are split according to the pileup conditions and analyzed separately. Each subchannel uses the WW transverse mass distribution, except for the 2-jet category, which does not use a discriminating variable.
- (ii) $H \rightarrow WW \rightarrow \ell\nu q\bar{q}'$: This analysis is performed for m_H hypotheses ranging from 300 GeV to 600 GeV. A leptonically decaying W boson is tagged with an isolated lepton and missing transverse momentum (E_T^{miss}). Additionally, two jets with an invariant mass compatible with a second W boson [21] are required. The W boson mass constraint allows the reconstruction of the Higgs boson candidate mass on an event-by-event basis by using a quadratic equation to solve for the component of the neutrino momentum along the beam axis. Events where this equation has imaginary solutions are discarded in order to reduce tails in the mass distribution. The analysis searches for a peak in the reconstructed $\ell\nu q\bar{q}'$ mass distribution. The background is modeled with a smooth function. The analysis is further divided by lepton flavor and by the number of additional jets (0, 1 or 2), where the 2-jet channel is optimized for the VBF production process.
- (4) $H \rightarrow \tau^+\tau^-$: The analyses [22] are categorized by the decay modes of the two τ leptons, for m_H hypotheses ranging from 110 GeV to 150 GeV (the leptonically decaying τ leptons are denoted τ_{lep} and the hadronically decaying τ leptons are denoted τ_{had}). Most of these subchannels are triggered using leptons, except for the fully hadronic channel $H \rightarrow \tau_{\text{had}}\tau_{\text{had}}$, which is triggered with specific double hadronic τ decay selections. All the searches using τ decay modes have a significant background from $Z \rightarrow \tau^+\tau^-$ decays, which are modeled using an embedding technique where $Z \rightarrow \mu^+\mu^-$ candidates selected in the data have the muons replaced by simulated τ decays [22]. These embedded events are used to describe this background process.
- (i) $H \rightarrow \tau_{\text{lep}}\tau_{\text{lep}}$: In this channel events are separately analyzed in four disjoint categories based on the number of reconstructed jets in the event [22]. There are two categories specifically aimed towards the gluon fusion production process, with or without a jet, one for the VBF production process and one for the Higgs boson production in association with a hadronically decaying vector boson. Each jet category requires at least one jet with p_T above 40 GeV. The collinear approximation [28] is used to reconstruct the $\tau\tau$ invariant mass, which is used as the discriminating variable. All three combinations of e and μ are used, except in the 0-jet category, which uses only the $e\mu$ candidate events where the effective mass is used as a discriminating variable.
- (ii) $H \rightarrow \tau_{\text{lep}}\tau_{\text{had}}$: There are seven separate categories in this subchannel. The selection of VBF-like events requires two jets with oppositely signed pseudorapidities η , $|\Delta\eta_{jj}| > 3.0$ and a dijet invariant mass larger than 300 GeV, in which events with electrons and muons are combined due to the limited number of candidates. In the other subchannels, electron and muon final states are considered separately. The remaining candidate events are categorized according to the number of jets with transverse momenta in

excess of 25 GeV, the 0-jet category being further subdivided based on whether the E_T^{miss} exceeds 20 GeV or not. The missing mass calculator (MMC) technique [29] is used to estimate the $\tau\tau$ invariant mass, which is used as a discriminating variable.

- (iii) $H + \text{jet} \rightarrow \tau_{\text{had}}\tau_{\text{had}} + \text{jet}$: Events are triggered using a selection of two hadronically decaying τ leptons with transverse energy thresholds varying according to the running conditions [22]. Two oppositely charged hadronically decaying τ candidates are required along with one jet with transverse momentum larger than 40 GeV, $E_T^{\text{miss}} > 20$ GeV, and a reconstructed invariant mass of the two τ leptons and the jet greater than 225 GeV. In addition to the Z background there is a significant multijet background which is estimated using data-driven methods. The $\tau\tau$ invariant mass is estimated via the collinear approximation and is used as a discriminating variable after further selections on the momentum fractions carried away by visible τ decay products.
- (5) $H \rightarrow b\bar{b}$: The $ZH \rightarrow \ell^+\ell^-b\bar{b}$, $ZH \rightarrow \nu\bar{\nu}b\bar{b}$, and $WH \rightarrow \ell\nu b\bar{b}$ analyses [23] are performed for m_H ranging from 110 GeV to 130 GeV. All three analyses require two b -tagged jets (one with $p_T > 45$ GeV and the other with $p_T > 25$ GeV) and the invariant mass of the two b -jets, m_{bb} , is used as a discriminating variable. The $ZH \rightarrow \ell^+\ell^-b\bar{b}$ analysis requires a dilepton invariant mass in the range $83 \text{ GeV} < m_{\ell\ell} < 99 \text{ GeV}$ and $E_T^{\text{miss}} < 50 \text{ GeV}$ to suppress the $t\bar{t}$ background. The $WH \rightarrow \ell\nu b\bar{b}$ analysis requires $E_T^{\text{miss}} > 25 \text{ GeV}$, the transverse mass of the lepton- E_T^{miss} system to be in excess of 40 GeV, and no additional leptons with $p_T > 20 \text{ GeV}$. The $ZH \rightarrow \nu\bar{\nu}b\bar{b}$ analysis requires $E_T^{\text{miss}} > 120 \text{ GeV}$, as well as $p_T^{\text{miss}} > 30 \text{ GeV}$, where p_T^{miss} is the missing transverse momentum determined from the tracks associated with the primary vertex. To increase the sensitivity of the search, the m_{bb} distribution is examined in subchannels with different signal-to-background ratios. In the searches with one or two charged leptons, the division is made according to four bins in transverse momentum p_T^V of the reconstructed vector boson V : $p_T^V < 50 \text{ GeV}$, $50 \text{ GeV} \leq p_T^V < 100 \text{ GeV}$, $100 \text{ GeV} \leq p_T^V < 200 \text{ GeV}$, and $p_T^V \geq 200 \text{ GeV}$. In the $ZH \rightarrow \nu\bar{\nu}b\bar{b}$ search the E_T^{miss} is used to define three subchannels corresponding to $120 \text{ GeV} < E_T^{\text{miss}} < 160 \text{ GeV}$, $160 \text{ GeV} \leq E_T^{\text{miss}} < 200 \text{ GeV}$, and $E_T^{\text{miss}} \geq 200 \text{ GeV}$. No categorization is made based on lepton flavor.

IV. SYSTEMATIC UNCERTAINTIES

The sources of systematic uncertainties and their effects on the signal and background rates $\nu_k(\alpha)$ and discriminating variable distributions $f_k(x|\alpha)$ are described in detail for

each channel in Refs. [16–23]. The sources of systematic uncertainty are decomposed into uncorrelated components, such that the constraint terms factorize as in Eq. (7). The main focus of the combination of channels is the correlated effect of given sources of uncertainties across channels. Typically, the correlated effects arise from the ingredients common to several channels, for example the simulation, the lepton and photon identification, and the integrated luminosity. The sources of systematic uncertainty affecting the signal model are frequently different from those affecting the backgrounds, which are often estimated from control regions in the data. The dominant uncertainties giving rise to correlated effects are those associated with theoretical predictions for the signal production cross sections and decay branching fractions, as well as those related to detector response affecting the reconstruction of electrons, photons, muons, jets, E_T^{miss} , and b -tagging. The log-normal constraint terms are used for uncertainties in the signal and background normalizations, while Gaussian constraints are used for uncertainties affecting the shapes of the pdfs.

A. Theoretical uncertainties affecting the signal

The Higgs boson production cross sections are computed up to next-to-next-to-leading order (NNLO) [30–35] in QCD for the gluon fusion ($gg \rightarrow H$) process, including soft-gluon resummation up to next-to-next-to-leading log (NNLL) [36] and next-to-leading-order (NLO) electroweak corrections [37,38]. These predictions are compiled in Refs. [39–41]. The cross section for the VBF process is estimated at NLO [42–44] and approximate NNLO QCD [45]. The cross sections for the associated production processes ($q\bar{q} \rightarrow WH/ZH$) are computed at NLO [46,47], NNLO [48] QCD, and NLO electroweak [47]. The cross sections for the associated production with a $t\bar{t}$ pair ($q\bar{q}/gg \rightarrow t\bar{t}H$) are estimated at NLO [49–53]. The Higgs boson production cross sections and decay branching ratios [54–58], as well as their related uncertainties, are compiled in Ref. [59]. The QCD scale uncertainties for $m_H = 120 \text{ GeV}$ amount to $^{+12}_{-8}\%$ for the $gg \rightarrow H$ process, $\pm 1\%$ for the $q\bar{q}' \rightarrow qq'H$ and associated WH/ZH processes, and $^{+3}_{-9}\%$ for the $q\bar{q}/gg \rightarrow t\bar{t}H$ process. The uncertainties related to the parton distribution functions (PDF) amount to $\pm 8\%$ for the predominantly gluon-initiated processes $gg \rightarrow H$ and $gg \rightarrow t\bar{t}H$, and $\pm 4\%$ for the predominantly quark-initiated processes $q\bar{q}' \rightarrow qq'H$ and WH/ZH [60]. The theoretical uncertainty associated with the exclusive Higgs boson production process with one additional jet in the $H \rightarrow WW^{(*)} \rightarrow \ell^+\nu\ell^-\bar{\nu}$ channel amounts to $\pm 20\%$ and is treated according to the prescription of Refs. [25,61]. An additional theoretical uncertainty on the signal normalization, to account for effects related to off-shell Higgs boson production and interference with other SM processes, is assigned at high Higgs boson masses ($m_H > 300 \text{ GeV}$) and estimated as $\pm 150\% \times (m_H/\text{TeV})^3$ [61–64].

B. Theoretical uncertainties affecting the background

In the $H \rightarrow \gamma\gamma$ and $H \rightarrow WW \rightarrow \ell\nu q\bar{q}'$ channels the backgrounds are estimated from a fit to the data. This removes almost all sensitivity to the corresponding theoretical uncertainties. In the case of the $H \rightarrow \gamma\gamma$ analysis an additional uncertainty is assigned to take into account possible inadequacies of the analytical background model chosen. Theoretical uncertainties enter in all other channels where theoretical calculations are used for background estimates. In particular, both signal and background processes are sensitive to the parton distribution functions, the underlying event simulation, and the parton shower model.

The $ZZ^{(*)}$ continuum process is the main background for the $H \rightarrow ZZ^{(*)} \rightarrow \ell^+\ell^-\ell^+\ell^-$ and $H \rightarrow ZZ \rightarrow \ell^+\ell^-\nu\bar{\nu}$ analyses and is also part of the backgrounds in the $H \rightarrow ZZ \rightarrow \ell^+\ell^-q\bar{q}$ channel. A NLO prediction [65] is used for the normalization. The QCD scale uncertainty has a $\pm 5\%$ effect on the expected $ZZ^{(*)}$ background, and the effects due to the PDF and α_s uncertainties are $\pm 4\%$ and $\pm 8\%$ for quark-initiated and gluon-initiated processes, respectively. An additional theoretical uncertainty of $\pm 10\%$ on the inclusive $ZZ^{(*)}$ cross section is conservatively included due to the missing higher-order QCD corrections for the gluon-initiated process. This theoretical uncertainty is treated as uncorrelated for the different channels due to the different acceptance in the $H \rightarrow ZZ^{(*)} \rightarrow \ell^+\ell^-\ell^+\ell^-$ and $H \rightarrow ZZ \rightarrow \ell^+\ell^-\nu\bar{\nu}$ channels and because its contribution to the $H \rightarrow ZZ \rightarrow \ell^+\ell^-q\bar{q}$ channel is small.

In most other channels the overall normalization of the main backgrounds is not estimated from theoretical predictions; however, simulations are used to model the pdfs $f(x|\alpha)$ or the scale factors used to extrapolate from the control regions to the signal regions. For example, in the $H \rightarrow WW^{(*)} \rightarrow \ell^+\nu\ell^-\bar{\nu}$ channel the main backgrounds are continuum $WW^{(*)}$ and $t\bar{t}$ production. Their normalizations are estimated in control regions; however, the factors used to extrapolate to the signal region are estimated with the NLO simulation [66].

C. Experimental uncertainties

The uncertainty on the integrated luminosity is considered as being fully correlated among channels and amounts to $\pm 3.9\%$ [67,68].

The detector-related sources of systematic uncertainty can affect various aspects of the analysis: (a) the overall normalization of the signal or background, (b) the migration of events between categories, and (c) the shape of the discriminating variable distributions $f(x|\alpha)$. Similarly to the theoretical uncertainties, experimental uncertainties on the event yields (a) are treated using a log-normal $f_p(a_p|\alpha_p)$ constraint pdf. In cases (b) and (c) a Gaussian constraint is applied.

The experimental sources of systematic uncertainty are modeled using the classification detailed below. Their

effect on the signal and background yields in each channel is reported separately in Table II. The various sources of systematic uncertainty have in some cases been grouped for a concise presentation (e.g. the jet energy scale and b -tagging efficiencies), while the full statistical model of the data provides a more detailed account of the various systematic effects including the effect on the pdfs $f(x|\alpha)$. The assumptions made in the treatment of systematics are outlined below.

- (i) The uncertainties in the trigger and identification efficiencies are treated as fully correlated for electrons and photons. The energy scale and resolution for photons and electrons are treated as uncorrelated sources of uncertainty.
- (ii) The uncertainties affecting muons are separated into those related to the inner detector (ID) and the muon spectrometer (MS) in order to provide a better description of the correlated effect among channels using different muon identification criteria and different ranges of muon transverse momenta.
- (iii) The jet energy scale (JES) and jet energy resolution (JER) are sensitive to a number of uncertain quantities, which depend on p_T , η , and flavor of the jet. Measurements of the JES and JER result in complicated correlations among these components. Building a complete model of the response to these correlated sources of uncertainty is intricate. Here, a simplified scheme is used in which independent JES and JER nuisance parameters are associated to channels with significantly different kinematic requirements and scattering processes with different kinematic distributions or flavor composition. This scheme includes a specific treatment for b -jets. The sensitivity of the results to various assumptions in the correlation between these sources of uncertainty has been found to be negligible. Furthermore, an additional component to the uncertainty in E_T^{miss} , which is uncorrelated with the JES uncertainty, is included.
- (iv) While the τ energy scale uncertainty is expected to be partially correlated with the JES, here it is treated as an uncorrelated source of uncertainty. This choice is based on the largely degenerate effect due to the uncertainty associated with the embedding procedure, in which the simulated detector response to hadronic τ decays is merged with a sample of $Z \rightarrow \mu^+\mu^-$ data events. Furthermore, the uncertainty of this embedding procedure is treated separately for signal and background processes, which is a conservative approach given that the $Z \rightarrow \tau^+\tau^-$ sideband effectively constrains this nuisance parameter.
- (v) The b -tagging systematic uncertainty is decomposed into five fundamental sources in the $H \rightarrow b\bar{b}$ channels, while a simplified model with a single source is

TABLE II. A summary of the main correlated experimental systematic uncertainties. The uncorrelated systematic uncertainties are summarized in a single combined number. The uncertainties indicate the $\pm 1\sigma$ relative variation in the signal and background yields in (%). The signal corresponds to a Higgs boson mass hypothesis of 125 GeV except for $H \rightarrow ZZ \rightarrow \ell^+ \ell^- q\bar{q}$, $H \rightarrow ZZ \rightarrow \ell^+ \ell^- \nu\bar{\nu}$, and $H \rightarrow WW \rightarrow \ell\nu q\bar{q}'$, which are quoted at 350 GeV.

	$H \rightarrow ZZ^{(*)}$			$H \rightarrow WW^{(*)}$			$H \rightarrow \tau^+ \tau^-$			$H \rightarrow b\bar{b}$	
	$H \rightarrow \gamma\gamma$	$\ell\ell\ell\ell$	$\ell\ell\nu\nu$	$\ell\ell q\bar{q}$	$\ell\nu\ell\nu$	$\ell\nu q\bar{q}$	$\tau_{\text{lep}}\tau_{\text{had}}$	$\tau_{\text{lep}}\tau_{\text{lep}}$	$\tau_{\text{had}}\tau_{\text{had}}$	ZH	WH
Relative uncertainty on signal yields											
Luminosity	± 3.9	± 3.9	± 3.9	± 3.9	± 3.9	± 3.9	± 3.9	± 3.9	± 3.9	± 3.9	± 3.9
e/γ efficiency	$^{+13.5}_{-11.9}$	± 3.2	± 1.3	...	± 1.5	± 0.9	± 2.9	± 2.0	...	± 1.2	...
e/γ energy scale	± 0.4	...	± 0.7	...	$^{+1.4}_{+0.3}$	± 0.3	...	$^{+0.3}_{-0.4}$	± 0.2
e/γ resolution	± 0.1	...	± 0.1	$^{+0.2}_{-0.5}$	$^{+0.2}_{-0.1}$
μ efficiency	...	± 0.2	± 0.4	...	± 0.1	± 0.3	± 1.0	± 2.0	...	± 0.4	...
μ resolution (ID)	± 0.1	...	± 0.1	$^{+0.2}_{-0.5}$...	± 0.1	...
μ resolution (MS)	± 0.1	...	± 0.1	$^{+0.2}_{-0.1}$...
Jet/ $E_{\text{T}}^{\text{miss}}$ energy scale	± 2.5	$^{+3.5}_{-3.4}$	$^{+2.2}_{-3.4}$	$^{+7.6}_{-7.0}$	$^{+1.3}_{-1.8}$	± 0.9	$^{+13.7}_{-16.5}$	$^{+4.1}_{-5.0}$	$^{+2.7}_{-5.1}$
Jet energy resolution	± 1.1	± 4.2	± 1.1	$^{+8.4}_{-7.8}$...	± 0.3	± 2.4	± 2.9	± 2.6
b -tag efficiency	± 0.9	± 0.02	± 0.02	$^{+6.1}_{-5.7}$	± 9.5	± 9.4
τ efficiency	± 4.2	...	± 8.0
Uncorrelated uncertainties	± 0.2	± 5.0	$^{+7.8}_{-7.2}$	$^{+12.0}_{-10.7}$	± 3.4	± 1.5	...	$^{+1.1}_{-2.0}$	$^{+3.7}_{-4.2}$	± 1.7	± 2.8
Relative uncertainty on background yields											
Luminosity	...	$^{+3.7}_{-3.5}$	$^{+2.8}_{-2.7}$	± 0.2	± 0.5	...	$^{+2.7}_{-2.6}$	$^{+3.5}_{-3.4}$
e/γ efficiency	...	± 1.8	± 0.9	...	± 1.4	± 0.9	± 2.0	$^{+0.5}_{-1.4}$
e/γ energy scale	$^{+3.1}_{-2.2}$...	$^{+0.5}_{-0.4}$...	$^{+0.8}_{-0.5}$	± 0.7	...	± 0.1	± 0.3
e/γ resolution	$^{+1.1}_{-0.8}$...	± 0.2	$^{+1.6}_{-1.7}$...	$^{+0.6}_{-0.2}$	± 0.1
μ efficiency	...	± 0.1	± 0.3	...	± 0.12	± 0.3	± 0.7	$^{+0.5}_{-1.5}$
μ resolution (ID)	± 0.2	...	± 0.2	$^{+1.6}_{-1.8}$...	± 0.1	...
μ resolution (MS)	± 0.2	...	± 0.2	± 0.1	...
Jet/ $E_{\text{T}}^{\text{miss}}$ energy scale	$^{+6.1}_{-4.6}$	± 0.4	$^{+4.0}_{-5.6}$	$^{+0.5}_{-0.0}$	$^{+2.2}_{-1.6}$
Jet energy resolution	± 1.7	± 0.1	± 1.2	± 0.3	± 0.9
b -tag efficiency	$^{+5.2}_{-4.4}$...	$^{+1.4}_{-1.1}$	± 0.1	...	± 1	± 1
τ efficiency	± 3.0
Uncorrelated uncertainties	...	± 10.0	± 4.9	$^{+2.3}_{-2.1}$	± 12.0	...	± 10.2	$^{+5.5}_{-6.3}$	± 10.3	± 5.5	$^{+2.8}_{-2.9}$

used in the $H \rightarrow ZZ \rightarrow \ell^+ \ell^- q\bar{q}$ channel. The uncertainty in the b -veto is considered uncorrelated with the uncertainty in the b -tagging efficiency.

The effect of these systematic uncertainties depends on the final state, but is typically small compared to the theoretical uncertainty of the production cross section.

The electron and muon energy scales are directly constrained by $Z \rightarrow e^+ e^-$ and $Z \rightarrow \mu^+ \mu^-$ events; the impact of the resulting systematic uncertainty on the four-lepton invariant mass is of the order of $\pm 0.5\%$ for electrons and negligible for muons. The impact of the photon energy scale systematic uncertainty on the diphoton invariant mass is approximately $\pm 0.6\%$.

D. Background measurement uncertainty

The estimates of background normalizations and model parameters from control regions or sidebands are the

main remaining sources of uncertainty. Because of the differences in control regions these uncertainties are not correlated across channels.

In the case of the $H \rightarrow b\bar{b}$ channels the background normalizations are constrained both from sideband fits and from auxiliary measurements based on the MC prediction of the main background processes ($Z + \text{jets}$, $W + \text{jets}$ and $t\bar{t}$).

The uncorrelated sources of systematic uncertainties are summarized as a single combined number in Table II for each channel.

E. Summary of the combined model

To cover the search range efficiently between $m_H = 110$ GeV and $m_H = 600$ GeV, the signal and backgrounds are modeled and the combination performed in m_H steps that reflect the interplay between the invariant mass resolution and the natural width of the Higgs boson. In the low

TABLE III. Step sizes in Higgs boson mass hypotheses at which the signal and backgrounds are modeled.

m_H (GeV)	Step size
110–120	1 GeV
120–130	0.5 GeV
130–150	1 GeV
150–290	2 GeV
290–350	5 GeV
350–400	10 GeV
400–600	20 GeV

mass range, where the high mass-resolution $H \rightarrow \gamma\gamma$ and $H \rightarrow ZZ^{(*)} \rightarrow \ell^+\ell^-\ell^+\ell^-$ channels dominate, the signal is modeled in steps from 500 MeV to 2 GeV. For higher masses the combination is performed with step sizes ranging from 2 GeV to 20 GeV. The m_H step sizes are given in Table III.

The combined model and statistical procedure are implemented within the ROOFIT, HISTFACTORY, and ROOSTATS software framework [26,69,70]. As shown in Table I, the number of channels included in the combination depends on the hypothesized value of m_H . The details for the number of channels, nuisance parameters, and constraint terms for various m_H ranges are shown in Table IV. For $m_H = 125$ GeV there are 70 channels included in the combined statistical model and the associated data set is comprised of more than 22 000 unbinned events and 8000 bins. For $m_H = 350$ GeV there are 46 channels included in the combined statistical model and the associated data set is comprised only of binned distributions, for which there are more than 4000 bins. Because of the limited size of the MC samples, additional nuisance parameters and constraint terms are included in the model to account for the statistical uncertainty in the MC templates. The difference between the number of nuisance parameters and the number of constraints reported in Table IV corresponds to the number of nuisance parameters without external constraints, which are estimated in data control regions or sidebands.

TABLE IV. Details of the combined model for different m_H ranges. The table shows the number of channels, nuisance parameters associated with systematic uncertainties, number of constraint terms, and number of additional nuisance parameters and constraints associated to limited MC sample sizes.

m_H (GeV)	Channels	Nuisance	Constraints	MC stat
110–130	70	287	159	180
131–150	67	210	119	140
152–198	46	83	80	78
200–278	52	199	119	120
280–295	52	208	118	119
300	58	281	120	121
305–400	46	269	111	112
420–480	46	238	111	112
500–600	46	201	111	112

V. STATISTICAL PROCEDURES

The procedures for computing frequentist p -values used for quantifying the agreement of the data with the background-only hypothesis and for determining exclusion limits are based on the profile likelihood ratio test statistic.

For a given data set \mathcal{D}_{com} and values for the global observables \mathcal{G} there is an associated likelihood function of μ and θ derived from the combined model over all channels including all constraint terms in Eq. (7),

$$L(\mu, \theta; m_H, \mathcal{D}_{\text{com}}, \mathcal{G}) = f_{\text{tot}}(\mathcal{D}_{\text{com}}, \mathcal{G} | \mu, m_H, \theta). \quad (9)$$

The notation $L(\mu, \theta)$ leaves the dependence on the data implicit.

A. The test statistics and estimators of μ and θ

The statistics used to test different values of the strength parameter μ are defined in terms of a likelihood function $L(\mu, \theta)$. The maximum likelihood estimates $\hat{\mu}$ and $\hat{\theta}$ are the values of the parameters that maximize the likelihood function $L(\mu, \theta)$. The conditional maximum likelihood estimate $\hat{\theta}(\mu)$ is the value of θ that maximizes the likelihood function with μ fixed. The tests are based on the profile likelihood ratio $\lambda(\mu)$, which reflects the level of compatibility between the data and μ . It is defined as

$$\lambda(\mu) = \frac{L(\mu, \hat{\theta}(\mu))}{L(\hat{\mu}, \hat{\theta})}. \quad (10)$$

Physically, the rate of signal events is non-negative; thus, $\mu \geq 0$. However, it is convenient to define the estimator $\hat{\mu}$ as the value of μ that maximizes the likelihood, even if it is negative [as long as the pdf $f_c(x_c | \mu, \theta) \geq 0$ everywhere]. In particular, $\hat{\mu} < 0$ indicates a deficit of events with respect to the background in the signal region. Following Ref. [71] a treatment equivalent to requiring $\mu \geq 0$ is to allow $\mu < 0$ and impose the constraint in the test statistic itself, i.e.

$$\tilde{\lambda}(\mu) = \begin{cases} \frac{L(\mu, \hat{\theta}(\mu))}{L(\hat{\mu}, \hat{\theta})} & \hat{\mu} \geq 0, \\ \frac{L(\mu, \hat{\theta}(\mu))}{L(0, \hat{\theta}(0))} & \hat{\mu} < 0. \end{cases} \quad (11)$$

To quantify the significance of an excess, the test statistic \tilde{q}_0 is used to test the background-only hypothesis $\mu = 0$ against the alternative hypothesis $\mu > 0$. It is defined as

$$\tilde{q}_0 = \begin{cases} -2 \ln \lambda(0) & \hat{\mu} > 0, \\ +2 \ln \lambda(0) & \hat{\mu} \leq 0. \end{cases} \quad (12)$$

Instead of defining the test statistic to be identically zero for $\hat{\mu} \leq 0$ as in Ref. [71], this sign change is introduced in order to probe p -values larger than 50%.

For setting an upper limit on μ , the test statistic \tilde{q}_μ is used to test the hypothesis of signal events being produced at a rate μ against the alternative hypothesis of signal events being produced at a lesser rate $\mu' < \mu$:

$$\tilde{q}_\mu = \begin{cases} -2 \ln \tilde{\lambda}(\mu) & \hat{\mu} \leq \mu, \\ +2 \ln \tilde{\lambda}(\mu) & \hat{\mu} > \mu. \end{cases} \quad (13)$$

Again, a sign change is introduced in order to probe p -values larger than 50%. The test statistic $-2 \ln \lambda(\mu)$ is used to differentiate signal events being produced at a rate μ from the alternative hypothesis of signal events being produced at a different rate $\mu' \neq \mu$.

Tests of μ are carried out with the Higgs mass m_H fixed to a particular value, and the entire procedure is repeated for values of m_H spaced in small steps.

B. The distribution of the test statistic and p -values

When calculating upper limits, a range of values of μ is explored using the test statistic \tilde{q}_μ . The value of the test statistic for the observed data is denoted $\tilde{q}_{\mu, \text{obs}}$. One can construct the distribution of \tilde{q}_μ assuming a different value of the signal strength μ' , which is denoted

$$f(\tilde{q}_\mu | \mu', m_H, \boldsymbol{\theta}). \quad (14)$$

The distribution depends explicitly on m_H and $\boldsymbol{\theta}$. The p -value is given by the tail probability of this distribution, and thus the p -value will also depend on m_H and $\boldsymbol{\theta}$. The reason for choosing the test statistic based on the profile likelihood ratio is that, with sufficiently large numbers of events, the distribution of the profile likelihood ratio with $\mu = \mu'$ is independent of the values of the nuisance parameters and, thus, also the associated p -values.

In practice, there is generally some residual dependence of the p -values on the value of $\boldsymbol{\theta}$. The values of the nuisance parameters that maximize the p -value are therefore sought. Following Refs. [25,72–75], the p -values for testing a particular value of μ are based on the distribution constructed at $\hat{\boldsymbol{\theta}}(\mu, \text{obs})$, the conditional maximum likelihood estimate with the observed data, as follows:

$$p_\mu = \int_{\tilde{q}_{\mu, \text{obs}}}^{\infty} f(\tilde{q}_\mu | \mu, m_H, \hat{\boldsymbol{\theta}}(\mu, \text{obs})) d\tilde{q}_\mu. \quad (15)$$

The ensemble includes randomizing both \mathcal{D} and \mathcal{G} .

Here the distribution of \tilde{q}_μ assumes that the data \mathcal{D} as well as the global observables \mathcal{G} are treated as measured quantities; i.e., they fluctuate upon repetition of the experiment according to the model $f_{\text{tot}}(\mathcal{D}_{\text{com}}, \mathcal{G} | \mu, m_H, \boldsymbol{\theta})$.

Upper limits for the strength parameter μ are calculated using the CL_s procedure [76]. To calculate this limit, the quantity CL_s is defined as the ratio

$$\text{CL}_s(\mu) = \frac{p_\mu}{1 - p_b}, \quad (16)$$

where p_b is the p -value derived from the same test statistic under the background-only hypothesis,

$$p_b = 1 - \int_{\tilde{q}_{\mu, \text{obs}}}^{\infty} f(\tilde{q}_\mu | 0, m_H, \hat{\boldsymbol{\theta}}(\mu = 0, \text{obs})) d\tilde{q}_\mu. \quad (17)$$

The CL_s upper limit on μ is denoted μ_{up} and obtained by solving for $\text{CL}_s(\mu_{\text{up}}) = 5\%$. A value of μ is regarded as excluded at the 95% confidence level if $\mu > \mu_{\text{up}}$.

The significance of an excess is based on the compatibility of the data with the background-only hypothesis. This compatibility is quantified by the following p -value:

$$p_0 = \int_{\tilde{q}_0, \text{obs}}^{\infty} f(\tilde{q}_0 | 0, m_H, \hat{\boldsymbol{\theta}}(\mu = 0, \text{obs})) d\tilde{q}_0. \quad (18)$$

Note that p_0 and p_b are both p -values of the background-only hypothesis, but the test statistic \tilde{q}_0 in Eq. (18) is optimized for discovery while the test statistic \tilde{q}_μ in Eq. (17) is optimized for upper limits.

It is customary to convert the background-only p -value into an equivalent Gaussian significance Z (often written $Z\sigma$). The conversion is defined as

$$Z = \Phi^{-1}(1 - p_0), \quad (19)$$

where Φ^{-1} is the inverse of the cumulative distribution for a standard Gaussian.

C. Experimental sensitivity and bands

It is useful to quantify the experimental sensitivity by means of the significance one would expect to find if a given signal hypothesis were true. Similarly, the expected upper limit is the median upper limit one would expect to find if the background-only hypothesis were true. Although these are useful quantities, they are subject to a certain degree of ambiguity because the median values depend on the assumed values of all of the parameters of the model, including the nuisance parameters.

Here, the expected upper limit is defined as the median of the distribution $f(\mu_{\text{up}} | 0, m_H, \hat{\boldsymbol{\theta}}(\mu = 0, \text{obs}))$ and the expected significance is based on the median of the distribution $f(p_0 | 1, m_H, \hat{\boldsymbol{\theta}}(\mu = 1, \text{obs}))$. The expected limit and significance thus have a small residual dependence on the observed data through $\hat{\boldsymbol{\theta}}(\mu, \text{obs})$.

These distributions are also used to define bands around the median upper limit. The standard presentation of upper limits includes the observed limit, the expected limit, and a $\pm 1\sigma$ and a $\pm 2\sigma$ band. More precisely, the edges of these bands, denoted $\mu_{\text{up}\pm 1}$ and $\mu_{\text{up}\pm 2}$, are defined by

$$\int_0^{\mu_{\text{up}\pm N}} f(\mu_{\text{up}} | 0, m_H, \hat{\boldsymbol{\theta}}(\mu = 0, \text{obs})) d\mu_{\text{up}} = \Phi(\pm N). \quad (20)$$

D. Asymptotic formalism

For large data samples, the asymptotic distributions $f(\tilde{q}_\mu | \mu', m_H, \boldsymbol{\theta})$ and $f(\tilde{q}_0 | \mu', m_H, \boldsymbol{\theta})$ are known and described in Ref. [71]. These formulas require the variance of the maximum likelihood estimate of μ , given μ' is the true value:

$$\sigma_{\mu'} = \sqrt{\text{var}[\hat{\mu}|\mu']}. \quad (21)$$

One result of Ref. [71] is that $\sigma_{\mu'}$ can be estimated with an artificial data set referred to as the *Asimov* data set. This data set is defined as a binned data set, where the number of events in bin b is exactly the number of events expected in bin b . The value of the test statistic evaluated on the Asimov data is denoted $\tilde{q}_{\mu, A_\alpha}$, where the subscript A_α denotes that this is the Asimov data set associated with α . A convenient way to estimate the variance of $\hat{\mu}$ is

$$\sigma_{\mu'} \approx \frac{\mu - \mu'}{\sqrt{\tilde{q}_{\mu, A_{\mu'}}}}. \quad (22)$$

In the asymptotic limit, \tilde{q}_μ is parabolic; thus $\sigma_{\mu'}$ is independent of μ . In Ref. [71], the bands around the expected limit are given by

$$\mu_{\text{up}+N} = \sigma(\Phi^{-1}(1 - 0.05\Phi(N)) + N). \quad (23)$$

An improved procedure is used here in order to capture the leading deviations of \tilde{q}_μ from a parabola, corresponding to departures in the distribution of $\hat{\mu}$ from a Gaussian distribution centered at μ' with variance $\sigma_{\mu'}^2$. The upper limit μ_{up} for an Asimov data set constructed with $\alpha_N = (\mu_N, m_H, \hat{\theta}(\mu_N, \text{obs}))$ (using the formulas in Ref. [71]) is found to be more accurate than Eq. (23) in reproducing the bands obtained with ensembles of pseudo-experiments, where μ_N is the value of μ corresponding to the edges of the $\mu_{\text{up}\pm N}$ band. The value of μ_N used for the $+N\sigma$ band is the value of μ that satisfies $\sqrt{\tilde{q}_{\mu_N, A_0}} = N$. The choice of $\hat{\theta}(\mu_N, \text{obs})$ is more indicative of $\hat{\theta}$ for the pseudoexperiments that have μ_{up} near the corresponding band.

E. Bayesian methods

A posterior distribution for the signal strength parameter μ can be obtained, via Bayes's theorem, with $f_{\text{tot}}(\mathcal{D}, \mathcal{G}|\alpha)$ and a prior $\eta(\alpha)$. The information about the nuisance parameters from auxiliary measurements is incorporated into $f_{\text{tot}}(\mathcal{D}, \mathcal{G}|\alpha)$ through the constraint terms $f_p(a_p|\alpha_p)$. As in Eq. (6), the prior on $\eta(\alpha_p)$ is taken as a uniform distribution. The upper limits are calculated for a given value of m_H , so no prior on m_H is needed. The prior on the signal strength parameter μ is taken to be uniform, as this choice leads to one-sided Bayesian credible intervals that correspond numerically to the CL_s upper limits in the frequentist formalism for the simple Gaussian and Poisson cases, and have been observed to coincide in more complex situations. The one-sided, 95% Bayesian credible region is defined as

$$\int_0^{\mu_{\text{up}}} f_{\text{tot}}(\mathcal{D}_{\text{sim}}, \mathcal{G}|\mu, m_H, \theta) \eta(\mu) \eta(\theta) d\mu d\theta = 0.95. \quad (24)$$

The integration over nuisance parameters is carried out with Markov chain Monte Carlo using the Metropolis-Hastings algorithm in the ROOSTATS package [26].

F. Correction for the look-elsewhere effect

By scanning over m_H and repeatedly testing the background-only hypothesis, the procedure is subject to effects of multiple testing referred to as the look-elsewhere effect. In principle, the confidence intervals can be constructed in the $\mu - m_H$ plane using the profile likelihood ratio $\lambda(\mu, m_H)$. For $\mu = 0$ there is no signal present; thus, the model is independent of m_H . This leads to a background-only distribution for $-2\ln\lambda(0, m_H)$ that departs from a chi-square distribution, thus complicating the calculation of a global p_0 when m_H is not specified. The global test statistic is the supremum of $q_0(m_H)$ with respect to m_H ,

$$q_0(\hat{m}_H) = \sup_{m_H} q_0(m_H). \quad (25)$$

In the asymptotic regime and for very small p -values, a procedure [77], based on the result of Ref. [78], exists to estimate the tail probability for $q_0(\hat{m}_H)$. The procedure requires an estimate for the average number of up-crossings of $q_0(m_H)$ above some threshold. Due to the m_H -dependence in the model, changes in cuts, and the list of channels included, it is technically difficult to estimate this quantity with ensembles of pseudoexperiments. Instead, a simple alternative method is used in which the average number of up-crossings is estimated by counting the number of up-crossings with the observed data. When the trials factor is large, the number of up-crossings at low thresholds is also large and thus a satisfactory estimate of the average [25]. This procedure has been checked using a large number of pseudoexperiments in a simplified test case, where it provided a good estimate of the trials factor.

VI. EXCLUSION LIMITS

The model discussed in Sec. II is used for all channels described in Sec. III and the systematic uncertainties summarized in Sec. IV. The statistical methods described in Sec. V are used to set limits on the signal strength as a function of m_H .

The expected and observed limits from the individual channels entering this combination are shown in Fig. 3. The combined 95% CL exclusion limits on μ are shown in Fig. 4 as a function of m_H . These results are based on the asymptotic approximation. The $\pm 1\sigma$ and $\pm 2\sigma$ variation bands around the median background expectation are calculated using the improved procedure described in Sec. VD, which yields slightly larger bands compared to those in Ref. [14]. Typically the increase in the bands is of the order of $\sim 5\%$ for the $\pm 1\sigma$ band and 10%–15% for the $\pm 2\sigma$ band. This procedure has been validated using ensemble tests and the Bayesian calculation of the exclusion

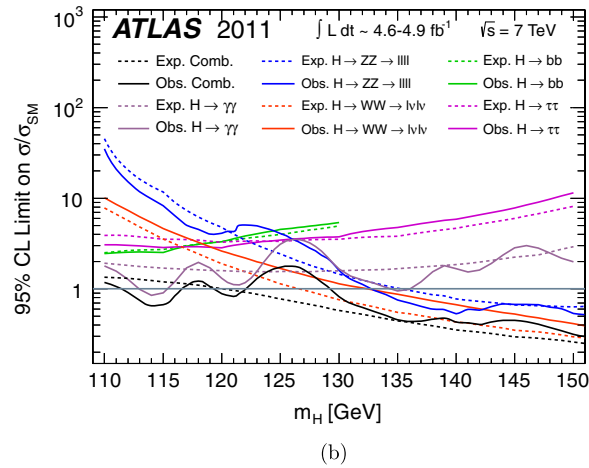
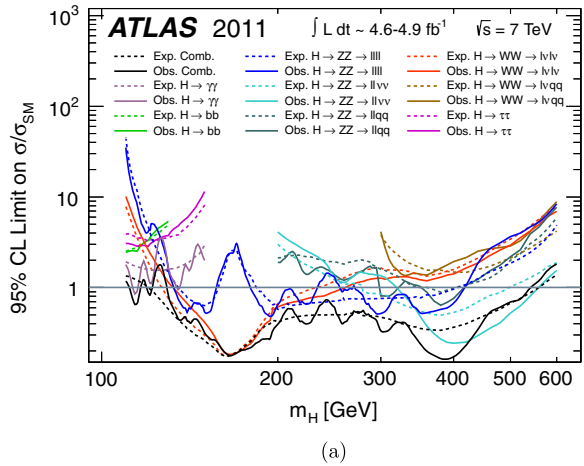


FIG. 3 (color online). The observed (solid lines) and expected (dashed lines) 95% CL cross section upper limits for the individual search channels and the combination, normalized to the SM Higgs boson production cross section, as a function of the Higgs boson mass, (a) for the full Higgs boson mass hypotheses range and (b) in the low mass range. The expected limits are those for the background-only hypothesis i.e. in the absence of a Higgs boson signal.

limits with a uniform prior on the signal strength described in Sec. VE. These approaches yield limits on μ which typically agree with the asymptotic results within a few percent.

The expected 95% CL exclusion region for the SM ($\mu = 1$) hypothesis covers the m_H range from 120 GeV to 560 GeV. The addition of the $H \rightarrow \tau^+ \tau^-$ and $H \rightarrow b\bar{b}$ channels, as well as the update of the $H \rightarrow WW^{(*)} \rightarrow \ell^+ \nu \ell^- \bar{\nu}$ channel, brings a significant gain in sensitivity in the low mass region with respect to the previous combined search. For Higgs boson mass hypotheses below approximately 122 GeV the dominant channel is $H \rightarrow \gamma\gamma$. For mass hypotheses larger than 122 GeV but smaller than 200 GeV the $H \rightarrow WW^{(*)} \rightarrow \ell^+ \nu \ell^- \bar{\nu}$ channel is the most sensitive. In the mass range between ~ 200 GeV and ~ 300 GeV the $H \rightarrow ZZ^{(*)} \rightarrow \ell^+ \ell^- \ell^+ \ell^-$ dominates. For

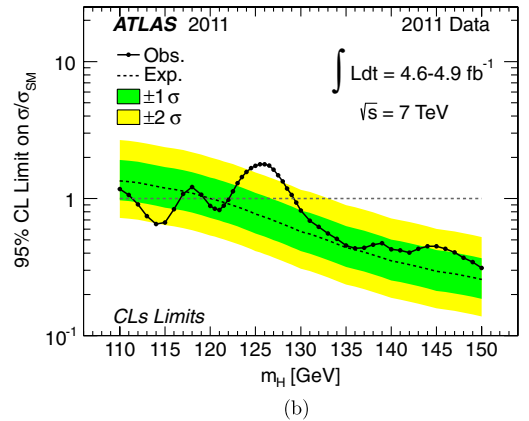
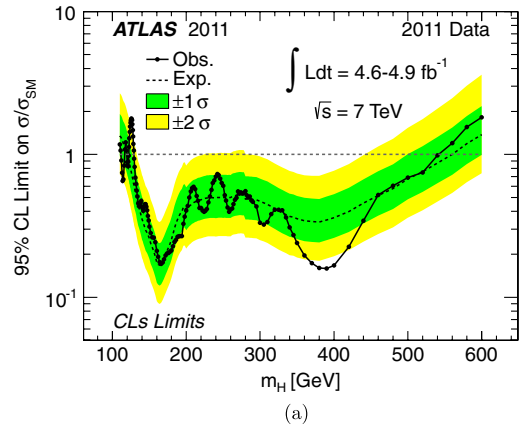


FIG. 4 (color online). The observed (solid line) and expected (dashed line) 95% CL combined upper limits on the SM Higgs boson production cross section divided by the SM expectation as a function of m_H , (a) in the full mass range considered in this analysis and (b) in the low mass range. The dotted curves show the median expected limit in the absence of a signal and the green and yellow bands indicate the corresponding $\pm 1\sigma$ and $\pm 2\sigma$ intervals.

higher mass hypotheses, the $H \rightarrow ZZ \rightarrow \ell^+ \ell^- \nu \bar{\nu}$ channel leads the search sensitivity. The updates of the $H \rightarrow WW^{(*)} \rightarrow \ell^+ \nu \ell^- \bar{\nu}$, $H \rightarrow WW \rightarrow \ell \nu q \bar{q}'$, $H \rightarrow ZZ \rightarrow \ell^+ \ell^- \nu \bar{\nu}$, and $H \rightarrow ZZ \rightarrow \ell^+ \ell^- q \bar{q}$ channels improve the sensitivity in the high mass region.

The observed exclusion regions range from 111.4 GeV to 116.6 GeV, from 119.4 GeV to 122.1 GeV, and from 129.2 GeV to 541 GeV at 95% CL under the SM ($\mu = 1$) hypothesis. The mass range 122.1 GeV to 129.2 GeV is not excluded due to the observation of an excess of events above the expected background. This excess and its significance are discussed in detail in Sec. VII.

Two mass regions where the observed exclusion is stronger than expected can be seen in Fig. 4. In the low mass range, Higgs mass hypotheses in the 111.4 GeV to 116.6 GeV range are excluded due mainly to a local deficit of events in the diphoton channel with respect to the expected background. A similar deficit is observed in the

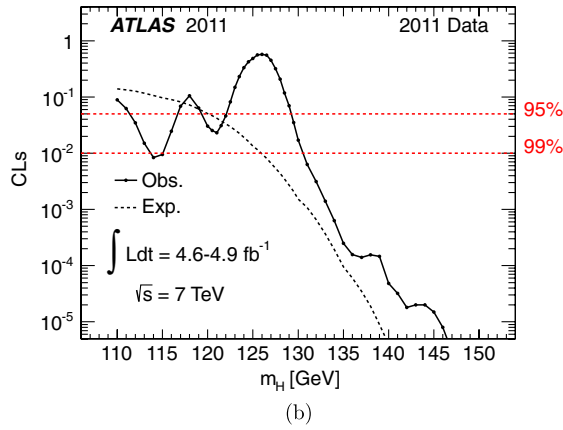
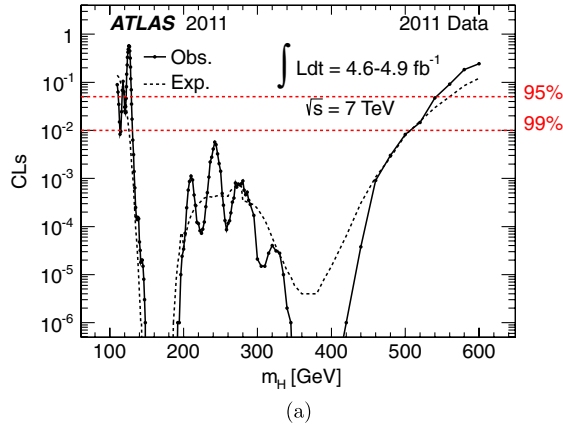


FIG. 5 (color online). The value of the combined CL_s for $\mu = 1$ (testing the SM Higgs boson hypothesis) as a function of m_H , (a) in the full mass range of this analysis and (b) in the low mass range. The regions with $CL_s < \alpha$ are excluded at the $(1 - \alpha)$ CL.

high mass region in the range 360 GeV to 420 GeV, resulting from deficits in the $H \rightarrow ZZ^{(*)} \rightarrow \ell^+ \ell^- \nu \bar{\nu}$ and $H \rightarrow ZZ \rightarrow \ell^+ \ell^- \nu \bar{\nu}$ channels. Both fluctuations correspond to approximately 2 standard deviations in the distribution of upper limits expected from background only.

A small mass region near $m_H \sim 245$ GeV was not excluded at the 95% CL in the combined search of Ref. [14], mainly due to a slight excess in the $H \rightarrow ZZ^{(*)} \rightarrow \ell^+ \ell^- \ell^+ \ell^-$ channel. This mass region is now excluded. The CL_s values for $\mu = 1$ as a function of the Higgs boson are shown in Fig. 5, where it can also be seen that the region between 130.7 GeV and 506 GeV is excluded at the 99% CL. The observed exclusion covers a large part of the expected exclusion range.

VII. SIGNIFICANCE OF THE EXCESS

The observed local p -values, calculated using the asymptotic approximation, as a function of m_H and the expected value in the presence of a SM Higgs boson signal at that mass are shown in Fig. 6 in the entire search mass

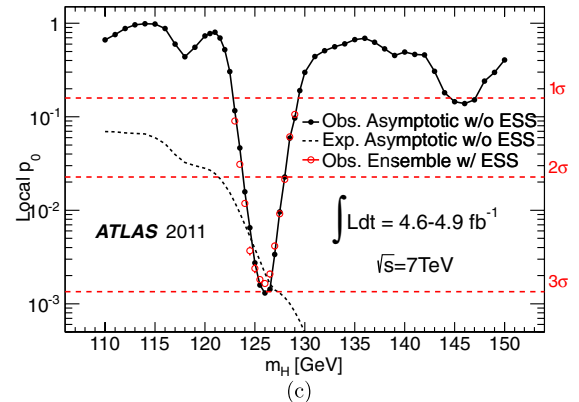
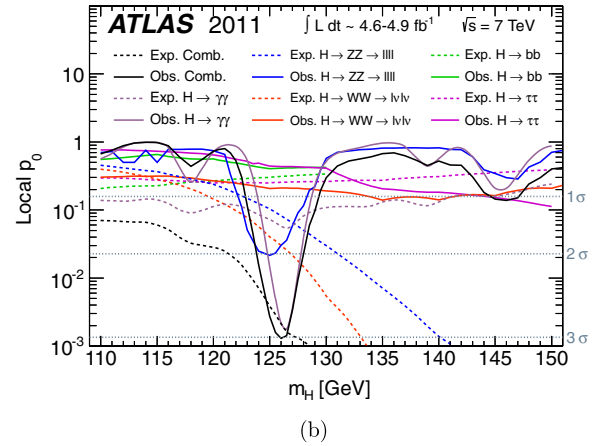
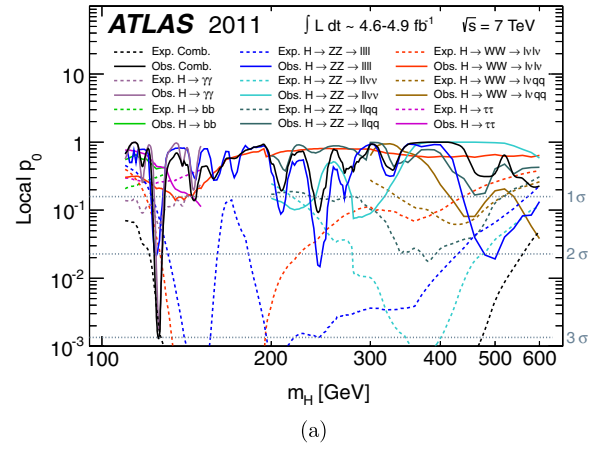


FIG. 6 (color online). The local probability p_0 for a background-only experiment to be more signal-like than the observation, for individual channels and the combination, (a) in the full mass range of 110–600 GeV and (b) in the low mass range of 110–150 GeV. The solid curves give the observed individual and combined p_0 . The dashed curves show the median expected value under the hypothesis of a SM Higgs boson signal at that mass. The combined observed local p_0 estimated using ensemble tests and taking into account energy scale systematic (ESS) uncertainties is illustrated in (c); the observed and expected combined results using asymptotic formulas are also shown. The horizontal dashed lines indicate the p_0 corresponding to significances of 1σ , 2σ , and 3σ for (a), (b), and (c).

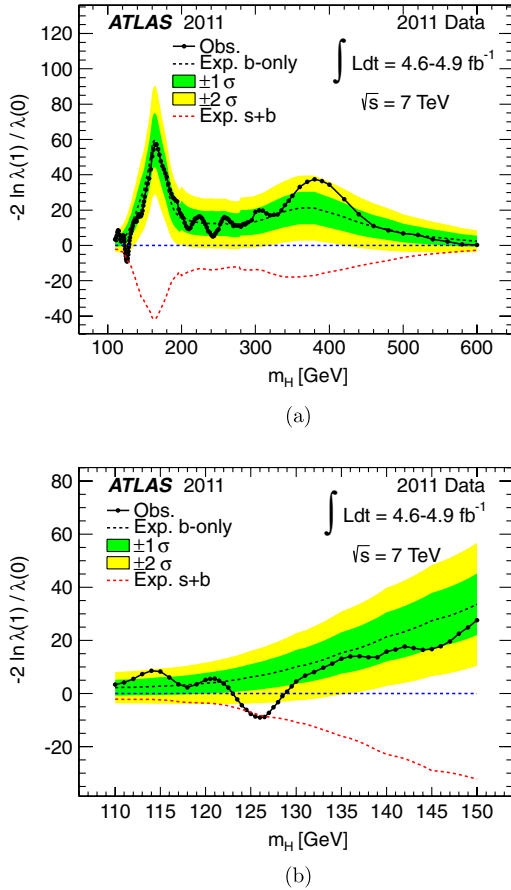


FIG. 7 (color online). The ratio of profile likelihoods for $\mu = 0$ and $\mu = 1$ as a function of the Higgs boson mass hypothesis. The solid line shows the observed ratio, the lower dashed line shows the median value expected under the signal-plus-background hypothesis, and the upper dashed line shows the median expected under the background-only hypothesis, (a) for the full mass range and (b) for the low mass range. The $\pm 1\sigma$ and $\pm 2\sigma$ intervals around the median background-only expectation are given by the green and yellow bands, respectively.

range and in the low mass range. The asymptotic approximation has been verified using ensemble tests which yield numerically consistent results.

The largest significance for the combination is observed for $m_H = 126$ GeV, where it reaches 3.0σ with an expected value in the presence of a signal at that mass of 2.9σ . The observed (expected) local significances for $m_H = 126$ GeV are 2.8σ (1.4σ) in the $H \rightarrow \gamma\gamma$ channel and 2.1σ (1.4σ) in the $H \rightarrow ZZ^{(*)} \rightarrow \ell^+\ell^-\ell^+\ell^-$ channel. In the $H \rightarrow WW^{(*)} \rightarrow \ell^+\nu\ell^-\bar{\nu}$ channel, which has been updated and includes additional data, the observed (expected) local significance for $m_H = 126$ GeV is 0.8σ (1.9σ); the observed significance was previously 1.4σ [14].

The significance of the excess is not very sensitive to energy scale and resolution systematic uncertainties for photons and electrons; however, the presence of these uncertainties leads to a small deviation from the

asymptotic approximation. The observed p_0 including these effects is therefore estimated using ensemble tests. The results are displayed in Fig. 6 as a function of m_H . The effect of the energy scale systematic uncertainties is an increase of approximately 30% of the corresponding local p_0 . The maximum local significance decreases slightly to 2.9σ . The muon momentum scale systematic uncertainties are smaller and therefore neglected.

The global p -values for the largest excess depend on the range of m_H and the channels considered. The global p_0 associated with a 2.8σ excess anywhere in the $H \rightarrow \gamma\gamma$ search domain of 110–150 GeV is approximately 7%. A 2.1σ excess anywhere in the $H \rightarrow ZZ^{(*)} \rightarrow \ell^+\ell^-\ell^+\ell^-$ search range of 110–600 GeV corresponds to a global p_0 of approximately 30%.

The global probability for a 2.9σ excess in the combined search to occur anywhere in the mass range 110–600 GeV is estimated to be approximately 15%, decreasing to 5%–7% in the range 110–146 GeV, which is not excluded at the 99% CL by the LHC combined SM Higgs boson search [62]. The data are observed to be consistent with the background-only hypothesis except for the region around

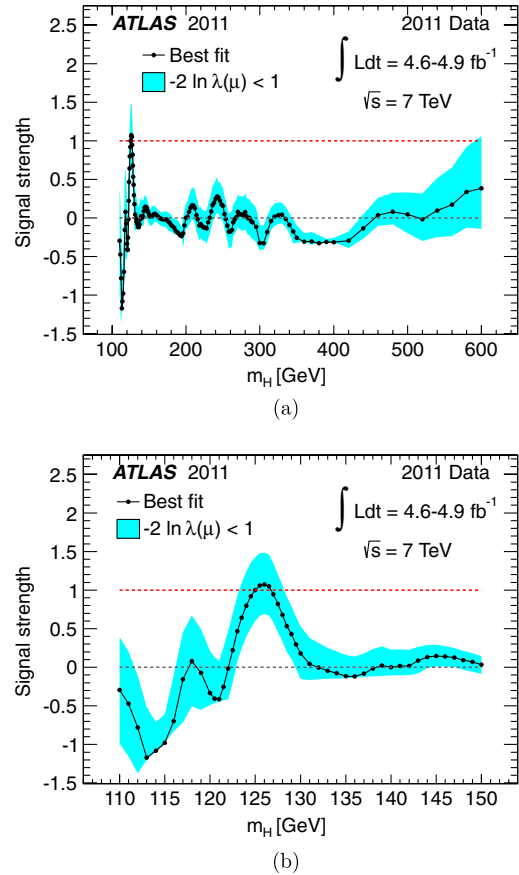


FIG. 8 (color online). The combined best-fit signal strength μ as a function of the Higgs boson mass hypothesis (a) in the full mass range of this analysis and (b) in the low mass range. The interval around $\hat{\mu}$ corresponds to a variation of $-2 \ln \lambda(\mu) < 1$.

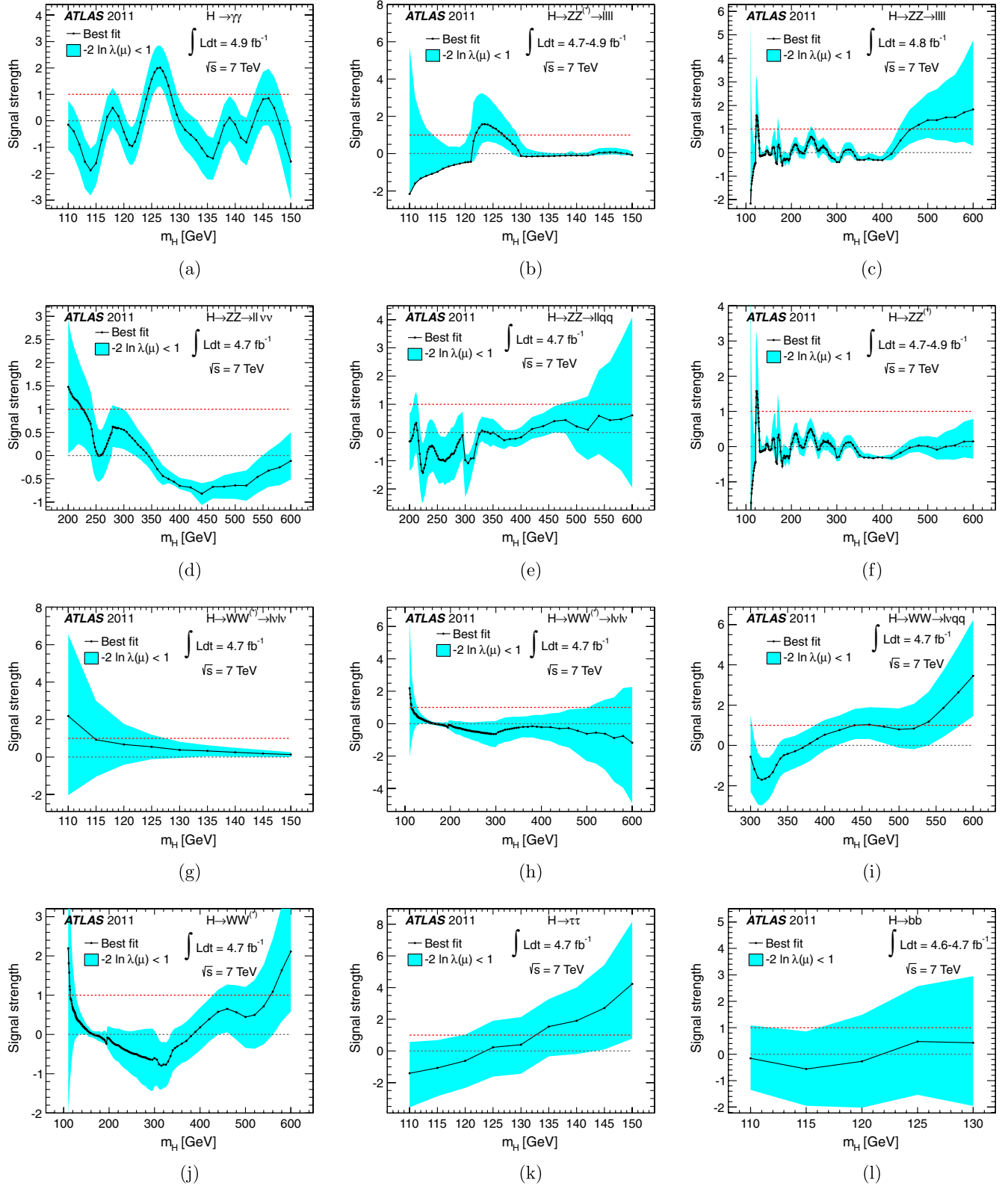


FIG. 9 (color online). The best-fit signal strength μ as a function of the Higgs boson mass hypothesis for the channels (a) $H \rightarrow \gamma\gamma$, (b) $H \rightarrow ZZ^{(*)} \rightarrow \ell^+\ell^-\ell^+\ell^-$ in the low mass region, (c) $H \rightarrow ZZ^{(*)} \rightarrow \ell^+\ell^-\ell^+\ell^-$ across the full search range, (d) $H \rightarrow ZZ \rightarrow \ell^+\ell^-\nu\nu$, (e) $H \rightarrow ZZ \rightarrow \ell^+\ell^-q\bar{q}$, (f) $H \rightarrow ZZ^{(*)}$ for all subchannels across the full search range, (g) $H \rightarrow WW^{(*)} \rightarrow \ell^+\nu\ell^-\bar{\nu}$ in the low mass region, (h) $H \rightarrow WW^{(*)} \rightarrow \ell^+\nu\ell^-\bar{\nu}$ across the full search range, (i) $H \rightarrow WW \rightarrow \ell\nu q\bar{q}'$, (j) $H \rightarrow WW^{(*)}$ for all subchannels in the full mass range, (k) $H \rightarrow \tau\tau$, and (l) $H \rightarrow b\bar{b}$. The band shows the interval around $\hat{\mu}$ corresponding to a variation of $-2 \ln \lambda(\mu) < 1$.

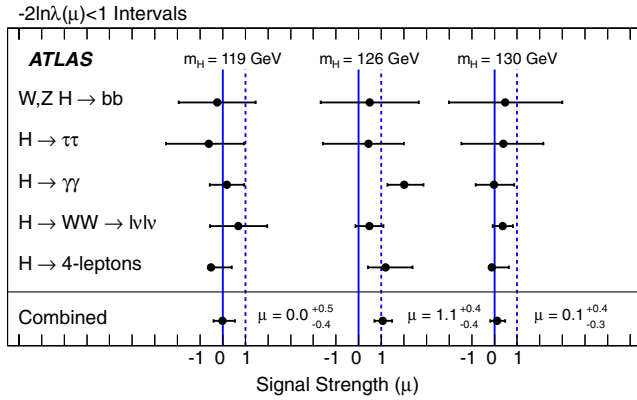


FIG. 10 (color online). Summary of the individual and combined best-fit values of the strength parameter for three sample Higgs boson mass hypotheses 119 GeV, 126 GeV (where the maximum observed significance is reached), and 130 GeV.

$m_H = 126$ GeV. The observed and expected ratio $-2\ln(\lambda(1)/\lambda(0))$ is shown in Fig. 7, which indicates a departure from the background-only hypothesis similar to the signal-plus-background expectation.

The best-fit value of μ , denoted $\hat{\mu}$, is displayed for the combination of all channels in Fig. 8 and for individual channels in Fig. 9 as a function of the m_H hypothesis. A summary of $-2\ln\lambda(\mu) < 1$ intervals at three specific Higgs boson mass hypotheses ($m_H = 119$ GeV, 126 GeV, and 130 GeV) for each Higgs decay mode and the combination is given in Fig. 10. The bands around $\hat{\mu}$ illustrate the μ interval corresponding to $-2\ln\lambda(\mu) < 1$ and represent an approximate $\pm 1\sigma$ variation. While the estimator $\hat{\mu}$ is allowed to be negative in Figs. 8 and 9 in order to illustrate the presence and extent of downward fluctuations, the μ parameter is bounded to ensure non-negative values of the probability density functions in the individual channels. Hence, for negative $\hat{\mu}$ values close to the boundary, the $-2\ln\lambda(\mu) < 1$ region does not reflect a calibrated 68% confidence interval. It should be noted that the $\hat{\mu}$ does not directly provide information on the relative strength of the production modes. The excess observed for $m_H = 126$ GeV corresponds to a $\hat{\mu}$ of 1.1 ± 0.4 , which is compatible with the signal strength expected from a SM Higgs boson at that mass ($\mu = 1$).

VIII. CONCLUSION

A combined search for the Standard Model Higgs boson has been performed with the ATLAS detector in the $\sqrt{s} = 7$ TeV pp collision data collected in 2011, corresponding to an integrated luminosity of 4.6–4.9 fb^{-1} . The channels used in this combination are $H \rightarrow \gamma\gamma$, $H \rightarrow b\bar{b}$, $H \rightarrow \tau^+\tau^-$, $H \rightarrow ZZ^{(*)} \rightarrow \ell^+\ell^-\ell^+\ell^-$, $H \rightarrow ZZ \rightarrow \ell^+\ell^-q\bar{q}$, $H \rightarrow ZZ \rightarrow \ell^+\ell^-\nu\bar{\nu}$, $H \rightarrow WW^{(*)} \rightarrow \ell^+\nu\ell^-\bar{\nu}$,

and $H \rightarrow WW \rightarrow \ell\nu q\bar{q}'$. The observed exclusion ranges at the 95% CL are 111.4 GeV to 116.6 GeV, 119.4 GeV to 122.1 GeV, and 129.2 GeV to 541 GeV, while Higgs boson masses between 120 GeV and 560 GeV are expected to be excluded at the 95% CL. The mass region between 130.7 GeV and 506 GeV is excluded at the 99% CL.

The local significance of the observed excess when all channels are combined is 2.9σ , in good agreement with the expected significance in the presence of a SM Higgs boson with $m_H = 126$ GeV of 2.9σ . An estimate of the global probability for such an excess to occur anywhere in the full explored Higgs boson mass region (from 110 GeV to 600 GeV) is approximately 15%. The global p_0 in the range not excluded at the 99% CL by the LHC combined Higgs boson search results [62] (from 110 GeV to 146 GeV) is approximately 5%–7%.

ACKNOWLEDGMENTS

We thank CERN for the very successful operation of the LHC, as well as the support staff from our institutions without whom ATLAS could not be operated efficiently. We acknowledge the support of ANPCyT, Argentina; YerPhI, Armenia; ARC, Australia; BMWF, Austria; ANAS, Azerbaijan; SSTC, Belarus; CNPq and FAPESP, Brazil; NSERC, NRC and CFI, Canada; CERN; CONICYT, Chile; CAS, MOST and NSFC, China; COLCIENCIAS, Colombia; MSMT CR, MPO CR and VSC CR, Czech Republic; DNRF, DNSRC and Lundbeck Foundation, Denmark; EPLANET and ERC, European Union; IN2P3-CNRS, CEA-DSM/IRFU, France; GNAS, Georgia; BMBF, DFG, HGF, MPG and AvH Foundation, Germany; GSRT, Greece; ISF, MINERVA, GIF, DIP and Benoziyo Center, Israel; INFN, Italy; MEXT and JSPS, Japan; CNRST, Morocco; FOM and NWO, Netherlands; RCN, Norway; MNiSW, Poland; GRICES and FCT, Portugal; MERYS (MECTS), Romania; MES of Russia and ROSATOM, Russian Federation; JINR; MSTD, Serbia; MSSR, Slovakia; ARRS and MVZT, Slovenia; DST/NRF, South Africa; MICINN, Spain; SRC and Wallenberg Foundation, Sweden; SER, SNSF and Cantons of Bern and Geneva, Switzerland; NSC, Taiwan; TAEK, Turkey; STFC, the Royal Society and Leverhulme Trust, United Kingdom; DOE and NSF, United States of America. The crucial computing support from all WLCG partners is acknowledged gratefully, in particular from CERN and the ATLAS Tier-1 facilities at TRIUMF (Canada), NDGF (Denmark, Norway, Sweden), CC-IN2P3 (France), KIT/GridKA (Germany), INFN-CNAF (Italy), NL-T1 (Netherlands), PIC (Spain), ASGC (Taiwan), RAL (UK) and BNL (USA) and in the Tier-2 facilities worldwide.

- [1] S. L. Glashow, *Nucl. Phys.* **22**, 579 (1961).
- [2] S. Weinberg, *Phys. Rev. Lett.* **19**, 1264 (1967).
- [3] A. Salam, in *Elementary Particle Theory* (Almqvist and Wiksell, Stockholm, 1968), p. 367.
- [4] F. Englert and R. Brout, *Phys. Rev. Lett.* **13**, 321 (1964).
- [5] P. W. Higgs, *Phys. Lett.* **12**, 132 (1964).
- [6] P. W. Higgs, *Phys. Rev. Lett.* **13**, 508 (1964).
- [7] G. Guralnik, C. Hagen, and T. Kibble, *Phys. Rev. Lett.* **13**, 585 (1964).
- [8] P. W. Higgs, *Phys. Rev.* **145**, 1156 (1966).
- [9] T. Kibble, *Phys. Rev.* **155**, 1554 (1967).
- [10] ALEPH Collaboration, DELPHI Collaboration, L3 Collaboration, OPAL Collaboration and The LEP Working Group for Higgs boson searches, *Phys. Lett. B* **565**, 61 (2003).
- [11] TEVNPH (Tevatron New Phenomena and Higgs Working Group), [arXiv:1107.5518](https://arxiv.org/abs/1107.5518).
- [12] ALEPH, CDF, D0, DELPHI, L3, OPAL, and SLD, LEP Electroweak Working Group, Tevatron Electroweak Working Group, SLD Electroweak and Heavy Flavour Groups Collaborations, [arXiv:1012.2367](https://arxiv.org/abs/1012.2367).
- [13] ATLAS Collaboration, *JINST* **3**, S08003 (2008).
- [14] ATLAS Collaboration, *Phys. Lett. B* **710**, 49 (2012).
- [15] CMS Collaboration, *Phys. Lett. B* **710**, 26 (2012).
- [16] ATLAS Collaboration, *Phys. Rev. Lett.* **108**, 111803 (2012).
- [17] ATLAS Collaboration, *Phys. Lett. B* **710**, 383 (2012).
- [18] ATLAS Collaboration, [arXiv:1205.6744](https://arxiv.org/abs/1205.6744).
- [19] ATLAS Collaboration, [arXiv:1206.2443](https://arxiv.org/abs/1206.2443).
- [20] ATLAS Collaboration, [arXiv:1206.0756](https://arxiv.org/abs/1206.0756).
- [21] ATLAS Collaboration, [arXiv:1206.6074](https://arxiv.org/abs/1206.6074).
- [22] ATLAS Collaboration, [arXiv:1206.5971](https://arxiv.org/abs/1206.5971).
- [23] ATLAS Collaboration, [arXiv:1207.0210](https://arxiv.org/abs/1207.0210).
- [24] A. L. Read, *Nucl. Instrum. Methods Phys. Res., Sect. A* **425**, 357 (1999).
- [25] ATLAS and CMS Collaborations, Report No. ATL-PHYS-PUB-2011-011, CERN-CMS-NOTE-2011-005, 2011.
- [26] L. Moneta, K. Belasco, K. S. Cranmer, S. Kreiss, A. Lazzaro *et al.*, Proc. Sci., ACAT2010 (2010) 057 [[arXiv:1009.1003](https://arxiv.org/abs/1009.1003)].
- [27] ATLAS Collaboration, Report No. ATLAS-CONF-2011-102, 2011, <https://cdsweb.cern.ch/record/1369219/>.
- [28] R. K. Ellis, I. Hinchliffe, M. Soldate, and J. van der Bij, *Nucl. Phys.* **B297**, 221 (1988).
- [29] A. Elagin, P. Murat, A. Pranko, and A. Safonov, *Nucl. Instrum. Methods Phys. Res., Sect. A* **654**, 481 (2011).
- [30] A. Djouadi, M. Spira, and P. M. Zerwas, *Phys. Lett. B* **264**, 440 (1991).
- [31] S. Dawson, *Nucl. Phys.* **B359**, 283 (1991).
- [32] M. Spira, A. Djouadi, D. Graudenz, and P. M. Zerwas, *Nucl. Phys.* **B453**, 17 (1995).
- [33] R. V. Harlander and W. B. Kilgore, *Phys. Rev. Lett.* **88**, 201801 (2002).
- [34] C. Anastasiou and K. Melnikov, *Nucl. Phys.* **B646**, 220 (2002).
- [35] V. Ravindran, J. Smith, and W. L. van Neerven, *Nucl. Phys.* **B665**, 325 (2003).
- [36] S. Catani, D. de Florian, M. Grazzini, and P. Nason, *J. High Energy Phys.* **07** (2003) 028.
- [37] U. Aglietti, R. Bonciani, G. Degrossi, and A. Vicini, *Phys. Lett. B* **595**, 432 (2004).
- [38] S. Actis, G. Passarino, C. Sturm, and S. Uccirati, *Phys. Lett. B* **670**, 12 (2008).
- [39] C. Anastasiou, R. Boughezal, and F. Petriello, *J. High Energy Phys.* **04** (2009) 003.
- [40] D. de Florian and M. Grazzini, *Phys. Lett. B* **674**, 291 (2009).
- [41] J. Baglio and A. Djouadi, *J. High Energy Phys.* **03** (2011) 055.
- [42] M. Ciccolini, A. Denner, and S. Dittmaier, *Phys. Rev. Lett.* **99**, 161803 (2007).
- [43] M. Ciccolini, A. Denner, and S. Dittmaier, *Phys. Rev. D* **77**, 013002 (2008).
- [44] K. Arnold *et al.*, *Comput. Phys. Commun.* **180**, 1661 (2009).
- [45] P. Bolzoni, F. Maltoni, S.-O. Moch, and M. Zaro, *Phys. Rev. Lett.* **105**, 011801 (2010).
- [46] T. Han and S. Willenbrock, *Phys. Lett. B* **273**, 167 (1991).
- [47] M. L. Ciccolini, S. Dittmaier, and M. Krämer, *Phys. Rev. D* **68**, 073003 (2003).
- [48] O. Brein, A. Djouadi, and R. Harlander, *Phys. Lett. B* **579**, 149 (2004).
- [49] W. Beenakker, S. Dittmaier, M. Krämer, B. Plümper, M. Spira, and P. M. Zerwas, *Phys. Rev. Lett.* **87**, 201805 (2001).
- [50] W. Beenakker, S. Dittmaier, M. Krämer, B. Plümper, M. Spira, and P. M. Zerwas, *Nucl. Phys.* **B653**, 151 (2003).
- [51] L. Reina and S. Dawson, *Phys. Rev. Lett.* **87**, 201804 (2001).
- [52] S. Dawson, L. H. Orr, L. Reina, and D. Wackerroth, *Phys. Rev. D* **67**, 071503 (2003).
- [53] S. Dawson, C. Jackson, L. Orr, L. Reina, and D. Wackerroth, *Phys. Rev. D* **68**, 034022 (2003).
- [54] A. Djouadi, J. Kalinowski, and M. Spira, *Comput. Phys. Commun.* **108**, 56 (1998).
- [55] A. Djouadi, J. Kalinowski, M. Mühlleitner, and M. Spira, [arXiv:1003.1643](https://arxiv.org/abs/1003.1643).
- [56] A. Bredenstein, A. Denner, S. Dittmaier, and M. M. Weber, *Phys. Rev. D* **74**, 013004 (2006).
- [57] A. Bredenstein, A. Denner, S. Dittmaier, and M. Weber, *J. High Energy Phys.* **02** (2007) 080.
- [58] S. Actis, G. Passarino, C. Sturm, and S. Uccirati, *Nucl. Phys.* **B811**, 182 (2009).
- [59] LHC Higgs Cross Section Working Group, edited by S. Dittmaier, C. Mariotti, G. Passarino, and R. Tanaka, Report No. CERN-2011-002, 2011.
- [60] M. Botje *et al.*, [arXiv:1101.0538](https://arxiv.org/abs/1101.0538).
- [61] S. Dittmaier, C. Mariotti, G. Passarino, R. Tanaka *et al.* (LHC Higgs Cross Section Working Group), [arXiv:1201.3084](https://arxiv.org/abs/1201.3084).
- [62] ATLAS and CMS Collaborations, Report No. ATLAS-CONF-2011-157, CMS-PAS-HIG-11-023, 2011, <https://cdsweb.cern.ch/record/1399599/>.
- [63] G. Passarino, C. Sturm, and S. Uccirati, *Nucl. Phys.* **B834**, 77 (2010).
- [64] C. Anastasiou, S. Buehler, F. Herzog, and A. Lazopoulos, *J. High Energy Phys.* **12** (2011) 058.
- [65] J. M. Campbell, R. K. Ellis, and C. Williams, *J. High Energy Phys.* **07** (2011) 018.
- [66] S. Frixione and B. Webber, *J. High Energy Phys.* **08** (2003) 007.
- [67] ATLAS Collaboration, *Eur. Phys. J. C* **71**, 1630 (2011).

- [68] ATLAS Collaboration, Report No. ATLAS-CONF-2011-116, 2011, <https://cdsweb.cern.ch/record/1376384>.
- [69] W. Verkerke and D. Kirkby, *Computing in High Energy and Nuclear Physics, 2003*, pp. 24–29 [[arXiv:physics/0306116](https://arxiv.org/abs/physics/0306116)].
- [70] K. Cranmer, G. Lewis, L. Moneta, A. Shibata, and W. Verkerke, Report No. CERN-OPEN-2012-016, 2012, <https://cdsweb.cern.ch/record/1456844>.
- [71] G. Cowan, K. Cranmer, E. Gross, and O. Vitells, *Eur. Phys. J. C* **71**, 1554 (2011).
- [72] K. Cranmer, PHYSTAT-LHC Workshop on Statistical Issues for LHC Physics, 2008, [oai:cds.cern.ch:1021125](https://cdsweb.cern.ch/record/1021125), <https://cdsweb.cern.ch/record/1021125>.
- [73] C. Chuang and T.L. Lai, *Statistica Sinica* **10**, 1 (2000).
- [74] B. Sen, M. Walker, and M. Woodroffe, *Statistica Sinica* **19**, 301 (2009).
- [75] ATLAS Collaboration, *Eur. Phys. J. C* **71**, 1728 (2011).
- [76] A.L. Read, *J. Phys. G* **28**, 2693 (2002).
- [77] E. Gross and O. Vitells, *Eur. Phys. J. C* **70**, 525 (2010).
- [78] R.B. Davies, *Biometrika* **74**, 33 (1987).

G. Aad,⁴⁷ T. Abajyan,²⁰ B. Abbott,¹¹⁰ J. Abdallah,¹¹ S. Abdel Khalek,¹¹⁴ A. A. Abdelalim,⁴⁸ O. Abdinov,¹⁰ R. Aben,¹⁰⁴ B. Abi,¹¹¹ M. Abolins,⁸⁷ O. S. AbouZeid,¹⁵⁷ H. Abramowicz,¹⁵² H. Abreu,¹³⁵ E. Acerbi,^{88a,88b} B. S. Acharya,^{163a,163b} L. Adamczyk,³⁷ D. L. Adams,²⁴ T. N. Addy,⁵⁵ J. Adelman,¹⁷⁵ S. Adomeit,⁹⁷ P. Adragna,⁷⁴ T. Adye,¹²⁸ S. Aefsky,²² J. A. Aguilar-Saavedra,^{123b,b} M. Agustoni,¹⁶ M. Aharrouche,⁸⁰ S. P. Ahlen,²¹ F. Ahles,⁴⁷ A. Ahmad,¹⁴⁷ M. Ahsan,⁴⁰ G. Aielli,^{132a,132b} T. Akdogan,^{19a} T. P. A. Åkesson,⁷⁸ G. Akimoto,¹⁵⁴ A. V. Akimov,⁹³ M. S. Alam,¹ M. A. Alam,⁷⁵ J. Albert,¹⁶⁸ S. Albrand,⁵⁴ M. Aleksa,²⁹ I. N. Aleksandrov,⁶³ F. Alessandria,^{88a} C. Alexa,^{25a} G. Alexander,¹⁵² G. Alexandre,⁴⁸ T. Alexopoulos,⁹ M. Alhroob,^{163a,163c} M. Aliev,¹⁵ G. Alimonti,^{88a} J. Alison,¹¹⁹ B. M. M. Allbrooke,¹⁷ P. P. Allport,⁷² S. E. Allwood-Spiers,⁵² J. Almond,⁸¹ A. Aloisio,^{101a,101b} R. Alon,¹⁷¹ A. Alonso,⁷⁸ F. Alonso,⁶⁹ B. Alvarez Gonzalez,⁸⁷ M. G. Alviggi,^{101a,101b} K. Amako,⁶⁴ C. Amelung,²² V. V. Ammosov,^{127,a} A. Amorim,^{123a,c} N. Amram,¹⁵² C. Anastopoulos,²⁹ L. S. Ancu,¹⁶ N. Andari,¹¹⁴ T. Andeen,³⁴ C. F. Anders,^{57b} G. Anders,^{57a} K. J. Anderson,³⁰ A. Andreazza,^{88a,88b} V. Andrei,^{57a} X. S. Anduaga,⁶⁹ P. Anger,⁴³ A. Angerami,³⁴ F. Anghinolfi,²⁹ A. Anisenkov,¹⁰⁶ N. Anjos,^{123a} A. Annovi,⁴⁶ A. Antonaki,⁸ M. Antonelli,⁴⁶ A. Antonov,⁹⁵ J. Antos,^{144b} F. Anulli,^{131a} M. Aoki,¹⁰⁰ S. Aoun,⁸² L. Aperio Bella,⁴ R. Apolle,^{117,d} G. Arabidze,⁸⁷ I. Aracena,¹⁴² Y. Arai,⁶⁴ A. T. H. Arce,⁴⁴ S. Arfaoui,¹⁴⁷ J-F. Arguin,¹⁴ E. Arik,^{18a,a} M. Arik,^{18a} A. J. Armbruster,⁸⁶ O. Arnaez,⁸⁰ V. Arnal,⁷⁹ C. Arnault,¹¹⁴ A. Artamonov,⁹⁴ G. Artoni,^{131a,131b} D. Arutinov,²⁰ S. Asai,¹⁵⁴ R. Asfandiyarov,¹⁷² S. Ask,²⁷ B. Åsman,^{145a,145b} L. Asquith,⁵ K. Assamagan,²⁴ A. Astbury,¹⁶⁸ B. Aubert,⁴ E. Auge,¹¹⁴ K. Augsten,¹²⁶ M. Auresseau,^{145a} G. Avolio,¹⁶² R. Avramidou,⁹ D. Axen,¹⁶⁷ G. Azuelos,^{92,e} Y. Azuma,¹⁵⁴ M. A. Baak,²⁹ G. Baccaglioni,^{88a} C. Bacci,^{133a,133b} A. M. Bach,¹⁴ H. Bachacou,¹³⁵ K. Bachas,²⁹ M. Backes,⁴⁸ M. Backhaus,²⁰ E. Badescu,^{25a} P. Bagnaia,^{131a,131b} S. Bahinipati,² Y. Bai,^{32a} D. C. Bailey,¹⁵⁷ T. Bain,¹⁵⁷ J. T. Baines,¹²⁸ O. K. Baker,¹⁷⁵ M. D. Baker,²⁴ S. Baker,⁷⁶ E. Banas,³⁸ P. Banerjee,⁹² Sw. Banerjee,¹⁷² D. Banfi,²⁹ A. Bangert,¹⁴⁹ V. Bansal,¹⁶⁸ H. S. Bansil,¹⁷ L. Barak,¹⁷¹ S. P. Baranov,⁹³ A. Barbaro Galtieri,¹⁴ T. Barber,⁴⁷ E. L. Barberio,⁸⁵ D. Barberis,^{49a,49b} M. Barbero,²⁰ D. Y. Bardin,⁶³ T. Barillari,⁹⁸ M. Barisonzi,¹⁷⁴ T. Barklow,¹⁴² N. Barlow,²⁷ B. M. Barnett,¹²⁸ R. M. Barnett,¹⁴ A. Baroncelli,^{133a} G. Barone,⁴⁸ A. J. Barr,¹¹⁷ F. Barreiro,⁷⁹ J. Barreiro Guimarães da Costa,⁵⁶ P. Barrillon,¹¹⁴ R. Bartoldus,¹⁴² A. E. Barton,⁷⁰ V. Bartsch,¹⁴⁸ R. L. Bates,⁵² L. Batkova,^{144a} J. R. Batley,²⁷ A. Battaglia,¹⁶ M. Battistin,²⁹ F. Bauer,¹³⁵ H. S. Bawa,^{142,f} S. Beale,⁹⁷ T. Beau,⁷⁷ P. H. Beauchemin,¹⁶⁰ R. Beccherle,^{49a} P. Bechtel,²⁰ H. P. Beck,¹⁶ A. K. Becker,¹⁷⁴ S. Becker,⁹⁷ M. Beckingham,¹³⁷ K. H. Becks,¹⁷⁴ A. J. Beddall,^{18c} A. Beddall,^{18c} S. Bedikian,¹⁷⁵ V. A. Bednyakov,⁶³ C. P. Bee,⁸² L. J. Beemster,¹⁰⁴ M. Begel,²⁴ S. Behar Harpaz,¹⁵¹ M. Beimforde,⁹⁸ C. Belanger-Champagne,⁸⁴ P. J. Bell,⁴⁸ W. H. Bell,⁴⁸ G. Bella,¹⁵² L. Bellagamba,^{19a} F. Bellina,²⁹ M. Bellomo,²⁹ A. Belloni,⁵⁶ O. Beloborodova,^{106,g} K. Belotskiy,⁹⁵ O. Beltramello,²⁹ O. Benary,¹⁵² D. Benchekroun,^{134a} K. Bendtz,^{145a,145b} N. Benekos,¹⁶⁴ Y. Benhammou,¹⁵² E. Benhar Noccioli,⁴⁸ J. A. Benitez Garcia,^{158b} D. P. Benjamin,⁴⁴ M. Benoit,¹¹⁴ J. R. Bensinger,²² K. Benslama,¹²⁹ S. Bentvelsen,¹⁰⁴ D. Berge,²⁹ E. Bergeaas Kuutmann,⁴¹ N. Berger,⁴ F. Berghaus,¹⁶⁸ E. Berglund,¹⁰⁴ J. Beringer,¹⁴ P. Bernat,⁷⁶ R. Bernhard,⁴⁷ C. Bernius,²⁴ T. Berry,⁷⁵ C. Bertella,⁸² A. Bertin,^{19a,19b} F. Bertolucci,^{121a,121b} M. I. Besana,^{88a,88b} G. J. Besjes,¹⁰³ N. Besson,¹³⁵ S. Bethke,⁹⁸ W. Bhimji,⁴⁵ R. M. Bianchi,²⁹ M. Bianco,^{71a,71b} O. Biebel,⁹⁷ S. P. Bieniek,⁷⁶ K. Bierwagen,⁵³ J. Biesiada,¹⁴ M. Biglietti,^{133a} H. Bilokon,⁴⁶ M. Bindi,^{19a,19b} S. Binet,¹¹⁴ A. Bingul,^{18c} C. Bini,^{131a,131b} C. Biscarat,¹⁷⁷ U. Bitenc,⁴⁷ K. M. Black,²¹ R. E. Blair,⁵ J.-B. Blanchard,¹³⁵ G. Blanchot,²⁹ T. Blazek,^{144a} C. Blocker,²² J. Blocki,³⁸ A. Blondel,⁴⁸ W. Blum,⁸⁰ U. Blumenschein,⁵³ G. J. Bobbink,¹⁰⁴ V. B. Bobrovnikov,¹⁰⁶ S. S. Bocchetta,⁷⁸ A. Bocci,⁴⁴ C. R. Boddy,¹¹⁷ M. Boehler,⁴⁷ J. Boek,¹⁷⁴ N. Boelaert,³⁵ J. A. Bogaerts,²⁹ A. Bogdanchikov,¹⁰⁶ A. Bogouch,^{89,a} C. Bohm,^{145a} J. Bohm,¹²⁴ V. Boisvert,⁷⁵ T. Bold,³⁷ V. Boldea,^{25a} N. M. Bolnet,¹³⁵ M. Bomben,⁷⁷ M. Bona,⁷⁴ M. Boonekamp,¹³⁵ C. N. Booth,¹³⁸ S. Bordonì,⁷⁷ C. Borer,¹⁶ A. Borisov,¹²⁷ G. Borissov,⁷⁰ I. Borjanovic,^{12a} M. Borri,⁸¹ S. Borroni,⁸⁶ V. Bortolotto,^{133a,133b} K. Bos,¹⁰⁴

- D. Boscherini,^{19a} M. Bosman,¹¹ H. Boterenbrood,¹⁰⁴ J. Bouchami,⁹² J. Boudreau,¹²² E. V. Bouhova-Thacker,⁷⁰
D. Boumediene,³³ C. Bourdarios,¹¹⁴ N. Bousson,⁸² A. Boveia,³⁰ J. Boyd,²⁹ I. R. Boyko,⁶³ I. Bozovic-Jelisavcic,^{12b}
J. Bracinik,¹⁷ P. Branchini,^{133a} A. Brandt,⁷ G. Brandt,¹¹⁷ O. Brandt,⁵³ U. Bratzler,¹⁵⁵ B. Brau,⁸³ J. E. Brau,¹¹³
H. M. Braun,^{174,a} S. F. Brazzale,^{163a,163c} B. Brelier,¹⁵⁷ J. Bremer,²⁹ K. Brendlinger,¹¹⁹ R. Brenner,¹⁶⁵ S. Bressler,¹⁷¹
D. Britton,⁵² F. M. Brochu,²⁷ I. Brock,²⁰ R. Brock,⁸⁷ F. Broggi,^{88a} C. Bromberg,⁸⁷ J. Bronner,⁹⁸ G. Brooijmans,³⁴
T. Brooks,⁷⁵ W. K. Brooks,^{31b} G. Brown,⁸¹ H. Brown,⁷ P. A. Bruckman de Renstrom,³⁸ D. Bruncko,^{143b}
R. Bruneliere,⁴⁷ S. Brunet,⁵⁹ A. Bruni,^{19a} G. Bruni,^{19a} M. Bruschi,^{19a} T. Buanes,¹³ Q. Buat,⁵⁴ F. Bucci,⁴⁸
J. Buchanan,¹¹⁷ P. Buchholz,¹⁴⁰ R. M. Buckingham,¹¹⁷ A. G. Buckley,⁴⁵ S. I. Buda,^{25a} I. A. Budagov,⁶³ B. Budick,¹⁰⁷
V. Büscher,⁸⁰ L. Bugge,¹¹⁶ O. Bulekov,⁹⁵ A. C. Bundock,⁷² M. Bunse,⁴² T. Buran,¹¹⁶ H. Burckhart,²⁹ S. Burdin,⁷²
T. Burgess,¹³ S. Burke,¹²⁸ E. Busato,³³ P. Bussey,⁵² C. P. Buszello,¹⁶⁵ B. Butler,¹⁴² J. M. Butler,²¹ C. M. Buttar,⁵²
J. M. Butterworth,⁷⁶ W. Buttinger,²⁷ S. Cabrera Urbán,¹⁶⁶ D. Caforio,^{19a,19b} O. Cakir,^{3a} P. Calafiura,¹⁴ G. Calderini,⁷⁷
P. Calfayan,⁹⁷ R. Calkins,¹⁰⁵ L. P. Caloba,^{23a} R. Caloi,^{131a,131b} D. Calvet,³³ S. Calvet,³³ R. Camacho Toro,³³
P. Camarri,^{132a,132b} D. Cameron,¹¹⁶ L. M. Caminada,¹⁴ S. Campana,²⁹ M. Campanelli,⁷⁶ V. Canale,^{101a,101b}
F. Canelli,^{30,h} A. Canepa,^{158a} J. Cantero,⁷⁹ R. Cantrill,⁷⁵ L. Capasso,^{101a,101b} M. D. M. Capeans Garrido,²⁹
I. Caprini,^{25a} M. Caprini,^{25a} D. Capriotti,⁹⁸ M. Capua,^{36a,36b} R. Caputo,⁸⁰ R. Cardarelli,^{132a} T. Carli,²⁹ G. Carlino,^{101a}
L. Carminati,^{88a,88b} B. Caron,⁸⁴ S. Caron,¹⁰³ E. Carquin,^{31b} G. D. Carrillo Montoya,¹⁷² A. A. Carter,⁷⁴ J. R. Carter,²⁷
J. Carvalho,^{123a,i} D. Casadei,¹⁰⁷ M. P. Casado,¹¹ M. Cascella,^{121a,121b} C. Caso,^{49a,49b,a}
A. M. Castaneda Hernandez,^{172,j} E. Castaneda-Miranda,¹⁷² V. Castillo Gimenez,¹⁶⁶ N. F. Castro,^{123a} G. Cataldi,^{71a}
P. Catastini,⁵⁶ A. Catinaccio,²⁹ J. R. Catmore,²⁹ A. Cattai,²⁹ G. Cattani,^{132a,132b} S. Caughron,⁸⁷ P. Cavalleri,⁷⁷
D. Cavalli,^{88a} M. Cavalli-Sforza,¹¹ V. Cavasinni,^{121a,121b} F. Ceradini,^{133a,133b} A. S. Cerqueira,^{23b} A. Cerri,²⁹
L. Cerrito,⁷⁴ F. Cerutti,⁴⁶ S. A. Cetin,^{18b} A. Chafaq,^{134a} D. Chakraborty,¹⁰⁵ I. Chalupkova,¹²⁵ K. Chan,²
B. Chapleau,⁸⁴ J. D. Chapman,²⁷ J. W. Chapman,⁸⁶ E. Chareyre,⁷⁷ D. G. Charlton,¹⁷ V. Chavda,⁸¹
C. A. Chavez Barajas,²⁹ S. Cheatham,⁸⁴ S. Chekanov,⁵ S. V. Chekulaev,^{158a} G. A. Chelkov,⁶³ M. A. Chelstowska,¹⁰³
C. Chen,⁶² H. Chen,²⁴ S. Chen,^{32c} X. Chen,¹⁷² Y. Chen,³⁴ A. Cheplakov,⁶³ R. Cherkaoui El Moursli,^{134e}
V. Chernyatin,²⁴ E. Cheu,⁶ S. L. Cheung,¹⁵⁷ L. Chevalier,¹³⁵ G. Chiefari,^{101a,101b} L. Chikovani,^{50a,a} J. T. Childers,²⁹
A. Chilingarov,⁷⁰ G. Chiodini,^{71a} A. S. Chisholm,¹⁷ R. T. Chislett,⁷⁶ A. Chitan,^{25a} M. V. Chizhov,⁶³ G. Choudalakis,³⁰
S. Chouridou,¹³⁶ I. A. Christidi,⁷⁶ A. Christov,⁴⁷ D. Chromek-Burckhart,²⁹ M. L. Chu,¹⁵⁰ J. Chudoba,¹²⁴
G. Ciapetti,^{131a,131b} A. K. Ciftci,^{3a} R. Ciftci,^{3a} D. Cinca,³³ V. Cindro,⁷³ C. Ciocca,^{19a,19b} A. Ciochio,¹⁴ M. Cirilli,⁸⁶
P. Cirkovic,^{12b} M. Citterio,^{88a} M. Ciubancan,^{25a} A. Clark,⁴⁸ P. J. Clark,⁴⁵ R. N. Clarke,¹⁴ W. Cleland,¹²²
J. C. Clemens,⁸² B. Clement,⁵⁴ C. Clement,^{145a,145b} Y. Coadou,⁸² M. Cobal,^{163a,163c} A. Cocco,¹³⁷ J. Cochran,⁶²
J. G. Cogan,¹⁴² J. Coggeshall,¹⁶⁴ E. Cogneras,¹⁷⁷ J. Colas,⁴ S. Cole,¹⁰⁵ A. P. Colijn,¹⁰⁴ N. J. Collins,¹⁷
C. Collins-Tooth,⁵² J. Collot,⁵⁴ T. Colombo,^{118a,118b} G. Colon,⁸³ P. Conde Muño,^{123a} E. Coniavitis,¹¹⁷
M. C. Conidi,¹¹ S. M. Consonni,^{88a,88b} V. Consorti,⁴⁷ S. Constantinescu,^{25a} C. Conta,^{118a,118b} G. Conti,⁵⁶
F. Conventi,^{101a,k} M. Cooke,¹⁴ B. D. Cooper,⁷⁶ A. M. Cooper-Sarkar,¹¹⁷ K. Copic,¹⁴ T. Cornelissen,¹⁷⁴ M. Corradi,^{19a}
F. Corriveau,^{84,l} A. Cortes-Gonzalez,¹⁶⁴ G. Cortiana,⁹⁸ G. Costa,^{88a} M. J. Costa,¹⁶⁶ D. Costanzo,¹³⁸ T. Costin,³⁰
D. Côté,²⁹ L. Courneyea,¹⁶⁸ G. Cowan,⁷⁵ C. Cowden,²⁷ B. E. Cox,⁸¹ K. Cranmer,¹⁰⁷ F. Crescioli,^{121a,121b}
M. Cristinziani,²⁰ G. Crosetti,^{36a,36b} S. Crépe-Renaudin,⁵⁴ C.-M. Cuciuc,^{25a} C. Cuenca Almenar,¹⁷⁵
T. Cuhadar Donszelmann,¹³⁸ M. Curatolo,⁴⁶ C. J. Curtis,¹⁷ C. Cuthbert,¹⁴⁹ P. Cwetanski,⁵⁹ H. Czirr,¹⁴⁰
P. Czodrowski,⁴³ Z. Czyczula,¹⁷⁵ S. D'Auria,⁵² M. D'Onofrio,⁷² A. D'Orazio,^{131a,131b}
M. J. Da Cunha Sargedas De Sousa,^{123a} C. Da Via,⁸¹ W. Dabrowski,³⁷ A. Dafinca,¹¹⁷ T. Dai,⁸⁶ C. Dallapiccola,⁸³
M. Dam,³⁵ M. Dameri,^{49a,49b} D. S. Damiani,¹³⁶ H. O. Danielsson,²⁹ V. Dao,⁴⁸ G. Darbo,^{49a} G. L. Darlea,^{25b}
J. A. Dassoulas,⁴¹ W. Davey,²⁰ T. Davidek,¹²⁵ N. Davidson,⁸⁵ R. Davidson,⁷⁰ E. Davies,^{117,d} M. Davies,⁹²
O. Davignon,⁷⁷ A. R. Davison,⁷⁶ Y. Davygora,^{57a} E. Dawe,¹⁴¹ I. Dawson,¹³⁸ R. K. Daya-Ishmukhametova,²² K. De,⁷
R. de Asmundis,^{101a} S. De Castro,^{19a,19b} S. De Cecco,⁷⁷ J. de Graat,⁹⁷ N. De Groot,¹⁰³ P. de Jong,¹⁰⁴
C. De La Taille,¹¹⁴ H. De la Torre,⁷⁹ F. De Lorenzi,⁶² L. de Mora,⁷⁰ L. De Nooij,¹⁰⁴ D. De Pedis,^{131a} A. De Salvo,^{131a}
U. De Sanctis,^{163a,163c} A. De Santo,¹⁴⁸ J. B. De Vivie De Regie,¹¹⁴ G. De Zorzi,^{131a,131b} W. J. Dearnaley,⁷⁰
R. Debebe,²⁴ C. Debenedetti,⁴⁵ B. Dechenaux,⁵⁴ D. V. Dedovich,⁶³ J. Degenhardt,¹¹⁹ C. Del Papa,^{163a,163c}
J. Del Peso,⁷⁹ T. Del Prete,^{121a,121b} T. Delemontex,⁵⁴ M. Deliyergiyev,⁷³ A. Dell'Acqua,²⁹ L. Dell'Asta,²¹
M. Della Pietra,^{101a,k} D. della Volpe,^{101a,101b} M. Delmastro,⁴ P. A. Delsart,⁵⁴ C. Deluca,¹⁰⁴ S. Demers,¹⁷⁵
M. Demichev,⁶³ B. Demirkoz,^{11,m} J. Deng,¹⁶² S. P. Denisov,¹²⁷ D. Derendarz,³⁸ J. E. Derkaoui,^{134d} F. Derue,⁷⁷
P. Dervan,⁷² K. Desch,²⁰ E. Devetak,¹⁴⁷ P. O. Deviveiros,¹⁰⁴ A. Dewhurst,¹²⁸ B. DeWilde,¹⁴⁷ S. Dhaliwal,¹⁵⁷

R. Dhullipudi,^{24,n} A. Di Ciaccio,^{132a,132b} L. Di Ciaccio,⁴ A. Di Girolamo,²⁹ B. Di Girolamo,²⁹ S. Di Luise,^{133a,133b}
A. Di Mattia,¹⁷² B. Di Micco,²⁹ R. Di Nardo,⁴⁶ A. Di Simone,^{132a,132b} R. Di Sipio,^{19a,19b} M. A. Diaz,^{31a} E. B. Diehl,⁸⁶
J. Dietrich,⁴¹ T. A. Dietzsch,^{57a} S. Diglio,⁸⁵ K. Dindar Yagci,³⁹ J. Dingfelder,²⁰ F. Dinut,^{25a} C. Dionisi,^{131a,131b}
P. Dita,^{25a} S. Dita,^{25a} F. Dittus,²⁹ F. Djama,⁸² T. Djobava,^{50b} M. A. B. do Vale,^{23c} A. Do Valle Wemans,^{123a,o}
T. K. O. Doan,⁴ M. Dobbs,⁸⁴ R. Dobinson,^{29,a} D. Dobos,²⁹ E. Dobson,^{29,p} J. Dodd,³⁴ C. Doglioni,⁴⁸ T. Doherty,⁵²
Y. Doi,^{64,a} J. Dolejsi,¹²⁵ I. Dolenc,⁷³ Z. Dolezal,¹²⁵ B. A. Dolgoshein,^{95,a} T. Dohmae,¹⁵⁴ M. Donadelli,^{23d} J. Donini,³³
J. Dopke,²⁹ A. Doria,^{101a} A. Dos Anjos,¹⁷² A. Dotti,^{121a,121b} M. T. Dova,⁶⁹ A. D. Doxiadis,¹⁰⁴ A. T. Doyle,⁵² M. Dris,⁹
J. Dubbert,⁹⁸ S. Dube,¹⁴ E. Duchovni,¹⁷¹ G. Duckeck,⁹⁷ A. Dudarev,²⁹ F. Dudziak,⁶² M. Dührssen,²⁹ I. P. Duerdoth,⁸¹
L. Dufloot,¹¹⁴ M-A. Dufour,⁸⁴ L. Duguid,⁷⁵ M. Dunford,²⁹ H. Duran Yildiz,^{3a} R. Duxfield,¹³⁸ M. Dwuznik,³⁷
F. Dydak,²⁹ M. Düren,⁵¹ J. Ebke,⁹⁷ S. Eckweiler,⁸⁰ K. Edmonds,⁸⁰ W. Edson,¹ C. A. Edwards,⁷⁵ N. C. Edwards,⁵²
W. Ehrenfeld,⁴¹ T. Eifert,¹⁴² G. Eigen,¹³ K. Einsweiler,¹⁴ E. Eisenhandler,⁷⁴ T. Ekelof,¹⁶⁵ M. El Kacimi,^{134c}
M. Ellert,¹⁶⁵ S. Elles,⁴ F. Ellinghaus,⁸⁰ K. Ellis,⁷⁴ N. Ellis,²⁹ J. Elmsheuser,⁹⁷ M. Elsing,²⁹ D. Emelianov,¹²⁸
R. Engelmann,¹⁴⁷ A. Engl,⁹⁷ B. Epp,⁶⁰ J. Erdmann,⁵³ A. Ereditato,¹⁶ D. Eriksson,^{145a} J. Ernst,¹ M. Ernst,²⁴
J. Ernwein,¹³⁵ D. Errede,¹⁶⁴ S. Errede,¹⁶⁴ E. Ertel,⁸⁰ M. Escalier,¹¹⁴ H. Esch,⁴² C. Escobar,¹²² X. Espinal Curull,¹¹
B. Esposito,⁴⁶ F. Etienne,⁸² A. I. Etienne,¹³⁵ E. Etzion,¹⁵² D. Evangelakou,⁵³ H. Evans,⁵⁹ L. Fabbri,^{19a,19b} C. Fabre,²⁹
R. M. Fakhruddinov,¹²⁷ S. Falciano,^{131a} Y. Fang,¹⁷² M. Fanti,^{88a,88b} A. Farbin,⁷ A. Farilla,^{133a} J. Farley,¹⁴⁷
T. Farooque,¹⁵⁷ S. Farrell,¹⁶² S. M. Farrington,¹⁶⁹ P. Farthouat,²⁹ P. Fassnacht,²⁹ D. Fassouliotis,⁸
B. Fatholahzadeh,¹⁵⁷ A. Favareto,^{88a,88b} L. Fayard,¹¹⁴ S. Fazio,^{36a,36b} R. Febbraro,³³ P. Federic,^{143a} O. L. Fedin,¹²⁰
W. Fedorko,⁸⁷ M. Fehling-Kaschek,⁴⁷ L. Felgioni,⁸² D. Fellmann,⁵ C. Feng,^{32d} E. J. Feng,⁵ A. B. Fenyuk,¹²⁷
J. Ferencei,^{143b} W. Fernando,⁵ S. Ferrag,⁵² J. Ferrando,⁵² V. Ferrara,⁴¹ A. Ferrari,¹⁶⁵ P. Ferrari,¹⁰⁴ R. Ferrari,^{118a}
D. E. Ferreira de Lima,⁵² A. Ferrer,¹⁶⁶ D. Ferrere,⁴⁸ C. Ferretti,⁸⁶ A. Ferretto Parodi,^{49a,49b} M. Fiascaris,³⁰
F. Fiedler,⁸⁰ A. Filipčič,⁷³ F. Filthaut,¹⁰³ M. Fincke-Keeler,¹⁶⁸ M. C. N. Fiolhais,^{123a,i} L. Fiorini,¹⁶⁶ A. Firan,³⁹
G. Fischer,⁴¹ M. J. Fisher,¹⁰⁸ M. Flechl,⁴⁷ I. Fleck,¹⁴⁰ J. Fleckner,⁸⁰ P. Fleischmann,¹⁷³ S. Fleischmann,¹⁷⁴ T. Flick,¹⁷⁴
A. Floderus,⁷⁸ L. R. Flores Castillo,¹⁷² M. J. Flowerdew,⁹⁸ T. Fonseca Martin,¹⁶ A. Formica,¹³⁵ A. Forti,⁸¹
D. Fortin,^{158a} D. Fournier,¹¹⁴ H. Fox,⁷⁰ P. Francavilla,¹¹ M. Franchini,^{19a,19b} S. Franchino,^{118a,118b} D. Francis,²⁹
T. Frank,¹⁷¹ S. Franz,²⁹ M. Fraternali,^{118a,118b} S. Fratina,¹¹⁹ S. T. French,²⁷ C. Friedrich,⁴¹ F. Friedrich,⁴³
R. Froeschl,²⁹ D. Froidevaux,²⁹ J. A. Frost,²⁷ C. Fukunaga,¹⁵⁵ E. Fullana Torregrosa,²⁹ B. G. Fulsom,¹⁴² J. Fuster,¹⁶⁶
C. Gabaldon,²⁹ O. Gabizon,¹⁷¹ T. Gadfort,²⁴ S. Gadomski,⁴⁸ G. Gagliardi,^{49a,49b} P. Gagnon,⁵⁹ C. Galea,⁹⁷
E. J. Gallas,¹¹⁷ V. Gallo,¹⁶ B. J. Gallop,¹²⁸ P. Gallus,¹²⁴ K. K. Gan,¹⁰⁸ Y. S. Gao,^{142,f} A. Gaponenko,¹⁴
F. Garberon,¹⁷⁵ M. Garcia-Sciveres,¹⁴ C. García,¹⁶⁶ J. E. García Navarro,¹⁶⁶ R. W. Gardner,³⁰ N. Garelli,²⁹
H. Garitaonandia,¹⁰⁴ V. Garonne,²⁹ C. Gatti,⁴⁶ G. Gaudio,^{118a} B. Gaur,¹⁴⁰ L. Gauthier,¹³⁵ P. Gauzzi,^{131a,131b}
I. L. Gavrilenko,⁹³ C. Gay,¹⁶⁷ G. Gaycken,²⁰ E. N. Gazis,⁹ P. Ge,^{32d} Z. Gecse,¹⁶⁷ C. N. P. Gee,¹²⁸ D. A. A. Geerts,¹⁰⁴
Ch. Geich-Gimbel,²⁰ K. Gellerstedt,^{145a,145b} C. Gemme,^{49a} A. Gemmell,⁵² M. H. Genest,⁵⁴ S. Gentile,^{131a,131b}
M. George,⁵³ S. George,⁷⁵ P. Gerlach,¹⁷⁴ A. Gershon,¹⁵² C. Geweniger,^{57a} H. Ghazlane,^{134b} N. Ghodbane,³³
B. Giacobbe,^{19a} S. Giagu,^{131a,131b} V. Giakoumopoulou,⁸ V. Giangiobbe,¹¹ F. Gianotti,²⁹ B. Gibbard,²⁴ A. Gibson,¹⁵⁷
S. M. Gibson,²⁹ D. Gillberg,²⁸ A. R. Gillman,¹²⁸ D. M. Gingrich,^{2,e} J. Ginzburg,¹⁵² N. Giokaris,⁸ M. P. Giordani,^{163c}
R. Giordano,^{101a,101b} F. M. Giorgi,¹⁵ P. Giovannini,⁹⁸ P. F. Giraud,¹³⁵ D. Giugni,^{88a} M. Giunta,⁹² P. Giusti,^{19a}
B. K. Gjelsten,¹¹⁶ L. K. Gladilin,⁹⁶ C. Glasman,⁷⁹ J. Glatzer,⁴⁷ A. Glazov,⁴¹ K. W. Glitza,¹⁷⁴ G. L. Glonti,⁶³
J. R. Goddard,⁷⁴ J. Godfrey,¹⁴¹ J. Godlewski,²⁹ M. Goebel,⁴¹ T. Göpfert,⁴³ C. Goeringer,⁸⁰ C. Gössling,⁴²
S. Goldfarb,⁸⁶ T. Golling,¹⁷⁵ A. Gomes,^{123a,c} L. S. Gomez Fajardo,⁴¹ R. Gonçalves,⁷⁵
J. Goncalves Pinto Firmino Da Costa,⁴¹ L. Gonella,²⁰ S. Gonzalez,¹⁷² S. González de la Hoz,¹⁶⁶ G. Gonzalez Parra,¹¹
M. L. Gonzalez Silva,²⁶ S. Gonzalez-Sevilla,⁴⁸ J. J. Goodson,¹⁴⁷ L. Goossens,²⁹ P. A. Gorbounov,⁹⁴ H. A. Gordon,²⁴
I. Gorelov,¹⁰² G. Gorfine,¹⁷⁴ B. Gorini,²⁹ E. Gorini,^{71a,71b} A. Gorišek,⁷³ E. Gornicki,³⁸ B. Gosdzik,⁴¹ A. T. Goshaw,⁵
M. Gosselink,¹⁰⁴ M. I. Gostkin,⁶³ I. Gough Eschrich,¹⁶² M. Gouighri,^{134a} D. Goujdami,^{134c} M. P. Goulette,⁴⁸
A. G. Goussiou,¹³⁷ C. Goy,⁴ S. Gozpinar,²² I. Grabowska-Bold,³⁷ P. Grafström,^{19a,19b} K-J. Grahn,⁴¹
F. Grancagnolo,^{71a} S. Grancagnolo,¹⁵ V. Grassi,¹⁴⁷ V. Gratchev,¹²⁰ N. Grau,³⁴ H. M. Gray,²⁹ J. A. Gray,¹⁴⁷
E. Graziani,^{133a} O. G. Grebenyuk,¹²⁰ T. Greenshaw,⁷² Z. D. Greenwood,^{24,n} K. Gregersen,³⁵ I. M. Gregor,⁴¹
P. Grenier,¹⁴² J. Griffiths,⁷ N. Grigalashvili,⁶³ A. A. Grillo,¹³⁶ S. Grinstein,¹¹ Y. V. Grishkevich,⁹⁶ J.-F. Grivaz,¹¹⁴
E. Gross,¹⁷¹ J. Grosse-Knetter,⁵³ J. Groth-Jensen,¹⁷¹ K. Grybel,¹⁴⁰ D. Guest,¹⁷⁵ C. Guichenev,³³ S. Guindon,⁵³
U. Gul,⁵² H. Guler,^{84,q} J. Gunther,¹²⁴ B. Guo,¹⁵⁷ J. Guo,³⁴ P. Gutierrez,¹¹⁰ N. Guttman,¹⁵² O. Gutzwiller,¹⁷²
C. Guyot,¹³⁵ C. Gwenlan,¹¹⁷ C. B. Gwilliam,⁷² A. Haas,¹⁴² S. Haas,²⁹ C. Haber,¹⁴ H. K. Hadavand,³⁹ D. R. Hadley,¹⁷

P. Haefner,²⁰ F. Hahn,²⁹ S. Haider,²⁹ Z. Hajduk,³⁸ H. Hakobyan,¹⁷⁶ D. Hall,¹¹⁷ J. Haller,⁵³ K. Hamacher,¹⁷⁴
P. Hamal,¹¹² M. Hamer,⁵³ A. Hamilton,^{144b,r} S. Hamilton,¹⁶⁰ L. Han,^{32b} K. Hanagaki,¹¹⁵ K. Hanawa,¹⁵⁹ M. Hance,¹⁴
C. Handel,⁸⁰ P. Hanke,^{57a} J. R. Hansen,³⁵ J. B. Hansen,³⁵ J. D. Hansen,³⁵ P. H. Hansen,³⁵ P. Hansson,¹⁴² K. Hara,¹⁵⁹
G. A. Hare,¹³⁶ T. Harenberg,¹⁷⁴ S. Harkusha,⁸⁹ D. Harper,⁸⁶ R. D. Harrington,⁴⁵ O. M. Harris,¹³⁷ J. Hartert,⁴⁷
F. Hartjes,¹⁰⁴ T. Haruyama,⁶⁴ A. Harvey,⁵⁵ S. Hasegawa,¹⁰⁰ Y. Hasegawa,¹³⁹ S. Hassani,¹³⁵ S. Haug,¹⁶
M. Hauschild,²⁹ R. Hauser,⁸⁷ M. Havranek,²⁰ C. M. Hawkes,¹⁷ R. J. Hawkings,²⁹ A. D. Hawkins,⁷⁸ D. Hawkins,¹⁶²
T. Hayakawa,⁶⁵ T. Hayashi,¹⁵⁹ D. Hayden,⁷⁵ C. P. Hays,¹¹⁷ H. S. Hayward,⁷² S. J. Haywood,¹²⁸ M. He,^{32d}
S. J. Head,¹⁷ V. Hedberg,⁷⁸ L. Heelan,⁷ S. Heim,⁸⁷ B. Heinemann,¹⁴ S. Heisterkamp,³⁵ L. Helary,²¹ C. Heller,⁹⁷
M. Heller,²⁹ S. Hellman,^{145a,145b} D. Hellmich,²⁰ C. Helsens,¹¹ R. C. W. Henderson,⁷⁰ M. Henke,^{57a} A. Henrichs,⁵³
A. M. Henriques Correia,²⁹ S. Henrot-Versille,¹¹⁴ C. Hensel,⁵³ T. Henß,¹⁷⁴ C. M. Hernandez,⁷
Y. Hernández Jiménez,¹⁶⁶ R. Herrberg,¹⁵ G. Herten,⁴⁷ R. Hertenberger,⁹⁷ L. Hervas,²⁹ G. G. Hesketh,⁷⁶
N. P. Hessey,¹⁰⁴ E. Higón-Rodríguez,¹⁶⁶ J. C. Hill,²⁷ K. H. Hiller,⁴¹ S. Hillert,²⁰ S. J. Hillier,¹⁷ I. Hinchliffe,¹⁴
E. Hines,¹¹⁹ M. Hirose,¹¹⁵ F. Hirsch,⁴² D. Hirschbuehl,¹⁷⁴ J. Hobbs,¹⁴⁷ N. Hod,¹⁵² M. C. Hodgkinson,¹³⁸
P. Hodgson,¹³⁸ A. Hoecker,²⁹ M. R. Hoferkamp,¹⁰² J. Hoffman,³⁹ D. Hoffmann,⁸² M. Hohlfeld,⁸⁰ M. Holder,¹⁴⁰
S. O. Holmgren,^{145a} T. Holy,¹²⁶ J. L. Holzbauer,⁸⁷ T. M. Hong,¹¹⁹ L. Hooft van Huysduynen,¹⁰⁷ C. Horn,¹⁴²
S. Horner,⁴⁷ J.-Y. Hostachy,⁵⁴ S. Hou,¹⁵⁰ A. Houmada,^{134a} J. Howard,¹¹⁷ J. Howarth,⁸¹ I. Hristova,¹⁵ J. Hrivnac,¹¹⁴
T. Hryn'ova,⁴ P. J. Hsu,⁸⁰ S.-C. Hsu,¹⁴ Z. Hubacek,¹²⁶ F. Hubaut,⁸² F. Huegging,²⁰ A. Huettmann,⁴¹ T. B. Huffman,¹¹⁷
E. W. Hughes,³⁴ G. Hughes,⁷⁰ M. Huhtinen,²⁹ M. Hurwitz,¹⁴ U. Husemann,⁴¹ N. Huseynov,^{63,s} J. Huston,⁸⁷ J. Huth,⁵⁶
G. Iacobucci,⁴⁸ G. Iakovidis,⁹ M. Ibbotson,⁸¹ I. Ibragimov,¹⁴⁰ L. Iconomidou-Fayard,¹¹⁴ J. Idarraga,¹¹⁴ P. Iengo,^{101a}
O. Igonkina,¹⁰⁴ Y. Ikegami,⁶⁴ M. Ikeno,⁶⁴ D. Iliadis,¹⁵³ N. Ilic,¹⁵⁷ T. Ince,²⁰ J. Inigo-Golfin,²⁹ P. Ioannou,⁸
M. Iodice,^{133a} K. Iordanidou,⁸ V. Ippolito,^{131a,131b} A. Irles Quiles,¹⁶⁶ C. Isaksson,¹⁶⁵ M. Ishino,⁶⁶ M. Ishitsuka,¹⁵⁶
R. Ishmukhametov,³⁹ C. Issever,¹¹⁷ S. Istin,^{18a} A. V. Ivashin,¹²⁷ W. Iwanski,³⁸ H. Iwasaki,⁶⁴ J. M. Izen,⁴⁰ V. Izzo,^{101a}
B. Jackson,¹¹⁹ J. N. Jackson,⁷² P. Jackson,¹⁴² M. R. Jaekel,²⁹ V. Jain,⁵⁹ K. Jakobs,⁴⁷ S. Jakobsen,³⁵ T. Jakoubek,¹²⁴
J. Jakubek,¹²⁶ D. K. Jana,¹¹⁰ E. Jansen,⁷⁶ H. Jansen,²⁹ A. Jantsch,⁹⁸ M. Janus,⁴⁷ G. Jarlskog,⁷⁸ L. Jeanty,⁵⁶
I. Jen-La Plante,³⁰ D. Jennens,⁸⁵ P. Jenni,²⁹ P. Jež,³⁵ S. Jézéquel,⁴ M. K. Jha,^{19a} H. Ji,¹⁷² W. Ji,⁸⁰ J. Jia,¹⁴⁷ Y. Jiang,^{32b}
M. Jimenez Belenguer,⁴¹ S. Jin,^{32a} O. Jinnouchi,¹⁵⁶ M. D. Joergensen,³⁵ D. Joffe,³⁹ M. Johansen,^{145a,145b}
K. E. Johansson,^{145a} P. Johansson,¹³⁸ S. Johnert,⁴¹ K. A. Johns,⁶ K. Jon-And,^{145a,145b} G. Jones,¹⁶⁹ R. W. L. Jones,⁷⁰
T. J. Jones,⁷² C. Joram,²⁹ P. M. Jorge,^{123a} K. D. Joshi,⁸¹ J. Jovicevic,¹⁴⁶ T. Jovin,^{12b} X. Ju,¹⁷² C. A. Jung,⁴²
R. M. Jungst,²⁹ V. Juranek,¹²⁴ P. Jussel,⁶⁰ A. Juste Rozas,¹¹ S. Kabana,¹⁶ M. Kaci,¹⁶⁶ A. Kaczmarska,³⁸ P. Kadlecik,³⁵
M. Kado,¹¹⁴ H. Kagan,¹⁰⁸ M. Kagan,⁵⁶ E. Kajomovitz,¹⁵¹ S. Kalinin,¹⁷⁴ L. V. Kalinovskaya,⁶³ S. Kama,³⁹
N. Kanaya,¹⁵⁴ M. Kaneda,²⁹ S. Kaneti,²⁷ T. Kanno,¹⁵⁶ V. A. Kantserov,⁹⁵ J. Kanzaki,⁶⁴ B. Kaplan,¹⁷⁵ A. Kapliy,³⁰
J. Kaplon,²⁹ D. Kar,⁵² M. Karagounis,²⁰ K. Karakostas,⁹ M. Karnevskiy,⁴¹ V. Kartvelishvili,⁷⁰ A. N. Karyukhin,¹²⁷
L. Kashif,¹⁷² G. Kasieczka,^{57b} R. D. Kass,¹⁰⁸ A. Kastanas,¹³ M. Kataoka,⁴ Y. Kataoka,¹⁵⁴ E. Katsoufis,⁹ J. Katzy,⁴¹
V. Kaushik,⁶ K. Kawagoe,⁶⁸ T. Kawamoto,¹⁵⁴ G. Kawamura,⁸⁰ M. S. Kayl,¹⁰⁴ V. A. Kazanin,¹⁰⁶ M. Y. Kazarinov,⁶³
R. Keeler,¹⁶⁸ R. Kehoe,³⁹ M. Keil,⁵³ G. D. Kekelidze,⁶³ J. S. Keller,¹³⁷ M. Kenyon,⁵² O. Kepka,¹²⁴ N. Kerschen,²⁹
B. P. Kerševan,⁷³ S. Kersten,¹⁷⁴ K. Kessoku,¹⁵⁴ J. Keung,¹⁵⁷ F. Khalil-zada,¹⁰ H. Khandanyan,¹⁶⁴ A. Khanov,¹¹¹
D. Kharchenko,⁶³ A. Khodinov,⁹⁵ A. Khomich,^{57a} T. J. Khoo,²⁷ G. Khorauli,²⁰ A. Khoroshilov,¹⁷⁴ V. Khovanskiy,⁹⁴
E. Khramov,⁶³ J. Khubua,^{50b} H. Kim,^{145a,145b} S. H. Kim,¹⁵⁹ N. Kimura,¹⁷⁰ O. Kind,¹⁵ B. T. King,⁷² M. King,⁶⁵
R. S. B. King,¹¹⁷ J. Kirk,¹²⁸ A. E. Kiryunin,⁹⁸ T. Kishimoto,⁶⁵ D. Kisielewska,³⁷ T. Kitamura,⁶⁵ T. Kittelmann,¹²²
E. Kladiva,^{143b} M. Klein,⁷² U. Klein,⁷² K. Kleinknecht,⁸⁰ M. Klemetti,⁸⁴ A. Klier,¹⁷¹ P. Klimek,^{145a,145b}
A. Klimentov,²⁴ R. Klingenberg,⁴² J. A. Klinger,⁸¹ E. B. Klinkby,³⁵ T. Klioutchnikova,²⁹ P. F. Klok,¹⁰³ S. Klous,¹⁰⁴
E.-E. Kluge,^{57a} T. Kluge,⁷² P. Kluit,¹⁰⁴ S. Kluth,⁹⁸ N. S. Knecht,¹⁵⁷ E. Kneringer,⁶⁰ E. B. F. G. Knoops,⁸² A. Knue,⁵³
B. R. Ko,⁴⁴ T. Kobayashi,¹⁵⁴ M. Kobel,⁴³ M. Kocian,¹⁴² P. Kodys,¹²⁵ K. Köneke,²⁹ A. C. König,¹⁰³ S. Koenig,⁸⁰
L. Köpke,⁸⁰ F. Koetsveld,¹⁰³ P. Koevesarki,²⁰ T. Koffas,²⁸ E. Koffeman,¹⁰⁴ L. A. Kogan,¹¹⁷ S. Kohlmann,¹⁷⁴
F. Kohn,⁵³ Z. Kohout,¹²⁶ T. Kohriki,⁶⁴ T. Koi,¹⁴² G. M. Kolachev,^{106,a} H. Kolanoski,¹⁵ V. Kolesnikov,⁶³
I. Koletsou,^{88a} J. Koll,⁸⁷ M. Kollefrath,⁴⁷ A. A. Komar,⁹³ Y. Komori,¹⁵⁴ T. Kondo,⁶⁴ T. Kono,^{41,t} A. I. Kononov,⁴⁷
R. Konoplich,^{107,u} N. Konstantinidis,⁷⁶ S. Koperny,³⁷ K. Korcyl,³⁸ K. Kordas,¹⁵³ A. Korn,¹¹⁷ A. Korol,¹⁰⁶
I. Korolkov,¹¹ E. V. Korolkova,¹³⁸ V. A. Korotkov,¹²⁷ O. Kortner,⁹⁸ S. Kortner,⁹⁸ V. V. Kostyukhin,²⁰ S. Kotov,⁹⁸
V. M. Kotov,⁶³ A. Kotwal,⁴⁴ C. Kourkoumelis,⁸ V. Kouskoura,¹⁵³ A. Koutsman,^{158a} R. Kowalewski,¹⁶⁸
T. Z. Kowalski,³⁷ W. Kozanecki,¹³⁵ A. S. Kozhin,¹²⁷ V. Kral,¹²⁶ V. A. Kramarenko,⁹⁶ G. Kramberger,⁷³
M. W. Krasny,⁷⁷ A. Krasznahorkay,¹⁰⁷ J. K. Kraus,²⁰ S. Kreiss,¹⁰⁷ F. Krejci,¹²⁶ J. Kretschmar,⁷² N. Krieger,⁵³

P. Krieger,¹⁵⁷ K. Kroeninger,⁵³ H. Kroha,⁹⁸ J. Kroll,¹¹⁹ J. Kroseberg,²⁰ J. Krstic,^{12a} U. Kruchonak,⁶³ H. Krüger,²⁰ T. Kruker,¹⁶ N. Krumnack,⁶² Z. V. KrumshTEYN,⁶³ T. Kubota,⁸⁵ S. Kuday,^{3a} S. Kuehn,⁴⁷ A. Kugel,^{57c} T. Kuhl,⁴¹ D. Kuhn,⁶⁰ V. Kukhtin,⁶³ Y. Kulchitsky,⁸⁹ S. Kuleshov,^{31b} C. Kummer,⁹⁷ M. Kuna,⁷⁷ J. Kunkle,¹¹⁹ A. Kupco,¹²⁴ H. Kurashige,⁶⁵ M. Kurata,¹⁵⁹ Y. A. Kurochkin,⁸⁹ V. Kus,¹²⁴ E. S. Kuwertz,¹⁴⁶ M. Kuze,¹⁵⁶ J. Kvita,¹⁴¹ R. Kwee,¹⁵ A. La Rosa,⁴⁸ L. La Rotonda,^{36a,36b} L. Labarga,⁷⁹ J. Labbe,⁴ S. Lablak,^{134a} C. Lacasta,¹⁶⁶ F. Lacava,^{131a,131b} H. Lacker,¹⁵ D. Lacour,⁷⁷ V. R. Lacuesta,¹⁶⁶ E. Ladygin,⁶³ R. Lafaye,⁴ B. Laforge,⁷⁷ T. Lagouri,⁷⁹ S. Lai,⁴⁷ E. Laisne,⁵⁴ M. Lamanna,²⁹ L. Lambourne,⁷⁶ C. L. Lampen,⁶ W. Lampl,⁶ E. Lancon,¹³⁵ U. Landgraf,⁴⁷ M. P. J. Landon,⁷⁴ J. L. Lane,⁸¹ V. S. Lang,^{57a} C. Lange,⁴¹ A. J. Lankford,¹⁶² F. Lanni,²⁴ K. LantzsCH,¹⁷⁴ S. Laplace,⁷⁷ C. Lapoire,²⁰ J. F. Laporte,¹³⁵ T. Lari,^{88a} A. Lerner,¹¹⁷ M. Lassnig,²⁹ P. Laurelli,⁴⁶ V. Lavorini,^{36a,36b} W. Lavrijsen,¹⁴ P. Laycock,⁷² O. Le Dortz,⁷⁷ E. Le Guirriec,⁸² C. Le Maner,¹⁵⁷ E. Le Menedeu,¹¹ T. LeCompte,⁵ F. Ledroit-Guillon,⁵⁴ H. Lee,¹⁰⁴ J. S. H. Lee,¹¹⁵ S. C. Lee,¹⁵⁰ L. Lee,¹⁷⁵ M. Lefebvre,¹⁶⁸ M. Legendre,¹³⁵ F. Legger,⁹⁷ C. Leggett,¹⁴ M. Lehmacher,²⁰ G. Lehmann Miotto,²⁹ X. Lei,⁶ M. A. L. Leite,^{23d} R. Leitner,¹²⁵ D. Lellouch,¹⁷¹ B. Lemmer,⁵³ V. Lendermann,^{57a} K. J. C. Leney,^{144b} T. Lenz,¹⁰⁴ G. Lenzen,¹⁷⁴ B. Lenzi,²⁹ K. Leonhardt,⁴³ S. Leontsinis,⁹ F. Lepold,^{57a} C. Leroy,⁹² J-R. Lessard,¹⁶⁸ C. G. Lester,²⁷ C. M. Lester,¹¹⁹ J. Levêque,⁴ D. Levin,⁸⁶ L. J. Levinson,¹⁷¹ A. Lewis,¹¹⁷ G. H. Lewis,¹⁰⁷ A. M. Leyko,²⁰ M. Leyton,¹⁵ B. Li,⁸² H. Li,^{172,v} S. Li,^{32b,w} X. Li,⁸⁶ Z. Liang,^{117,x} H. Liao,³³ B. Liberti,^{132a} P. Lichard,²⁹ M. Lichtnecker,⁹⁷ K. Lie,¹⁶⁴ W. Liebig,¹³ C. Limbach,²⁰ A. Limosani,⁸⁵ M. Limper,⁶¹ S. C. Lin,^{150,y} F. Linde,¹⁰⁴ J. T. Linnemann,⁸⁷ E. Lipeles,¹¹⁹ A. Lipniacka,¹³ T. M. Liss,¹⁶⁴ D. Lissauer,²⁴ A. Lister,⁴⁸ A. M. Litke,¹³⁶ C. Liu,²⁸ D. Liu,¹⁵⁰ H. Liu,⁸⁶ J. B. Liu,⁸⁶ L. Liu,⁸⁶ M. Liu,^{32b} Y. Liu,^{32b} M. Livan,^{118a,118b} S. S. A. Livermore,¹¹⁷ A. Lleres,⁵⁴ J. Llorente Merino,⁷⁹ S. L. Lloyd,⁷⁴ E. Lobodzinska,⁴¹ P. Loch,⁶ W. S. Lockman,¹³⁶ T. Loddenkoetter,²⁰ F. K. Loebinger,⁸¹ A. Loginov,¹⁷⁵ C. W. Loh,¹⁶⁷ T. Lohse,¹⁵ K. Lohwasser,⁴⁷ M. Lokajicek,¹²⁴ V. P. Lombardo,⁴ R. E. Long,⁷⁰ L. Lopes,^{123a} D. Lopez Mateos,⁵⁶ J. Lorenz,⁹⁷ N. Lorenzo Martinez,¹¹⁴ M. Losada,¹⁶¹ P. Loscutoff,¹⁴ F. Lo Sterzo,^{131a,131b} M. J. Losty,^{158a} X. Lou,⁴⁰ A. Lounis,¹¹⁴ K. F. Loureiro,¹⁶¹ J. Love,²¹ P. A. Love,⁷⁰ A. J. Lowe,^{142,f} F. Lu,^{32a} H. J. Lubatti,¹³⁷ C. Luci,^{131a,131b} A. Lucotte,⁵⁴ A. Ludwig,⁴³ D. Ludwig,⁴¹ I. Ludwig,⁴⁷ J. Ludwig,⁴⁷ F. Luehring,⁵⁹ G. Luijckx,¹⁰⁴ W. Lukas,⁶⁰ D. Lumb,⁴⁷ L. Luminari,^{131a} E. Lund,¹¹⁶ B. Lund-Jensen,¹⁴⁶ B. Lundberg,⁷⁸ J. Lundberg,^{145a,145b} O. Lundberg,^{145a,145b} J. Lundquist,³⁵ M. Lungwitz,⁸⁰ D. Lynn,²⁴ E. Lytken,⁷⁸ H. Ma,²⁴ L. L. Ma,¹⁷² G. Maccarrone,⁴⁶ A. Macchiolo,⁹⁸ B. Maček,⁷³ J. Machado Miguens,^{123a} R. Mackeprang,³⁵ R. J. Madaras,¹⁴ H. J. Maddocks,⁷⁰ W. F. Mader,⁴³ R. Maenner,^{57c} T. Maeno,²⁴ P. Mättig,¹⁷⁴ S. Mättig,⁴¹ L. Magnoni,²⁹ E. Magradze,⁵³ K. Mahboubi,⁴⁷ S. Mahmoud,⁷² G. Mahout,¹⁷ C. Maiani,¹³⁵ C. Maidantchik,^{23a} A. Maio,^{123a,c} S. Majewski,²⁴ Y. Makida,⁶⁴ N. Makovec,¹¹⁴ P. Mal,¹³⁵ B. Malaescu,²⁹ Pa. Malecki,³⁸ P. Malecki,³⁸ V. P. Maleev,¹²⁰ F. Malek,⁵⁴ U. Mallik,⁶¹ D. Malon,⁵ C. Malone,¹⁴² S. Maltezos,⁹ V. Malyshev,¹⁰⁶ S. Malyukov,²⁹ R. Mameghani,⁹⁷ J. Mamuzic,^{12b} A. Manabe,⁶⁴ L. Mandelli,^{88a} I. Mandić,⁷³ R. Mandrysch,¹⁵ J. Maneira,^{123a} P. S. Mangeard,⁸⁷ L. Manhaes de Andrade Filho,^{23b} J. A. Manjarres Ramos,¹³⁵ A. Mann,⁵³ P. M. Manning,¹³⁶ A. Manousakis-Katsikakis,⁸ B. Mansoulie,¹³⁵ A. Mapelli,²⁹ L. Mapelli,²⁹ L. March,⁷⁹ J. F. Marchand,²⁸ F. Marchese,^{132a,132b} G. Marchiori,⁷⁷ M. Marcisovsky,¹²⁴ C. P. Marino,¹⁶⁸ F. Marroquim,^{23a} Z. Marshall,²⁹ F. K. Martens,¹⁵⁷ L. F. Marti,¹⁶ S. Marti-Garcia,¹⁶⁶ B. Martin,²⁹ B. Martin,⁸⁷ J. P. Martin,⁹² T. A. Martin,¹⁷ V. J. Martin,⁴⁵ B. Martin dit Latour,⁴⁸ S. Martin-Haugh,¹⁴⁸ M. Martinez,¹¹ V. Martinez Outschoorn,⁵⁶ A. C. Martyniuk,¹⁶⁸ M. Marx,⁸¹ F. Marzano,^{131a} A. Marzin,¹¹⁰ L. Masetti,⁸⁰ T. Mashimo,¹⁵⁴ R. Mashinistov,⁹³ J. Masik,⁸¹ A. L. Maslennikov,¹⁰⁶ I. Massa,^{19a,19b} G. Massaro,¹⁰⁴ N. Massol,⁴ P. Mastrandrea,¹⁴⁷ A. Mastroberardino,^{36a,36b} T. Masubuchi,¹⁵⁴ P. Matricon,¹¹⁴ H. Matsunaga,¹⁵⁴ T. Matsushita,⁶⁵ C. Mattravers,^{117,d} J. Maurer,⁸² S. J. Maxfield,⁷² A. Mayne,¹³⁸ R. Mazini,¹⁵⁰ M. Mazur,²⁰ L. Mazzaferro,^{132a,132b} M. Mazzanti,^{88a} S. P. Mc Kee,⁸⁶ A. McCarn,¹⁶⁴ R. L. McCarthy,¹⁴⁷ T. G. McCarthy,²⁸ N. A. McCubbin,¹²⁸ K. W. McFarlane,^{55,a} J. A. Mcfayden,¹³⁸ G. Mchedlidze,^{50b} T. McLaughlan,¹⁷ S. J. McMahon,¹²⁸ R. A. McPherson,^{168,l} A. Meade,⁸³ J. Mechnich,¹⁰⁴ M. Mechtel,¹⁷⁴ M. Medinnis,⁴¹ R. Meera-Lebbai,¹¹⁰ T. Meguro,¹¹⁵ R. Mehdiyev,⁹² S. Mehlhase,³⁵ A. Mehta,⁷² K. Meier,^{57a} B. Meirose,⁷⁸ C. Melachrinos,³⁰ B. R. Mellado Garcia,¹⁷² F. Meloni,^{88a,88b} L. Mendoza Navas,¹⁶¹ Z. Meng,^{150,v} A. Mengarelli,^{19a,19b} S. Menke,⁹⁸ E. Meoni,¹⁶⁰ K. M. Mercurio,⁵⁶ P. Mermod,⁴⁸ L. Merola,^{101a,101b} C. Meroni,^{88a} F. S. Merritt,³⁰ H. Merritt,¹⁰⁸ A. Messina,^{29,z} J. Metcalfe,¹⁰² A. S. Mete,¹⁶² C. Meyer,⁸⁰ C. Meyer,³⁰ J-P. Meyer,¹³⁵ J. Meyer,¹⁷³ J. Meyer,⁵³ T. C. Meyer,²⁹ J. Miao,^{32d} S. Michal,²⁹ L. Micu,^{25a} R. P. Middleton,¹²⁸ S. Migas,⁷² L. Mijović,¹³⁵ G. Mikenberg,¹⁷¹ M. Mikestikova,¹²⁴ M. Mikuž,⁷³ D. W. Miller,³⁰ R. J. Miller,⁸⁷ W. J. Mills,¹⁶⁷ C. Mills,⁵⁶ A. Milov,¹⁷¹ D. A. Milstead,^{145a,145b} D. Milstein,¹⁷¹ A. A. Minaenko,¹²⁷ M. Miñano Moya,¹⁶⁶ I. A. Minashvili,⁶³ A. I. Mincer,¹⁰⁷ B. Mindur,³⁷ M. Mineev,⁶³ Y. Ming,¹⁷² L. M. Mir,¹¹

G. Mirabelli,^{131a} J. Mitrevski,¹³⁶ V. A. Mitsou,¹⁶⁶ S. Mitsui,⁶⁴ P. S. Miyagawa,¹³⁸ J. U. Mjörnmark,⁷⁸ T. Moa,^{145a,145b} V. Moeller,²⁷ K. Mönig,⁴¹ N. Möser,²⁰ S. Mohapatra,¹⁴⁷ W. Mohr,⁴⁷ R. Moles-Valls,¹⁶⁶ J. Monk,⁷⁶ E. Monnier,⁸² J. Montejo Berlingen,¹¹ F. Monticelli,⁶⁹ S. Monzani,^{19a,19b} R. W. Moore,² G. F. Moorhead,⁸⁵ C. Mora Herrera,⁴⁸ A. Moraes,⁵² N. Morange,¹³⁵ J. Morel,⁵³ G. Morello,^{36a,36b} D. Moreno,⁸⁰ M. Moreno Llácer,¹⁶⁶ P. Morettini,^{49a} M. Morgenstern,⁴³ M. Morii,⁵⁶ A. K. Morley,²⁹ G. Mornacchi,²⁹ J. D. Morris,⁷⁴ L. Morvaj,¹⁰⁰ H. G. Moser,⁹⁸ M. Mosidze,^{50b} J. Moss,¹⁰⁸ R. Mount,¹⁴² E. Mountricha,^{9,aa} S. V. Mouraviev,^{93,a} E. J. W. Moyse,⁸³ F. Mueller,^{57a} J. Mueller,¹²² K. Mueller,²⁰ T. A. Müller,⁹⁷ T. Mueller,⁸⁰ D. Muenstermann,²⁹ Y. Munwes,¹⁵² W. J. Murray,¹²⁸ I. Mussche,¹⁰⁴ E. Musto,^{101a,101b} A. G. Myagkov,¹²⁷ M. Myska,¹²⁴ J. Nadal,¹¹ K. Nagai,¹⁵⁹ R. Nagai,¹⁵⁶ K. Nagano,⁶⁴ A. Nagarkar,¹⁰⁸ Y. Nagasaka,⁵⁸ M. Nagel,⁹⁸ A. M. Nairz,²⁹ Y. Nakahama,²⁹ K. Nakamura,¹⁵⁴ T. Nakamura,¹⁵⁴ I. Nakano,¹⁰⁹ G. Nanava,²⁰ A. Napier,¹⁶⁰ R. Narayan,^{57b} M. Nash,^{76,d} T. Nattermann,²⁰ T. Naumann,⁴¹ G. Navarro,¹⁶¹ H. A. Neal,⁸⁶ P. Yu. Nechaeva,⁹³ T. J. Neep,⁸¹ A. Negri,^{118a,118b} G. Negri,²⁹ M. Negrini,^{19a} S. Nektarijevic,⁴⁸ A. Nelson,¹⁶² T. K. Nelson,¹⁴² S. Nemecek,¹²⁴ P. Nemethy,¹⁰⁷ A. A. Nepomuceno,^{23a} M. Nessi,^{29,bb} M. S. Neubauer,¹⁶⁴ A. Neusiedl,⁸⁰ R. M. Neves,¹⁰⁷ P. Nevski,²⁴ P. R. Newman,¹⁷ V. Nguyen Thi Hong,¹³⁵ R. B. Nickerson,¹¹⁷ R. Nicolaidou,¹³⁵ B. Nicquevert,²⁹ F. Niedercorn,¹¹⁴ J. Nielsen,¹³⁶ N. Nikiforou,³⁴ A. Nikiforov,¹⁵ V. Nikolaenko,¹²⁷ I. Nikolic-Audit,⁷⁷ K. Nikolics,⁴⁸ K. Nikolopoulos,¹⁷ H. Nilsen,⁴⁷ P. Nilsson,⁷ Y. Ninomiya,¹⁵⁴ A. Nisati,^{131a} R. Nisius,⁹⁸ T. Nobe,¹⁵⁶ L. Nodulman,⁵ M. Nomachi,¹¹⁵ I. Nomidis,¹⁵³ S. Norberg,¹¹⁰ M. Nordberg,²⁹ P. R. Norton,¹²⁸ J. Novakova,¹²⁵ M. Nozaki,⁶⁴ L. Nozka,¹¹² I. M. Nugent,^{158a} A.-E. Nuncio-Quiroz,²⁰ G. Nunes Hanninger,⁸⁵ T. Nunnemann,⁹⁷ E. Nurse,⁷⁶ B. J. O'Brien,⁴⁵ S. W. O'Neale,^{17,a} D. C. O'Neil,¹⁴¹ V. O'Shea,⁵² L. B. Oakes,⁹⁷ F. G. Oakham,^{28,e} H. Oberlack,⁹⁸ J. Ocariz,⁷⁷ A. Ochi,⁶⁵ S. Oda,⁶⁸ S. Odaka,⁶⁴ J. Odier,⁸² H. Ogren,⁵⁹ A. Oh,⁸¹ S. H. Oh,⁴⁴ C. C. Ohm,²⁹ T. Ohshima,¹⁰⁰ H. Okawa,²⁴ Y. Okumura,³⁰ T. Okuyama,¹⁵⁴ A. Olariu,^{25a} A. G. Olchevski,⁶³ S. A. Olivares Pino,^{31a} M. Oliveira,^{123a,i} D. Oliveira Damazio,²⁴ E. Oliver Garcia,¹⁶⁶ D. Olivito,¹¹⁹ A. Olszewski,³⁸ J. Olszowska,³⁸ A. Onofre,^{123a,cc} P. U. E. Onyisi,³⁰ C. J. Oram,^{158a} M. J. Oreglia,³⁰ Y. Oren,¹⁵² D. Orestano,^{133a,133b} N. Orlando,^{71a,71b} I. Orlov,¹⁰⁶ C. Oropeza Barrera,⁵² R. S. Orr,¹⁵⁷ B. Osculati,^{49a,49b} R. Ospanov,¹¹⁹ C. Osuna,¹¹ G. Otero y Garzon,²⁶ J. P. Ottersbach,¹⁰⁴ M. Ouchrif,^{134d} E. A. Ouellette,¹⁶⁸ F. Ould-Saada,¹¹⁶ A. Ouraou,¹³⁵ Q. Ouyang,^{32a} A. Ovcharova,¹⁴ M. Owen,⁸¹ S. Owen,¹³⁸ V. E. Ozcan,^{18a} N. Ozturk,⁷ A. Pacheco Pages,¹¹ C. Padilla Aranda,¹¹ S. Pagan Griso,¹⁴ E. Paganis,¹³⁸ C. Pahl,⁹⁸ F. Paige,²⁴ P. Pais,⁸³ K. Pajchel,¹¹⁶ G. Palacino,^{158b} C. P. Paleari,⁶ S. Palestini,²⁹ D. Pallin,³³ A. Palma,^{123a} J. D. Palmer,¹⁷ Y. B. Pan,¹⁷² E. Panagiotopoulou,⁹ P. Pani,¹⁰⁴ N. Panikashvili,⁸⁶ S. Panitkin,²⁴ D. Pantea,^{25a} A. Papadelis,^{145a} Th. D. Papadopoulou,⁹ A. Paramonov,⁵ D. Paredes Hernandez,³³ W. Park,^{24,dd} M. A. Parker,²⁷ F. Parodi,^{49a,49b} J. A. Parsons,³⁴ U. Parzefall,⁴⁷ S. Pashapour,⁵³ E. Pasqualucci,^{131a} S. Passaggio,^{49a} A. Passeri,^{133a} F. Pastore,^{133a,133b,a} Fr. Pastore,⁷⁵ G. Pásztor,^{48,ee} S. Pataria,¹⁷⁴ N. Patel,¹⁴⁹ J. R. Pater,⁸¹ S. Patricelli,^{101a,101b} T. Pauly,²⁹ M. Pecszy,^{143a} S. Pedraza Lopez,¹⁶⁶ M. I. Pedraza Morales,¹⁷² S. V. Peleganchuk,¹⁰⁶ D. Pelikan,¹⁶⁵ H. Peng,^{32b} B. Penning,³⁰ A. Penson,³⁴ J. Penwell,⁵⁹ M. Perantoni,^{23a} K. Perez,^{34,ff} T. Perez Cavalcanti,⁴¹ E. Perez Codina,^{158a} M. T. Pérez García-Estañ,¹⁶⁶ V. Perez Reale,³⁴ L. Perini,^{88a,88b} H. Pernegger,²⁹ R. Perrino,^{71a} P. Perrodo,⁴ V. D. Peshekhonov,⁶³ K. Peters,²⁹ B. A. Petersen,²⁹ J. Petersen,²⁹ T. C. Petersen,³⁵ E. Petit,⁴ A. Petridis,¹⁵³ C. Petridou,¹⁵³ E. Petrolo,^{131a} F. Petrucci,^{133a,133b} D. Petschull,⁴¹ M. Petteni,¹⁴¹ R. Pezoa,^{31b} A. Phan,⁸⁵ P. W. Phillips,¹²⁸ G. Piacquadio,²⁹ A. Picazio,⁴⁸ E. Piccaro,⁷⁴ M. Piccinini,^{19a,19b} S. M. Piec,⁴¹ R. Piegai,²⁶ D. T. Pignotti,¹⁰⁸ J. E. Pilcher,³⁰ A. D. Pilkington,⁸¹ J. Pina,^{123a,c} M. Pinamonti,^{163a,163c} A. Pinder,¹¹⁷ J. L. Pinfold,² B. Pinto,^{123a} C. Pizio,^{88a,88b} M. Plamondon,¹⁶⁸ M.-A. Pleier,²⁴ E. Plotnikova,⁶³ A. Poblaguev,²⁴ S. Poddar,^{57a} F. Podlyski,³³ L. Poggioli,¹¹⁴ M. Pohl,⁴⁸ G. Polesello,^{118a} A. Policicchio,^{36a,36b} A. Polini,^{19a} J. Poll,⁷⁴ V. Polychronakos,²⁴ D. Pomeroy,²² K. Pommès,²⁹ L. Pontecorvo,^{131a} B. G. Pope,⁸⁷ G. A. Popeneciu,^{25a} D. S. Popovic,^{12a} A. Poppleton,²⁹ X. Portell Bueso,²⁹ G. E. Pospelov,⁹⁸ S. Pospisil,¹²⁶ I. N. Potrap,⁹⁸ C. J. Potter,¹⁴⁸ C. T. Potter,¹¹³ G. Poulard,²⁹ J. Poveda,⁵⁹ V. Pozdnyakov,⁶³ R. Prabhu,⁷⁶ P. Pralavorio,⁸² A. Pranko,¹⁴ S. Prasad,²⁹ R. Pravahan,²⁴ S. Prell,⁶² K. Pretzl,¹⁶ D. Price,⁵⁹ J. Price,⁷² L. E. Price,⁵ D. Prieur,¹²² M. Primavera,^{71a} K. Prokofiev,¹⁰⁷ F. Prokoshin,^{31b} S. Protopopescu,²⁴ J. Proudfoot,⁵ X. Prudent,⁴³ M. Przybycien,³⁷ H. Przysieznik,⁴ S. Psoroulas,²⁰ E. Ptacek,¹¹³ E. Pueschel,⁸³ J. Purdham,⁸⁶ M. Purohit,^{24,dd} P. Puzo,¹¹⁴ Y. Pylypchenko,⁶¹ J. Qian,⁸⁶ A. Quadt,⁵³ D. R. Quarrie,¹⁴ W. B. Quayle,¹⁷² F. Quinonez,^{31a} M. Raas,¹⁰³ V. Radescu,⁴¹ P. Radloff,¹¹³ T. Rador,^{18a} F. Ragusa,^{88a,88b} G. Rahal,¹⁷⁷ A. M. Rahimi,¹⁰⁸ D. Rahm,²⁴ S. Rajagopalan,²⁴ M. Rammensee,⁴⁷ M. Rammes,¹⁴⁰ A. S. Randle-Conde,³⁹ K. Randrianarivony,²⁸ F. Rauscher,⁹⁷ T. C. Rave,⁴⁷ M. Raymond,²⁹ A. L. Read,¹¹⁶ D. M. Rebuffi,^{118a,118b} A. Redelbach,¹⁷³ G. Redlinger,²⁴ R. Reece,¹¹⁹ K. Reeves,⁴⁰ E. Reinherz-Aronis,¹⁵² A. Reinsch,¹¹³ I. Reisinger,⁴² C. Rembser,²⁹ Z. L. Ren,¹⁵⁰ A. Renaud,¹¹⁴ M. Rescigno,^{131a} S. Resconi,^{88a}

B. Resende,¹³⁵ P. Reznicek,⁹⁷ R. Rezvani,¹⁵⁷ R. Richter,⁹⁸ E. Richter-Was,^{4,gg} M. Ridel,⁷⁷ M. Rijpstra,¹⁰⁴ M. Rijssenbeek,¹⁴⁷ A. Rimoldi,^{118a,118b} L. Rinaldi,^{19a} R. R. Rios,³⁹ I. Riu,¹¹ G. Rivoltella,^{88a,88b} F. Rizatdinova,¹¹¹ E. Rizvi,⁷⁴ S. H. Robertson,^{84,l} A. Robichaud-Veronneau,¹¹⁷ D. Robinson,²⁷ J. E. M. Robinson,⁸¹ A. Robson,⁵² J. G. Rocha de Lima,¹⁰⁵ C. Roda,^{121a,121b} D. Roda Dos Santos,²⁹ A. Roe,⁵³ S. Roe,²⁹ O. Røhne,¹¹⁶ S. Rolli,¹⁶⁰ A. Romaniouk,⁹⁵ M. Romano,^{19a,19b} G. Romeo,²⁶ E. Romero Adam,¹⁶⁶ L. Roos,⁷⁷ E. Ros,¹⁶⁶ S. Rosati,^{131a} K. Rosbach,⁴⁸ A. Rose,¹⁴⁸ M. Rose,⁷⁵ G. A. Rosenbaum,¹⁵⁷ E. I. Rosenberg,⁶² P. L. Rosendahl,¹³ O. Rosenthal,¹⁴⁰ L. Rosselet,⁴⁸ V. Rossetti,¹¹ E. Rossi,^{131a,131b} L. P. Rossi,^{49a} M. Rotaru,^{25a} I. Roth,¹⁷¹ J. Rothberg,¹³⁷ D. Rousseau,¹¹⁴ C. R. Royon,¹³⁵ A. Rozanov,⁸² Y. Rozen,¹⁵¹ X. Ruan,^{32a,hh} F. Rubbo,¹¹ I. Rubinskiy,⁴¹ B. Ruckert,⁹⁷ N. Ruckstuhl,¹⁰⁴ V. I. Rud,⁹⁶ C. Rudolph,⁴³ G. Rudolph,⁶⁰ F. Rühr,⁶ A. Ruiz-Martinez,⁶² L. Rumyantsev,⁶³ Z. Rurikova,⁴⁷ N. A. Rusakovich,⁶³ J. P. Rutherford,⁶ C. Ruwiedel,^{14,a} P. Ruzicka,¹²⁴ Y. F. Ryabov,¹²⁰ P. Ryan,⁸⁷ M. Rybar,¹²⁵ G. Rybkin,¹¹⁴ N. C. Ryder,¹¹⁷ A. F. Saavedra,¹⁴⁹ I. Sadeh,¹⁵² H. F. W. Sadrozinski,¹³⁶ R. Sadykov,⁶³ F. Safai Tehrani,^{131a} H. Sakamoto,¹⁵⁴ G. Salamanna,⁷⁴ A. Salamon,^{132a} M. Saleem,¹¹⁰ D. Salek,²⁹ D. Salihagic,⁹⁸ A. Salnikov,¹⁴² J. Salt,¹⁶⁶ B. M. Salvachua Ferrando,⁵ D. Salvatore,^{36a,36b} F. Salvatore,¹⁴⁸ A. Salvucci,¹⁰³ A. Salzburger,²⁹ D. Sampsonidis,¹⁵³ B. H. Samset,¹¹⁶ A. Sanchez,^{101a,101b} V. Sanchez Martinez,¹⁶⁶ H. Sandaker,¹³ H. G. Sander,⁸⁰ M. P. Sanders,⁹⁷ M. Sandhoff,¹⁷⁴ T. Sandoval,²⁷ C. Sandoval,¹⁶¹ R. Sandstroem,⁹⁸ D. P. C. Sankey,¹²⁸ A. Sansoni,⁴⁶ C. Santamarina Rios,⁸⁴ C. Santoni,³³ R. Santonico,^{132a,132b} H. Santos,^{123a} J. G. Saraiva,^{123a} T. Sarangi,¹⁷² E. Sarkisyan-Grinbaum,⁷ F. Sarri,^{121a,121b} G. Sartisohn,¹⁷⁴ O. Sasaki,⁶⁴ Y. Sasaki,¹⁵⁴ N. Sasao,⁶⁶ I. Satsounkevitch,⁸⁹ G. Sauvage,^{4,a} E. Sauvan,⁴ J. B. Sauvan,¹¹⁴ P. Savard,^{157,e} V. Savinov,¹²² D. O. Savu,²⁹ L. Sawyer,^{24,n} D. H. Saxon,⁵² J. Saxon,¹¹⁹ C. Sbarra,^{19a} A. Sbrizzi,^{19a,19b} D. A. Scannicchio,¹⁶² M. Scarcella,¹⁴⁹ J. Schaarschmidt,¹¹⁴ P. Schacht,⁹⁸ D. Schaefer,¹¹⁹ U. Schäfer,⁸⁰ S. Schaepe,²⁰ S. Schaezel,^{57b} A. C. Schaffer,¹¹⁴ D. Schaile,⁹⁷ R. D. Schamberger,¹⁴⁷ A. G. Schamov,¹⁰⁶ V. Scharf,^{57a} V. A. Schegelsky,¹²⁰ D. Scheirich,⁸⁶ M. Schernau,¹⁶² M. I. Scherzer,³⁴ C. Schiavi,^{49a,49b} J. Schieck,⁹⁷ M. Schioppa,^{36a,36b} S. Schlenker,²⁹ E. Schmidt,⁴⁷ K. Schmieden,²⁰ C. Schmitt,⁸⁰ S. Schmitt,^{57b} M. Schmitz,²⁰ B. Schneider,¹⁶ U. Schnoor,⁴³ A. Schoening,^{57b} A. L. S. Schorlemmer,⁵³ M. Schott,²⁹ D. Schouten,^{158a} J. Schovancova,¹²⁴ M. Schram,⁸⁴ C. Schroeder,⁸⁰ N. Schroer,^{57c} M. J. Schultens,²⁰ J. Schultes,¹⁷⁴ H.-C. Schultz-Coulon,^{57a} H. Schulz,¹⁵ M. Schumacher,⁴⁷ B. A. Schumm,¹³⁶ Ph. Schune,¹³⁵ C. Schwanenberger,⁸¹ A. Schwartzman,¹⁴² Ph. Schwemling,⁷⁷ R. Schwienhorst,⁸⁷ R. Schwierz,⁴³ J. Schwindling,¹³⁵ T. Schwindt,²⁰ M. Schwoerer,⁴ G. Sciolla,²² W. G. Scott,¹²⁸ J. Searcy,¹¹³ G. Sedov,⁴¹ E. Sedykh,¹²⁰ S. C. Seidel,¹⁰² A. Seiden,¹³⁶ F. Seifert,⁴³ J. M. Seixas,^{23a} G. Sekhniadze,^{101a} S. J. Sekula,³⁹ K. E. Selbach,⁴⁵ D. M. Seliverstov,¹²⁰ B. Sellden,^{145a} G. Sellers,⁷² M. Seman,^{143b} N. Semprini-Cesari,^{19a,19b} C. Serfon,⁹⁷ L. Serin,¹¹⁴ L. Serkin,⁵³ R. Seuster,⁹⁸ H. Severini,¹¹⁰ A. Sfyrta,²⁹ E. Shabalina,⁵³ M. Shamim,¹¹³ L. Y. Shan,^{32a} J. T. Shank,²¹ Q. T. Shao,⁸⁵ M. Shapiro,¹⁴ P. B. Shatalov,⁹⁴ K. Shaw,^{163a,163c} D. Sherman,¹⁷⁵ P. Sherwood,⁷⁶ A. Shibata,¹⁰⁷ S. Shimizu,²⁹ M. Shimojima,⁹⁹ T. Shin,⁵⁵ M. Shiyakova,⁶³ A. Shmeleva,⁹³ M. J. Shochet,³⁰ D. Short,¹¹⁷ S. Shrestha,⁶² E. Shulga,⁹⁵ M. A. Shupe,⁶ P. Sicho,¹²⁴ A. Sidoti,^{131a} F. Siegert,⁴⁷ Dj. Sijacki,^{12a} O. Silbert,¹⁷¹ J. Silva,^{123a} Y. Silver,¹⁵² D. Silverstein,¹⁴² S. B. Silverstein,^{145a} V. Simak,¹²⁶ O. Simard,¹³⁵ Lj. Simic,^{12a} S. Simion,¹¹⁴ E. Simioni,⁸⁰ B. Simmons,⁷⁶ R. Simoniello,^{88a,88b} M. Simonyan,³⁵ P. Sinervo,¹⁵⁷ N. B. Sinev,¹¹³ V. Sipica,¹⁴⁰ G. Siragusa,¹⁷³ A. Sircar,²⁴ A. N. Sisakyan,^{63,a} S. Yu. Sivoklov,⁹⁶ J. Sjölin,^{145a,145b} T. B. Sjrursen,¹³ L. A. Skinnari,¹⁴ H. P. Skottowe,⁵⁶ K. Skovpen,¹⁰⁶ P. Skubic,¹¹⁰ M. Slater,¹⁷ T. Slavicek,¹²⁶ K. Sliwa,¹⁶⁰ V. Smakhtin,¹⁷¹ B. H. Smart,⁴⁵ S. Yu. Smirnov,⁹⁵ Y. Smirnov,⁹⁵ L. N. Smirnova,⁹⁶ O. Smirnova,⁷⁸ B. C. Smith,⁵⁶ D. Smith,¹⁴² K. M. Smith,⁵² M. Smizanska,⁷⁰ K. Smolek,¹²⁶ A. A. Snesarev,⁹³ S. W. Snow,⁸¹ J. Snow,¹¹⁰ S. Snyder,²⁴ R. Sobie,^{168,l} J. Sodomka,¹²⁶ A. Soffer,¹⁵² C. A. Solans,¹⁶⁶ M. Solar,¹²⁶ J. Solc,¹²⁶ E. Yu. Soldatov,⁹⁵ U. Soldevila,¹⁶⁶ E. Solfaroli Camillocci,^{131a,131b} A. A. Solodkov,¹²⁷ O. V. Solovyanov,¹²⁷ V. Solovyeu,¹²⁰ N. Soni,⁸⁵ V. Sopko,¹²⁶ B. Sopko,¹²⁶ M. Sosebee,⁷ R. Soualah,^{163a,163c} A. Soukharev,¹⁰⁶ S. Spagnolo,^{71a,71b} F. Spanò,⁷⁵ R. Spighi,^{19a} G. Spigo,²⁹ R. Spiwoks,²⁹ M. Spousta,^{125,ii} T. Spreitzer,¹⁵⁷ B. Spurlock,⁷ R. D. St. Denis,⁵² J. Stahlman,¹¹⁹ R. Stamen,^{57a} E. Stanecka,³⁸ R. W. Stanek,⁵ C. Stanescu,^{133a} M. Stanescu-Bellu,⁴¹ S. Stapnes,¹¹⁶ E. A. Starchenko,¹²⁷ J. Stark,⁵⁴ P. Staroba,¹²⁴ P. Starovoitov,⁴¹ R. Staszewski,³⁸ A. Staude,⁹⁷ P. Stavina,^{143a,a} G. Steele,⁵² P. Steinbach,⁴³ P. Steinberg,²⁴ I. Stekl,¹²⁶ B. Stelzer,¹⁴¹ H. J. Stelzer,⁸⁷ O. Stelzer-Chilton,^{158a} H. Stenzel,⁵¹ S. Stern,⁹⁸ G. A. Stewart,²⁹ J. A. Stillings,²⁰ M. C. Stockton,⁸⁴ K. Stoerig,⁴⁷ G. Stoicea,^{25a} S. Stonjek,⁹⁸ P. Strachota,¹²⁵ A. R. Stradling,⁷ A. Straessner,⁴³ J. Strandberg,¹⁴⁶ S. Strandberg,^{145a,145b} A. Strandlie,¹¹⁶ M. Strang,¹⁰⁸ E. Strauss,¹⁴² M. Strauss,¹¹⁰ P. Strizenec,^{143b} R. Ströhmer,¹⁷³ D. M. Strom,¹¹³ J. A. Strong,^{75,a} R. Stroynowski,³⁹ J. Strube,¹²⁸ B. Stugu,¹³ I. Stumer,^{24,a} J. Stupak,¹⁴⁷ P. Sturm,¹⁷⁴ N. A. Styles,⁴¹ D. A. Soh,^{150,x}

- D. Su,¹⁴² H.S. Subramania,² A. Succurro,¹¹ Y. Sugaya,¹¹⁵ C. Suhr,¹⁰⁵ M. Suk,¹²⁵ V. V. Sulin,⁹³ S. Sultansoy,^{3d} T. Sumida,⁶⁶ X. Sun,⁵⁴ J. E. Sundermann,⁴⁷ K. Suruliz,¹³⁸ G. Susinno,^{36a,36b} M. R. Sutton,¹⁴⁸ Y. Suzuki,⁶⁴ Y. Suzuki,⁶⁵ M. Svatos,¹²⁴ S. Swedish,¹⁶⁷ I. Sykora,^{143a} T. Sykora,¹²⁵ J. Sánchez,¹⁶⁶ D. Ta,¹⁰⁴ K. Tackmann,⁴¹ A. Taffard,¹⁶² R. Tafirout,^{158a} N. Taiblum,¹⁵² Y. Takahashi,¹⁰⁰ H. Takai,²⁴ R. Takashima,⁶⁷ H. Takeda,⁶⁵ T. Takeshita,¹³⁹ Y. Takubo,⁶⁴ M. Talby,⁸² A. Talyshev,^{106,g} M. C. Tamssett,²⁴ J. Tanaka,¹⁵⁴ R. Tanaka,¹¹⁴ S. Tanaka,¹³⁰ S. Tanaka,⁶⁴ A. J. Tanasijczuk,¹⁴¹ K. Tani,⁶⁵ N. Tannoury,⁸² S. Tapprogge,⁸⁰ D. Tardif,¹⁵⁷ S. Tarem,¹⁵¹ F. Tarrade,²⁸ G. F. Tartarelli,^{88a} P. Tas,¹²⁵ M. Tasevsky,¹²⁴ E. Tassi,^{36a,36b} M. Tatarikhanov,¹⁴ Y. Tayalati,^{134d} C. Taylor,⁷⁶ F. E. Taylor,⁹¹ G. N. Taylor,⁸⁵ W. Taylor,^{158b} M. Teinturier,¹¹⁴ M. Teixeira Dias Castanheira,⁷⁴ P. Teixeira-Dias,⁷⁵ K. K. Temming,⁴⁷ H. Ten Kate,²⁹ P. K. Teng,¹⁵⁰ S. Terada,⁶⁴ K. Terashi,¹⁵⁴ J. Terron,⁷⁹ M. Testa,⁴⁶ R. J. Teuscher,^{157,l} J. Therhaag,²⁰ T. Theveneaux-Pelzer,⁷⁷ S. Thoma,⁴⁷ J. P. Thomas,¹⁷ E. N. Thompson,³⁴ P. D. Thompson,¹⁷ P. D. Thompson,¹⁵⁷ A. S. Thompson,⁵² L. A. Thomsen,³⁵ E. Thomson,¹¹⁹ M. Thomson,²⁷ W. M. Thong,⁸⁵ R. P. Thun,⁸⁶ F. Tian,³⁴ M. J. Tibbetts,¹⁴ T. Tic,¹²⁴ V. O. Tikhomirov,⁹³ Y. A. Tikhonov,^{106,g} S. Timoshenko,⁹⁵ P. Tipton,¹⁷⁵ S. Tisserant,⁸² T. Todorov,⁴ S. Todorova-Nova,¹⁶⁰ B. Toggerson,¹⁶² J. Tojo,⁶⁸ S. Tokár,^{143a} K. Tokushuku,⁶⁴ K. Tollefson,⁸⁷ M. Tomoto,¹⁰⁰ L. Tompkins,³⁰ K. Toms,¹⁰² A. Tonoyan,¹³ C. Topfel,¹⁶ N. D. Topilin,⁶³ I. Torchiani,²⁹ E. Torrence,¹¹³ H. Torres,⁷⁷ E. Torró Pastor,¹⁶⁶ J. Toth,^{82,ee} F. Touchard,⁸² D. R. Tovey,¹³⁸ T. Trefzger,¹⁷³ L. Tremblet,²⁹ A. Tricoli,²⁹ I. M. Trigger,^{158a} S. Trincaz-Duvoid,⁷⁷ M. F. Tripiana,⁶⁹ N. Triplett,²⁴ W. Trischuk,¹⁵⁷ B. Trocmé,⁵⁴ C. Troncon,^{88a} M. Trotter-McDonald,¹⁴¹ M. Trzebinski,³⁸ A. Trzupek,³⁸ C. Tsarouchas,²⁹ J. C-L. Tseng,¹¹⁷ M. Tsiakiris,¹⁰⁴ P. V. Tsiarehsha,⁸⁹ D. Tsiou,^{4,jj} G. Tsipolitis,⁹ S. Tsisikaridze,¹¹ V. Tsiskaridze,⁴⁷ E. G. Tskhadadze,^{50a} I. I. Tsukerman,⁹⁴ V. Tsulaia,¹⁴ J.-W. Tsung,²⁰ S. Tsuno,⁶⁴ D. Tsybychev,¹⁴⁷ A. Tua,¹³⁸ A. Tudorache,^{25a} V. Tudorache,^{25a} J. M. Tuggle,³⁰ M. Turala,³⁸ D. Turecek,¹²⁶ I. Turk Cakir,^{3e} E. Turlay,¹⁰⁴ R. Turra,^{88a,88b} P. M. Tuts,³⁴ A. Tykhonov,⁷³ M. Tylmad,^{145a,145b} M. Tyndel,¹²⁸ G. Tzanakos,⁸ K. Uchida,²⁰ I. Ueda,¹⁵⁴ R. Ueno,²⁸ M. Ugland,¹³ M. Uhlenbrock,²⁰ M. Uhrmacher,⁵³ F. Ukegawa,¹⁵⁹ G. Unal,²⁹ A. Undrus,²⁴ G. Unel,¹⁶² Y. Unno,⁶⁴ D. Urbaniec,³⁴ G. Usai,⁷ M. Uslenghi,^{118a,118b} L. Vacavant,⁸² V. Vacek,¹²⁶ B. Vachon,⁸⁴ S. Vahsen,¹⁴ J. Valenta,¹²⁴ S. Valentinetti,^{19a,19b} A. Valero,¹⁶⁶ S. Valkar,¹²⁵ E. Valladolid Gallego,¹⁶⁶ S. Vallecorsa,¹⁵¹ J. A. Valls Ferrer,¹⁶⁶ P. C. Van Der Deijl,¹⁰⁴ R. van der Geer,¹⁰⁴ H. van der Graaf,¹⁰⁴ R. Van Der Leeuw,¹⁰⁴ E. van der Poel,¹⁰⁴ D. van der Ster,²⁹ N. van Eldik,²⁹ P. van Gemmeren,⁵ I. van Vulpen,¹⁰⁴ M. Vanadia,⁹⁸ W. Vandelli,²⁹ A. Vaniachine,⁵ P. Vankov,⁴¹ F. Vannucci,⁷⁷ R. Vari,^{131a} T. Varol,⁸³ D. Varouchas,¹⁴ A. Vartapetian,⁷ K. E. Varvell,¹⁴⁹ V. I. Vassilakopoulos,⁵⁵ F. Vazeille,³³ T. Vazquez Schroeder,⁵³ G. Vegni,^{88a,88b} J. J. Veillet,¹¹⁴ F. Veloso,^{123a} R. Veness,²⁹ S. Veneziano,^{131a} A. Ventura,^{71a,71b} D. Ventura,⁸³ M. Venturi,⁴⁷ N. Venturi,¹⁵⁷ V. Vercesi,^{118a} M. Verducci,¹³⁷ W. Verkerke,¹⁰⁴ J. C. Vermeulen,¹⁰⁴ A. Vest,⁴³ M. C. Vetterli,^{141,e} I. Vichou,¹⁶⁴ T. Vickey,^{144b,kk} O. E. Vickey Boeriu,^{144b} G. H. A. Viehhauser,¹¹⁷ S. Viel,¹⁶⁷ M. Villa,^{19a,19b} M. Villaplana Perez,¹⁶⁶ E. Vilucchi,⁴⁶ M. G. Vincker,²⁸ E. Vinek,²⁹ V. B. Vinogradov,⁶³ M. Virchaux,^{135,a} J. Virzi,¹⁴ O. Vitells,¹⁷¹ M. Viti,⁴¹ I. Vivarelli,⁴⁷ F. Vives Vaque,² S. Vlachos,⁹ D. Vladoiu,⁹⁷ M. Vlasak,¹²⁶ A. Vogel,²⁰ P. Vokac,¹²⁶ G. Volpi,⁴⁶ M. Volpi,⁸⁵ G. Volpini,^{88a} H. von der Schmitt,⁹⁸ H. von Radziewski,⁴⁷ E. von Toerne,²⁰ V. Vorobel,¹²⁵ V. Vorwerk,¹¹ M. Vos,¹⁶⁶ R. Voss,²⁹ T. T. Voss,¹⁷⁴ J. H. Vosseveld,⁷² N. Vranjes,¹³⁵ M. Vranjes Milosavljevic,¹⁰⁴ V. Vrba,¹²⁴ M. Vreeswijk,¹⁰⁴ T. Vu Anh,⁴⁷ R. Vuillermet,²⁹ I. Vukotic,³⁰ W. Wagner,¹⁷⁴ P. Wagner,¹¹⁹ H. Wahlen,¹⁷⁴ S. Währmund,⁴³ J. Wakabayashi,¹⁰⁰ S. Walch,⁸⁶ J. Walder,⁷⁰ R. Walker,⁹⁷ W. Walkowiak,¹⁴⁰ R. Wall,¹⁷⁵ P. Waller,⁷² B. Walsh,¹⁷⁵ C. Wang,⁴⁴ H. Wang,¹⁷² H. Wang,^{32b,ll} J. Wang,¹⁵⁰ J. Wang,⁵⁴ R. Wang,¹⁰² S. M. Wang,¹⁵⁰ T. Wang,²⁰ A. Warburton,⁸⁴ C. P. Ward,²⁷ M. Warsinsky,⁴⁷ A. Washbrook,⁴⁵ C. Wasicki,⁴¹ I. Watanabe,⁶⁵ P. M. Watkins,¹⁷ A. T. Watson,¹⁷ I. J. Watson,¹⁴⁹ M. F. Watson,¹⁷ G. Watts,¹³⁷ S. Watts,⁸¹ A. T. Waugh,¹⁴⁹ B. M. Waugh,⁷⁶ M. S. Weber,¹⁶ P. Weber,⁵³ A. R. Weidberg,¹¹⁷ P. Weigell,⁹⁸ J. Weingarten,⁵³ C. Weiser,⁴⁷ H. Wellenstein,²² P. S. Wells,²⁹ T. Wenaus,²⁴ D. Wendland,¹⁵ Z. Weng,^{150,x} T. Wengler,²⁹ S. Wenig,²⁹ N. Wermes,²⁰ M. Werner,⁴⁷ P. Werner,²⁹ M. Werth,¹⁶² M. Wessels,^{57a} J. Wetter,¹⁶⁰ C. Weydert,⁵⁴ K. Whalen,²⁸ S. J. Wheeler-Ellis,¹⁶² A. White,⁷ M. J. White,⁸⁵ S. White,^{121a,121b} S. R. Whitehead,¹¹⁷ D. Whiteson,¹⁶² D. Whittington,⁵⁹ F. Wicek,¹¹⁴ D. Wicke,¹⁷⁴ F. J. Wickens,¹²⁸ W. Wiedenmann,¹⁷² M. Wielers,¹²⁸ P. Wienemann,²⁰ C. Wigglesworth,⁷⁴ L. A. M. Wiik-Fuchs,⁴⁷ P. A. Wijeratne,⁷⁶ A. Wildauer,⁹⁸ M. A. Wildt,^{41,t} I. Wilhelm,¹²⁵ H. G. Wilkens,²⁹ J. Z. Will,⁹⁷ E. Williams,³⁴ H. H. Williams,¹¹⁹ W. Willis,³⁴ S. Willocq,⁸³ J. A. Wilson,¹⁷ M. G. Wilson,¹⁴² A. Wilson,⁸⁶ I. Wingerter-Seez,⁴ S. Winkelmann,⁴⁷ F. Winklmeier,²⁹ M. Wittgen,¹⁴² S. J. Wollstadt,⁸⁰ M. W. Wolter,³⁸ H. Wolters,^{123a,i} W. C. Wong,⁴⁰ G. Wooden,⁸⁶ B. K. Wosiek,³⁸ J. Wotschack,²⁹ M. J. Woudstra,⁸¹ K. W. Wozniak,³⁸ K. Wraight,⁵² C. Wright,⁵² M. Wright,⁵² B. Wrona,⁷² S. L. Wu,¹⁷² X. Wu,⁴⁸ Y. Wu,^{32b,mm} E. Wulf,³⁴ B. M. Wynne,⁴⁵ S. Xella,³⁵ M. Xiao,¹³⁵ S. Xie,⁴⁷ C. Xu,^{32b,aa} D. Xu,¹³⁸ B. Yabsley,¹⁴⁹

S. Yacoob,^{144b} M. Yamada,⁶⁴ H. Yamaguchi,¹⁵⁴ A. Yamamoto,⁶⁴ K. Yamamoto,⁶² S. Yamamoto,¹⁵⁴ T. Yamamura,¹⁵⁴
 T. Yamanaka,¹⁵⁴ J. Yamaoka,⁴⁴ T. Yamazaki,¹⁵⁴ Y. Yamazaki,⁶⁵ Z. Yan,²¹ H. Yang,⁸⁶ U. K. Yang,⁸¹ Y. Yang,⁵⁹
 Z. Yang,^{145a,145b} S. Yanush,⁹⁰ L. Yao,^{32a} Y. Yao,¹⁴ Y. Yasu,⁶⁴ G. V. Ybeles Smit,¹²⁹ J. Ye,³⁹ S. Ye,²⁴ M. Yilmaz,^{3c}
 R. Yoosoofmiya,¹²² K. Yorita,¹⁷⁰ R. Yoshida,⁵ C. Young,¹⁴² C. J. Young,¹¹⁷ S. Youssef,²¹ D. Yu,²⁴ J. Yu,⁷ J. Yu,¹¹¹
 L. Yuan,⁶⁵ A. Yurkewicz,¹⁰⁵ M. Byszewski,²⁹ B. Zabinski,³⁸ R. Zaidan,⁶¹ A. M. Zaitsev,¹²⁷ Z. Zajacova,²⁹
 L. Zanello,^{131a,131b} A. Zaytsev,¹⁰⁶ C. Zeitnitz,¹⁷⁴ M. Zeman,¹²⁴ A. Zemla,³⁸ C. Zender,²⁰ O. Zenin,¹²⁷ T. Ženiš,^{143a}
 Z. Zinonos,^{121a,121b} S. Zenz,¹⁴ D. Zerwas,¹¹⁴ G. Zevi della Porta,⁵⁶ Z. Zhan,^{32d} D. Zhang,^{32b,II} H. Zhang,⁸⁷ J. Zhang,⁵
 X. Zhang,^{32d} Z. Zhang,¹¹⁴ L. Zhao,¹⁰⁷ T. Zhao,¹³⁷ Z. Zhao,^{32b} A. Zhemchugov,⁶³ J. Zhong,¹¹⁷ B. Zhou,⁸⁶ N. Zhou,¹⁶²
 Y. Zhou,¹⁵⁰ C. G. Zhu,^{32d} H. Zhu,⁴¹ J. Zhu,⁸⁶ Y. Zhu,^{32b} X. Zhuang,⁹⁷ V. Zhuravlov,⁹⁸ D. Zieminska,⁵⁹ N. I. Zimin,⁶³
 R. Zimmermann,²⁰ S. Zimmermann,²⁰ S. Zimmermann,⁴⁷ M. Ziolkowski,¹⁴⁰ R. Zitoun,⁴ L. Živković,³⁴
 V. V. Zmouchko,^{127,a} G. Zobernig,¹⁷² A. Zoccoli,^{19a,19b} M. zur Nedden,¹⁵ V. Zutshi,¹⁰⁵ and L. Zwalinski²⁹

(ATLAS Collaboration)

¹Physics Department, SUNY Albany, Albany, New York, USA

²Department of Physics, University of Alberta, Edmonton, Alberta, Canada

^{3a}Department of Physics, Ankara University, Ankara, Turkey

^{3b}Department of Physics, Dumlupinar University, Kutahya, Turkey

^{3c}Department of Physics, Gazi University, Ankara, Turkey

^{3d}Division of Physics, TOBB University of Economics and Technology, Ankara, Turkey

^{3e}Turkish Atomic Energy Authority, Ankara, Turkey

⁴LAPP, CNRS/IN2P3 and Université de Savoie, Annecy-le-Vieux, France

⁵High Energy Physics Division, Argonne National Laboratory, Argonne, Illinois, USA

⁶Department of Physics, University of Arizona, Tucson, Arizona, USA

⁷Department of Physics, The University of Texas at Arlington, Arlington, Texas, USA

⁸Physics Department, University of Athens, Athens, Greece

⁹Physics Department, National Technical University of Athens, Zografou, Greece

¹⁰Institute of Physics, Azerbaijan Academy of Sciences, Baku, Azerbaijan

¹¹Institut de Física d'Altes Energies and Departament de Física de la Universitat Autònoma de Barcelona and ICREA, Barcelona, Spain

^{12a}Institute of Physics, University of Belgrade, Belgrade, Serbia

^{12b}Vinca Institute of Nuclear Sciences, University of Belgrade, Belgrade, Serbia

¹³Department for Physics and Technology, University of Bergen, Bergen, Norway

¹⁴Physics Division, Lawrence Berkeley National Laboratory and University of California, Berkeley, California, USA

¹⁵Department of Physics, Humboldt University, Berlin, Germany

¹⁶Albert Einstein Center for Fundamental Physics and Laboratory for High Energy Physics, University of Bern, Bern, Switzerland

¹⁷School of Physics and Astronomy, University of Birmingham, Birmingham, United Kingdom

^{18a}Department of Physics, Bogazici University, Istanbul, Turkey

^{18b}Division of Physics, Dogus University, Istanbul, Turkey

^{18c}Department of Physics Engineering, Gaziantep University, Gaziantep, Turkey

^{18d}Department of Physics, Istanbul Technical University, Istanbul, Turkey

^{19a}INFN Sezione di Bologna, Italy

^{19b}Dipartimento di Fisica, Università di Bologna, Bologna, Italy

²⁰Physikalisches Institut, University of Bonn, Bonn, Germany

²¹Department of Physics, Boston University, Boston, Massachusetts, USA

²²Department of Physics, Brandeis University, Waltham, Massachusetts, USA

^{23a}Universidade Federal do Rio De Janeiro COPPE/EE/IF, Rio de Janeiro, Brazil

^{23b}Federal University of Juiz de Fora (UFJF), Juiz de Fora, Brazil

^{23c}Federal University of Sao Joao del Rei (UFSJ), Sao Joao del Rei, Brazil

^{23d}Instituto de Física, Universidade de Sao Paulo, Sao Paulo, Brazil

²⁴Physics Department, Brookhaven National Laboratory, Upton, New York, USA

^{25a}National Institute of Physics and Nuclear Engineering, Bucharest, Romania

^{25b}University Politehnica Bucharest, Bucharest, Romania

^{25c}West University in Timisoara, Timisoara, Romania

²⁶Departamento de Física, Universidad de Buenos Aires, Buenos Aires, Argentina

²⁷Cavendish Laboratory, University of Cambridge, Cambridge, United Kingdom

²⁸Department of Physics, Carleton University, Ottawa, Ontario, Canada

²⁹CERN, Geneva, Switzerland

- ³⁰Enrico Fermi Institute, University of Chicago, Chicago, Illinois, USA
- ^{31a}Departamento de Física, Pontificia Universidad Católica de Chile, Santiago, Chile
- ^{31b}Departamento de Física, Universidad Técnica Federico Santa María, Valparaíso, Chile
- ^{32a}Institute of High Energy Physics, Chinese Academy of Sciences, Beijing, China
- ^{32b}Department of Modern Physics, University of Science and Technology of China, Anhui, China
- ^{32c}Department of Physics, Nanjing University, Jiangsu, China
- ^{32d}School of Physics, Shandong University, Shandong, China
- ³³Laboratoire de Physique Corpusculaire, Clermont Université and Université Blaise Pascal and CNRS/IN2P3, Aubiere Cedex, France
- ³⁴Nevis Laboratory, Columbia University, Irvington, New York, USA
- ³⁵Niels Bohr Institute, University of Copenhagen, Kobenhavn, Denmark
- ^{36a}INFN Gruppo Collegato di Cosenza, Italy
- ^{36b}Dipartimento di Fisica, Università della Calabria, Arcavata di Rende, Italy
- ³⁷AGH University of Science and Technology, Faculty of Physics and Applied Computer Science, Krakow, Poland
- ³⁸The Henryk Niewodniczanski Institute of Nuclear Physics, Polish Academy of Sciences, Krakow, Poland
- ³⁹Physics Department, Southern Methodist University, Dallas, Texas, USA
- ⁴⁰Physics Department, University of Texas at Dallas, Richardson, Texas, USA
- ⁴¹DESY, Hamburg and Zeuthen, Germany
- ⁴²Institut für Experimentelle Physik IV, Technische Universität Dortmund, Dortmund, Germany
- ⁴³Institut für Kern- und Teilchenphysik, Technical University Dresden, Dresden, Germany
- ⁴⁴Department of Physics, Duke University, Durham, North Carolina, USA
- ⁴⁵SUPA-School of Physics and Astronomy, University of Edinburgh, Edinburgh, United Kingdom
- ⁴⁶INFN Laboratori Nazionali di Frascati, Frascati, Italy
- ⁴⁷Fakultät für Mathematik und Physik, Albert-Ludwigs-Universität, Freiburg i.Br., Germany
- ⁴⁸Section de Physique, Université de Genève, Geneva, Switzerland
- ^{49a}INFN Sezione di Genova, Italy
- ^{49b}Dipartimento di Fisica, Università di Genova, Genova, Italy
- ^{50a}E. Andronikashvili Institute of Physics, Tbilisi State University, Tbilisi, Georgia
- ^{50b}High Energy Physics Institute, Tbilisi State University, Tbilisi, Georgia
- ⁵¹II Physikalisches Institut, Justus-Liebig-Universität Giessen, Giessen, Germany
- ⁵²SUPA-School of Physics and Astronomy, University of Glasgow, Glasgow, United Kingdom
- ⁵³II Physikalisches Institut, Georg-August-Universität, Göttingen, Germany
- ⁵⁴Laboratoire de Physique Subatomique et de Cosmologie, Université Joseph Fourier and CNRS/IN2P3 and Institut National Polytechnique de Grenoble, Grenoble, France
- ⁵⁵Department of Physics, Hampton University, Hampton, Virginia, USA
- ⁵⁶Laboratory for Particle Physics and Cosmology, Harvard University, Cambridge, Massachusetts, USA
- ^{57a}Kirchhoff-Institut für Physik, Ruprecht-Karls-Universität Heidelberg, Heidelberg, Germany
- ^{57b}Physikalisches Institut, Ruprecht-Karls-Universität Heidelberg, Heidelberg, Germany
- ^{57c}ZITI Institut für technische Informatik, Ruprecht-Karls-Universität Heidelberg, Mannheim, Germany
- ⁵⁸Faculty of Applied Information Science, Hiroshima Institute of Technology, Hiroshima, Japan
- ⁵⁹Department of Physics, Indiana University, Bloomington, Indiana, USA
- ⁶⁰Institut für Astro- und Teilchenphysik, Leopold-Franzens-Universität, Innsbruck, Austria
- ⁶¹University of Iowa, Iowa City, Iowa, USA
- ⁶²Department of Physics and Astronomy, Iowa State University, Ames, Iowa, USA
- ⁶³Joint Institute for Nuclear Research, JINR Dubna, Dubna, Russia
- ⁶⁴KEK, High Energy Accelerator Research Organization, Tsukuba, Japan
- ⁶⁵Graduate School of Science, Kobe University, Kobe, Japan
- ⁶⁶Faculty of Science, Kyoto University, Kyoto, Japan
- ⁶⁷Kyoto University of Education, Kyoto, Japan
- ⁶⁸Department of Physics, Kyushu University, Fukuoka, Japan
- ⁶⁹Instituto de Física La Plata, Universidad Nacional de La Plata and CONICET, La Plata, Argentina
- ⁷⁰Physics Department, Lancaster University, Lancaster, United Kingdom
- ^{71a}INFN Sezione di Lecce, Italy
- ^{71b}Dipartimento di Matematica e Fisica, Università del Salento, Lecce, Italy
- ⁷²Oliver Lodge Laboratory, University of Liverpool, Liverpool, United Kingdom
- ⁷³Department of Physics, Jozef Stefan Institute and University of Ljubljana, Ljubljana, Slovenia
- ⁷⁴School of Physics and Astronomy, Queen Mary University of London, London, United Kingdom
- ⁷⁵Department of Physics, Royal Holloway University of London, Surrey, United Kingdom
- ⁷⁶Department of Physics and Astronomy, University College London, London, United Kingdom
- ⁷⁷Laboratoire de Physique Nucléaire et de Hautes Energies, UPMC and Université Paris-Diderot and CNRS/IN2P3, Paris, France
- ⁷⁸Fysiska institutionen, Lunds universitet, Lund, Sweden

- ⁷⁹*Departamento de Fisica Teorica C-15, Universidad Autonoma de Madrid, Madrid, Spain*
⁸⁰*Institut für Physik, Universität Mainz, Mainz, Germany*
- ⁸¹*School of Physics and Astronomy, University of Manchester, Manchester, United Kingdom*
⁸²*CPPM, Aix-Marseille Université and CNRS/IN2P3, Marseille, France*
- ⁸³*Department of Physics, University of Massachusetts, Amherst, Massachusetts, USA*
⁸⁴*Department of Physics, McGill University, Montreal, Quebec, Canada*
⁸⁵*School of Physics, University of Melbourne, Victoria, Australia*
- ⁸⁶*Department of Physics, The University of Michigan, Ann Arbor, Michigan, USA*
⁸⁷*Department of Physics and Astronomy, Michigan State University, East Lansing, Michigan, USA*
^{88a}*INFN Sezione di Milano, Italy*
^{88b}*Dipartimento di Fisica, Università di Milano, Milano, Italy*
- ⁸⁹*B.I. Stepanov Institute of Physics, National Academy of Sciences of Belarus, Minsk, Republic of Belarus*
⁹⁰*National Scientific and Educational Centre for Particle and High Energy Physics, Minsk, Republic of Belarus*
⁹¹*Department of Physics, Massachusetts Institute of Technology, Cambridge, Massachusetts, USA*
⁹²*Group of Particle Physics, University of Montreal, Montreal, Quebec, Canada*
⁹³*P.N. Lebedev Institute of Physics, Academy of Sciences, Moscow, Russia*
⁹⁴*Institute for Theoretical and Experimental Physics (ITEP), Moscow, Russia*
⁹⁵*Moscow Engineering and Physics Institute (MEPhI), Moscow, Russia*
- ⁹⁶*Skobeltsyn Institute of Nuclear Physics, Lomonosov Moscow State University, Moscow, Russia*
⁹⁷*Fakultät für Physik, Ludwig-Maximilians-Universität München, München, Germany*
⁹⁸*Max-Planck-Institut für Physik (Werner-Heisenberg-Institut), München, Germany*
⁹⁹*Nagasaki Institute of Applied Science, Nagasaki, Japan*
- ¹⁰⁰*Graduate School of Science and Kobayashi-Maskawa Institute, Nagoya University, Nagoya, Japan*
^{101a}*INFN Sezione di Napoli, Italy*
^{101b}*Dipartimento di Scienze Fisiche, Università di Napoli, Napoli, Italy*
- ¹⁰²*Department of Physics and Astronomy, University of New Mexico, Albuquerque, New Mexico, USA*
¹⁰³*Institute for Mathematics, Astrophysics and Particle Physics, Radboud University Nijmegen/Nikhef, Nijmegen, Netherlands*
¹⁰⁴*Nikhef National Institute for Subatomic Physics and University of Amsterdam, Amsterdam, Netherlands*
¹⁰⁵*Department of Physics, Northern Illinois University, DeKalb, Illinois, USA*
¹⁰⁶*Budker Institute of Nuclear Physics, SB RAS, Novosibirsk, Russia*
¹⁰⁷*Department of Physics, New York University, New York, New York, USA*
¹⁰⁸*Ohio State University, Columbus, Ohio, , USA*
¹⁰⁹*Faculty of Science, Okayama University, Okayama, Japan*
- ¹¹⁰*Homer L. Dodge Department of Physics and Astronomy, University of Oklahoma, Norman, Oklahoma, USA*
¹¹¹*Department of Physics, Oklahoma State University, Stillwater, Oklahoma, USA*
¹¹²*Palacký University, RCPTM, Olomouc, Czech Republic*
¹¹³*Center for High Energy Physics, University of Oregon, Eugene, Oregon, USA*
¹¹⁴*LAL, Université Paris-Sud and CNRS/IN2P3, Orsay, France*
¹¹⁵*Graduate School of Science, Osaka University, Osaka, Japan*
¹¹⁶*Department of Physics, University of Oslo, Oslo, Norway*
- ¹¹⁷*Department of Physics, Oxford University, Oxford, United Kingdom*
^{118a}*INFN Sezione di Pavia, Italy*
^{118b}*Dipartimento di Fisica, Università di Pavia, Pavia, Italy*
- ¹¹⁹*Department of Physics, University of Pennsylvania, Philadelphia, Pennsylvania, USA*
¹²⁰*Petersburg Nuclear Physics Institute, Gatchina, Russia*
^{121a}*INFN Sezione di Pisa, Italy*
^{121b}*Dipartimento di Fisica E. Fermi, Università di Pisa, Pisa, Italy*
- ¹²²*Department of Physics and Astronomy, University of Pittsburgh, Pittsburgh, Pennsylvania, USA*
^{123a}*Laboratorio de Instrumentacao e Fisica Experimental de Particulas-LIP, Lisboa, Portugal*
^{123b}*Departamento de Fisica Teorica y del Cosmos and CAFPE, Universidad de Granada, Granada, Spain*
¹²⁴*Institute of Physics, Academy of Sciences of the Czech Republic, Praha, Czech Republic*
¹²⁵*Faculty of Mathematics and Physics, Charles University in Prague, Praha, Czech Republic*
¹²⁶*Czech Technical University in Prague, Praha, Czech Republic*
- ¹²⁷*State Research Center Institute for High Energy Physics, Protvino, Russia*
¹²⁸*Particle Physics Department, Rutherford Appleton Laboratory, Didcot, United Kingdom*
¹²⁹*Physics Department, University of Regina, Regina, Saskatchewan, Canada*
¹³⁰*Ritsumeikan University, Kusatsu, Shiga, Japan*
^{131a}*INFN Sezione di Roma I, Italy*
^{131b}*Dipartimento di Fisica, Università La Sapienza, Roma, Italy*
^{132a}*INFN Sezione di Roma Tor Vergata, Italy*
^{132b}*Dipartimento di Fisica, Università di Roma Tor Vergata, Roma, Italy*

- ^{133a}INFN Sezione di Roma Tre, Italy
^{133b}Dipartimento di Fisica, Università Roma Tre, Roma, Italy
- ^{134a}Faculté des Sciences Ain Chock, Réseau Universitaire de Physique des Hautes Energies-Université Hassan II, Casablanca, Morocco
^{134b}Centre National de l'Energie des Sciences Techniques Nucleaires, Rabat, Morocco
^{134c}Faculté des Sciences Semlalia, Université Cadi Ayyad, LPHEA-Marrakech, Morocco
^{134d}Faculté des Sciences, Université Mohamed Premier and LPTPM, Oujda, Morocco
^{134e}Faculté des sciences, Université Mohammed V-Agdal, Rabat, Morocco
- ¹³⁵DSM/IRFU (Institut de Recherches sur les Lois Fondamentales de l'Univers), CEA Saclay (Commissariat a l'Energie Atomique), Gif-sur-Yvette, France
- ¹³⁶Santa Cruz Institute for Particle Physics, University of California Santa Cruz, Santa Cruz, California, USA
¹³⁷Department of Physics, University of Washington, Seattle, Washington, USA
- ¹³⁸Department of Physics and Astronomy, University of Sheffield, Sheffield, United Kingdom
¹³⁹Department of Physics, Shinshu University, Nagano, Japan
¹⁴⁰Fachbereich Physik, Universität Siegen, Siegen, Germany
- ¹⁴¹Department of Physics, Simon Fraser University, Burnaby, British Columbia, Canada
¹⁴²SLAC National Accelerator Laboratory, Stanford, California, USA
- ^{143a}Faculty of Mathematics, Physics & Informatics, Comenius University, Bratislava, Slovak Republic
^{143b}Department of Subnuclear Physics, Institute of Experimental Physics of the Slovak Academy of Sciences, Kosice, Slovak Republic
^{144a}Department of Physics, University of Johannesburg, Johannesburg, South Africa
^{144b}School of Physics, University of the Witwatersrand, Johannesburg, South Africa
^{145a}Department of Physics, Stockholm University, Sweden
^{145b}The Oskar Klein Centre, Stockholm, Sweden
- ¹⁴⁶Physics Department, Royal Institute of Technology, Stockholm, Sweden
- ¹⁴⁷Departments of Physics & Astronomy and Chemistry, Stony Brook University, Stony Brook, New York, USA
¹⁴⁸Department of Physics and Astronomy, University of Sussex, Brighton, United Kingdom
¹⁴⁹School of Physics, University of Sydney, Sydney, Australia
¹⁵⁰Institute of Physics, Academia Sinica, Taipei, Taiwan
- ¹⁵¹Department of Physics, Technion: Israel Institute of Technology, Haifa, Israel
¹⁵²Raymond and Beverly Sackler School of Physics and Astronomy, Tel Aviv University, Tel Aviv, Israel
¹⁵³Department of Physics, Aristotle University of Thessaloniki, Thessaloniki, Greece
- ¹⁵⁴International Center for Elementary Particle Physics and Department of Physics, The University of Tokyo, Tokyo, Japan
¹⁵⁵Graduate School of Science and Technology, Tokyo Metropolitan University, Tokyo, Japan
¹⁵⁶Department of Physics, Tokyo Institute of Technology, Tokyo, Japan
¹⁵⁷Department of Physics, University of Toronto, Toronto, Ontario, Canada
^{158a}TRIUMF, Vancouver, British Columbia, Canada
^{158b}Department of Physics and Astronomy, York University, Toronto, Ontario, Canada
- ¹⁵⁹Institute of Pure and Applied Sciences, University of Tsukuba, 1-1-1 Tennodai, Tsukuba, Ibaraki 305-8571, Japan
¹⁶⁰Science and Technology Center, Tufts University, Medford, Massachusetts, USA
¹⁶¹Centro de Investigaciones, Universidad Antonio Narino, Bogota, Colombia
- ¹⁶²Department of Physics and Astronomy, University of California Irvine, Irvine, California, USA
^{163a}INFN Gruppo Collegato di Udine, Italy
^{163b}ICTP, Trieste, Italy
^{163c}Dipartimento di Chimica, Fisica e Ambiente, Università di Udine, Udine, Italy
¹⁶⁴Department of Physics, University of Illinois, Urbana, Illinois, USA
¹⁶⁵Department of Physics and Astronomy, University of Uppsala, Uppsala, Sweden
- ¹⁶⁶Instituto de Física Corpuscular (IFIC) and Departamento de Física Atómica, Molecular y Nuclear and Departamento de Ingeniería Electrónica and Instituto de Microelectrónica de Barcelona (IMB-CNM), University of Valencia and CSIC, Valencia, Spain
- ¹⁶⁷Department of Physics, University of British Columbia, Vancouver, British Columbia, Canada
¹⁶⁸Department of Physics and Astronomy, University of Victoria, Victoria, British Columbia, Canada
¹⁶⁹Department of Physics, University of Warwick, Coventry, United Kingdom
¹⁷⁰Waseda University, Tokyo, Japan
- ¹⁷¹Department of Particle Physics, The Weizmann Institute of Science, Rehovot, Israel
¹⁷²Department of Physics, University of Wisconsin, Madison, Wisconsin, USA
- ¹⁷³Fakultät für Physik und Astronomie, Julius-Maximilians-Universität, Würzburg, Germany
¹⁷⁴Fachbereich C Physik, Bergische Universität Wuppertal, Wuppertal, Germany
¹⁷⁵Department of Physics, Yale University, New Haven, Connecticut, USA
¹⁷⁶Yerevan Physics Institute, Yerevan, Armenia
- ¹⁷⁷Domaine scientifique de la Doua, Centre de Calcul CNRS/IN2P3, Villeurbanne Cedex, France

- ^aDeceased.
- ^bAlso at Laboratorio de Instrumentacao e Fisica Experimental de Particulas-LIP, Lisboa, Portugal.
- ^cAlso at Faculdade de Ciencias and CFNUL, Universidade de Lisboa, Lisboa, Portugal.
- ^dAlso at Particle Physics Department, Rutherford Appleton Laboratory, Didcot, United Kingdom.
- ^eAlso at TRIUMF, Vancouver, British Columbia, Canada.
- ^fAlso at Department of Physics, California State University, Fresno CA, USA.
- ^gAlso at Novosibirsk State University, Novosibirsk, Russia.
- ^hAlso at Fermilab, Batavia, IL, USA.
- ⁱAlso at Department of Physics, University of Coimbra, Coimbra, Portugal.
- ^jAlso at Department of Physics, UASLP, San Luis Potosi, Mexico.
- ^kAlso at Università di Napoli Parthenope, Napoli, Italy
- ^lAlso at Institute of Particle Physics (IPP), Canada.
- ^mAlso at Department of Physics, Middle East Technical University, Ankara, Turkey.
- ⁿAlso at Louisiana Tech University, Ruston, LA, USA
- ^oAlso at Dep Fisica and CEFITEC of Faculdade de Ciencias e Tecnologia, Universidade Nova de Lisboa, Caparica, Portugal.
- ^pAlso at Department of Physics and Astronomy, University College London, London, United Kingdom.
- ^qAlso at Group of Particle Physics, University of Montreal, Montreal, Quebec, Canada.
- ^rAlso at Department of Physics, University of Cape Town, Cape Town, South Africa.
- ^sAlso at Institute of Physics, Azerbaijan Academy of Sciences, Baku, Azerbaijan.
- ^tAlso at Institut für Experimentalphysik, Universität Hamburg, Hamburg, Germany.
- ^uAlso at Manhattan College, New York, NY, USA
- ^vAlso at School of Physics, Shandong University, Shandong, China.
- ^wAlso at CPPM, Aix-Marseille Université and CNRS/IN2P3, Marseille, France.
- ^xAlso at School of Physics and Engineering, Sun Yat-sen University, Guanzhou, China.
- ^yAlso at Academia Sinica Grid Computing, Institute of Physics, Academia Sinica, Taipei, Taiwan.
- ^zAlso at Dipartimento di Fisica, Università La Sapienza, Roma, Italy.
- ^{aa}Also at DSM/IRFU (Institut de Recherches sur les Lois Fondamentales de l'Univers), CEA Saclay (Commissariat a l'Energie Atomique), Gif-sur-Yvette, France.
- ^{bb}Also at Section de Physique, Université de Genève, Geneva, Switzerland.
- ^{cc}Also at Departamento de Fisica, Universidade de Minho, Braga, Portugal.
- ^{dd}Also at Department of Physics and Astronomy, University of South Carolina, Columbia, SC, USA
- ^{ee}Also at Institute for Particle and Nuclear Physics, Wigner Research Centre for Physics, Budapest, Hungary.
- ^{ff}Also at California Institute of Technology, Pasadena, CA, USA.
- ^{gg}Also at Institute of Physics, Jagiellonian University, Krakow, Poland.
- ^{hh}Also at LAL, Université Paris-Sud and CNRS/IN2P3, Orsay, France.
- ⁱⁱAlso at Nevis Laboratory, Columbia University, Irvington, NY, USA
- ^{jj}Also at Department of Physics and Astronomy, University of Sheffield, Sheffield, United Kingdom.
- ^{kk}Also at Department of Physics, Oxford University, Oxford, United Kingdom.
- ^{ll}Also at Institute of Physics, Academia Sinica, Taipei, Taiwan.
- ^{mm}Also at Department of Physics, The University of Michigan, Ann Arbor, MI, USA.